Liquefaction Phenomena
Field and Experimental Observations

Ahmed Elgamal

Acknowledgements

Professor T. L. Youd of Brigham Young University, graciously provided references and slides for use in preparing these notes. This assistance is gratefully acknowledged.

Professor T. Leslie Youd
Brigham Young University
Dept. of Civil Engineering 368 CB
Provo, UT 84602
Tel. 801 378 6327, Fax. 801 378 4449
E-mail: tyoud@byu.edu

Mechanics of Liquefaction

- Propagation of seismic waves through soil layers generates shear deformations within the layer
- Shear deformations cause collapse of loose granular soil structure
- Collapse of granular structure transfers stresses from particle contacts to the pore water

Courtesy of Professor T. L. Youd

Packing changes of particulate group during cyclic loading (after Youd 1977)

A. PARTICULATE GROUP CONTAINING LARGE HOLE — B. SMALL SHEAR STRAIN COLLAPSES HOLE — C. LARGE STRAIN CREATES SMALL HOLES (DILATION)

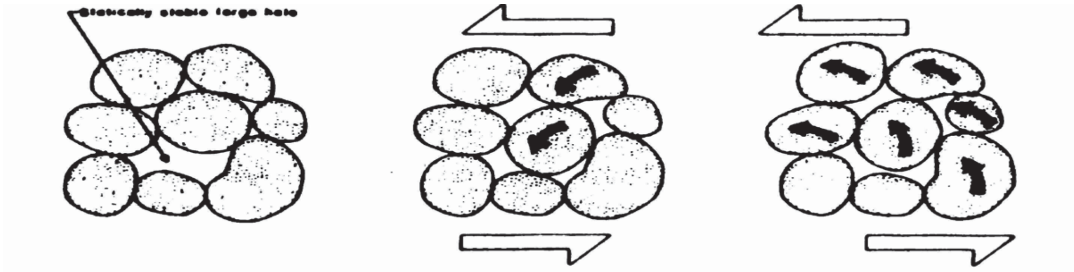

D. STRAIN REVERSAL COLLAPSES HOLES — E. LARGE STRAIN CREATES SMALL HOLES (DILATION) — F. AFTER A STRAIN CYCLE, VOLUME DECREASES

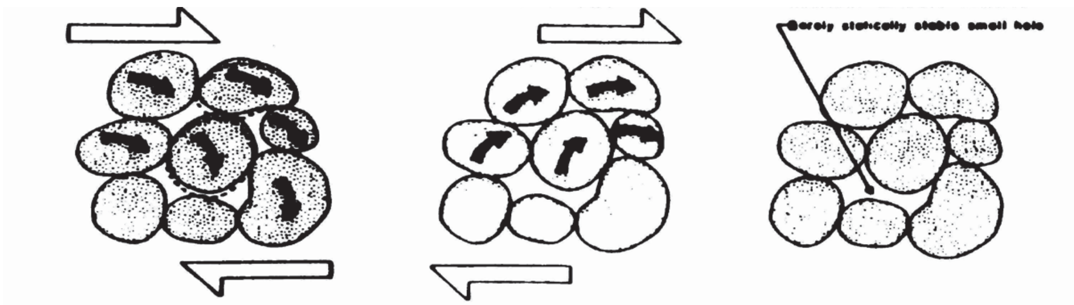

Mechanics of Liquefaction

- An increase of pore water pressure reduces intergranular or effective stress
- When the pore water pressure reaches a critical level, liquefaction occurs

Liquefaction

The transformation of a granular material from a solid state to a liquefied state as a consequence of increased pore water pressure and reduced effective stress.

» ASCE Comm. On Soil Dynamics, 1978

Courtesy of Professor T. L. Youd

Consequences of Liquefaction

- **Sand boils**
- Flow failure
- Lateral spread
- Ground oscillation
- Loss of bearing strength
- Ground settlement

Courtesy of Professor T. L. Youd

Adalier, K., Elgamal, A.W., 1992. Post-liquefaction behavior of soil systems. Technical Report. Dept. of Civil and Environ. Eng., Rensselaer Polytechnic Institute, Troy, NY. 203 pp.

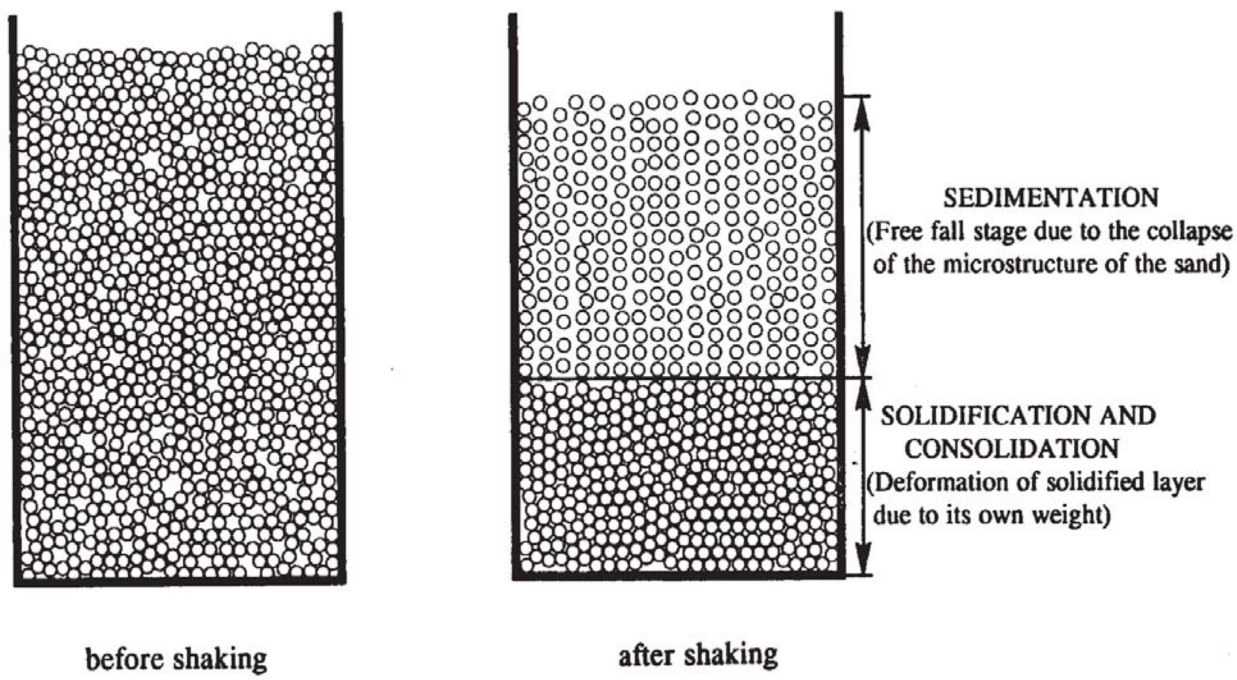

Sand boil generated by 1979 Imperial Valley, Calif. earthquake

Courtesy of Professor T. L. Youd

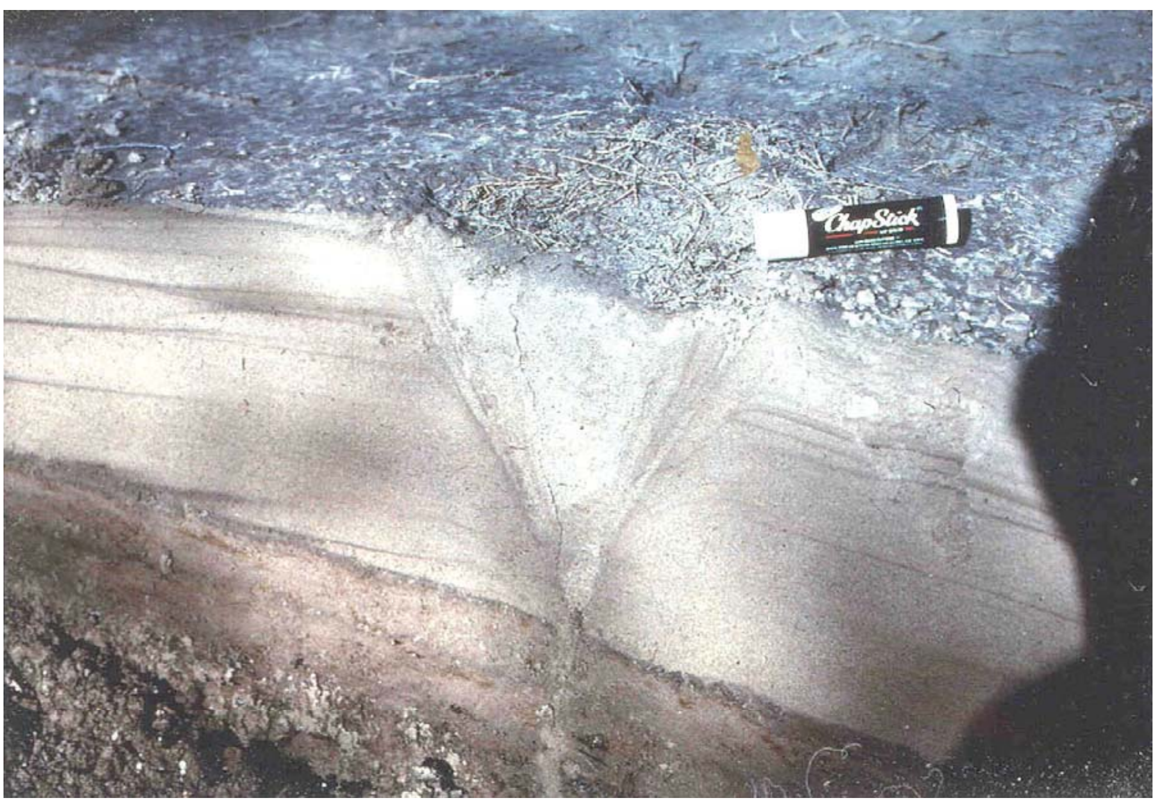

Cross section of sand boil generated by 1981 Westmorland, Calif. earthquake

Courtesy of Professor T. L. Youd

Sand Boil Erupted within House in Caucete during the 1977 San Juan, Argentina Earthquake

Courtesy of Professor T. L. Youd

Sand Boil Within House
Caucete, Argentina, 1977

- Total volume of sand and water =11.99 m^3
- Volume of sand and silt particles = 2.77 m^3
- Volume of water = 9.22 m^3
- Ratio of water to solids = 3.33:1

Courtesy of Professor T. L. Youd

Consequences of Liquefaction

- Sand boils
- **Flow failure**
- Lateral spread
- Ground oscillation
- Loss of bearing strength
- Ground settlement

Courtesy of Professor T. L. Youd

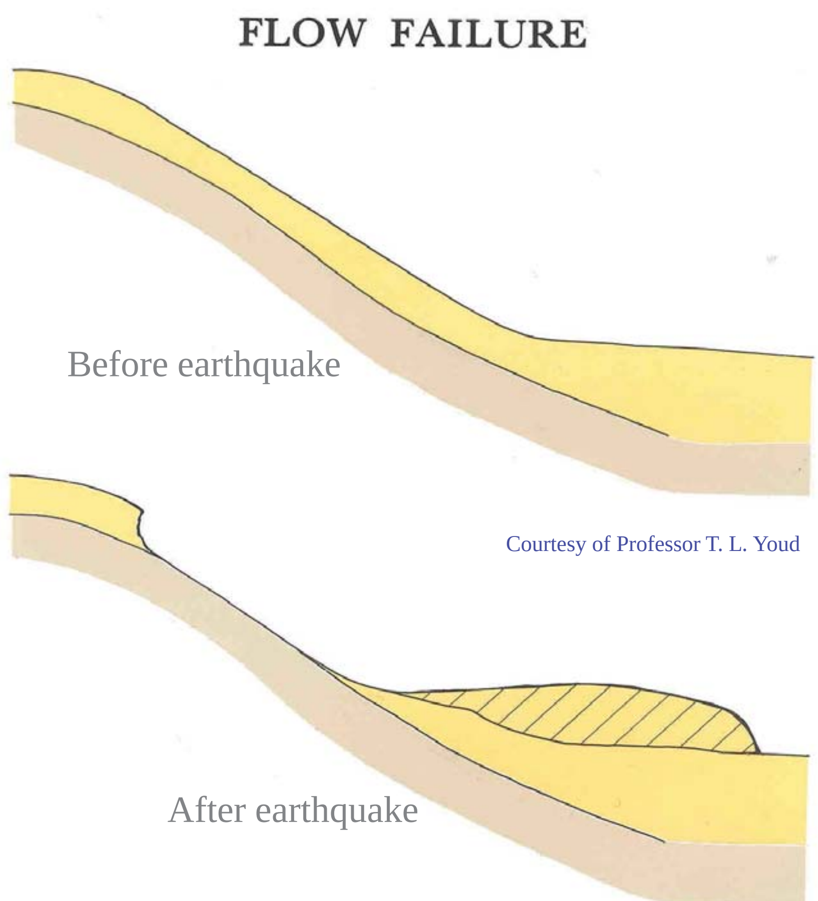

Flow landslide, Half Moon Bay, Calif., 1906 San Francisco Earthquake

Courtesy of Professor T. L. Youd

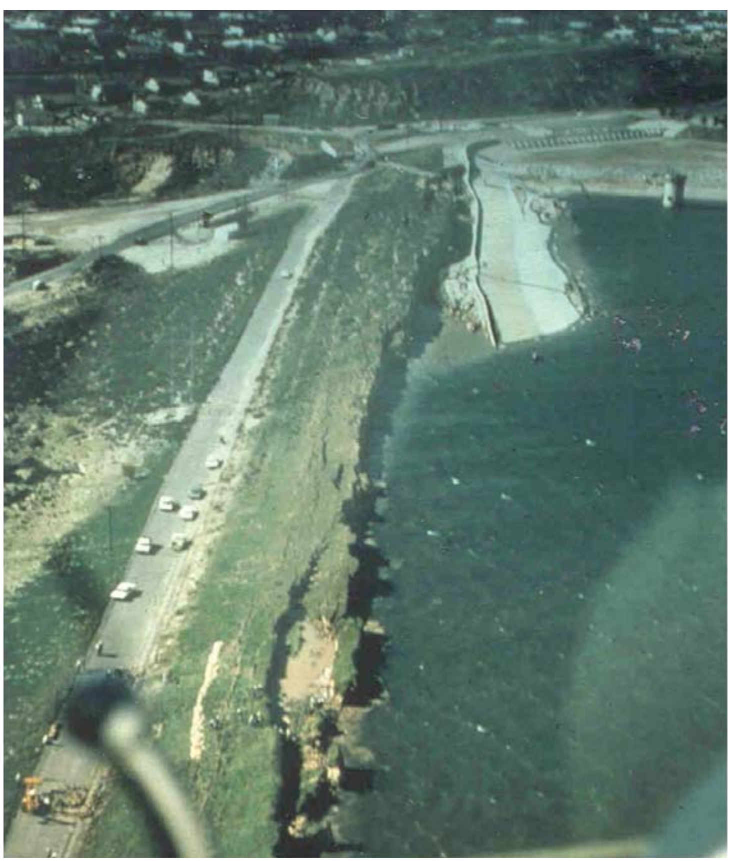

Crest and Upstream Embankment of Lower San Fernando Dam Slipped Upstream and into Reservoir Due to Liquefaction-Induced Flow Failure During 1971 San Fernando, California Earthquake

Courtesy of Professor T. L. Youd

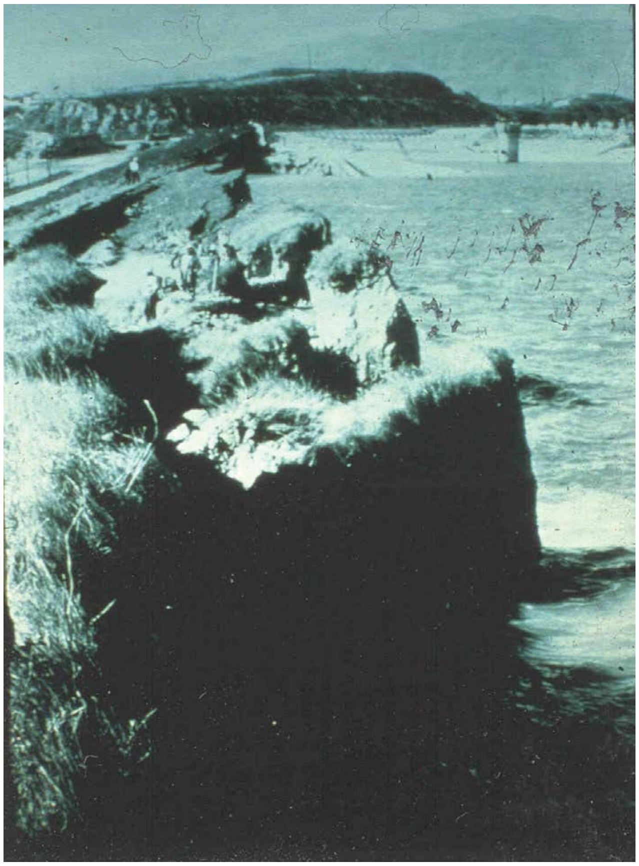

Crest and Upstream Embankment of Lower San Fernando Dam Slipped Upstream and into Reservoir Due to Liquefaction-Induced Flow Failure During 1971 San Fernando, California Earthquake

Courtesy of Professor T. L. Youd

View of Failed Lower San Fernando Dam after Draining of Reservoir

Courtesy of Professor T. L. Youd

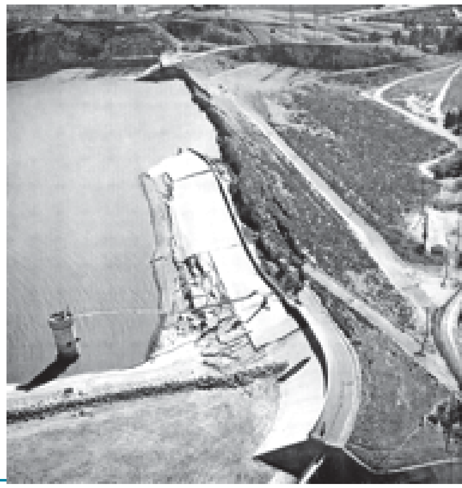

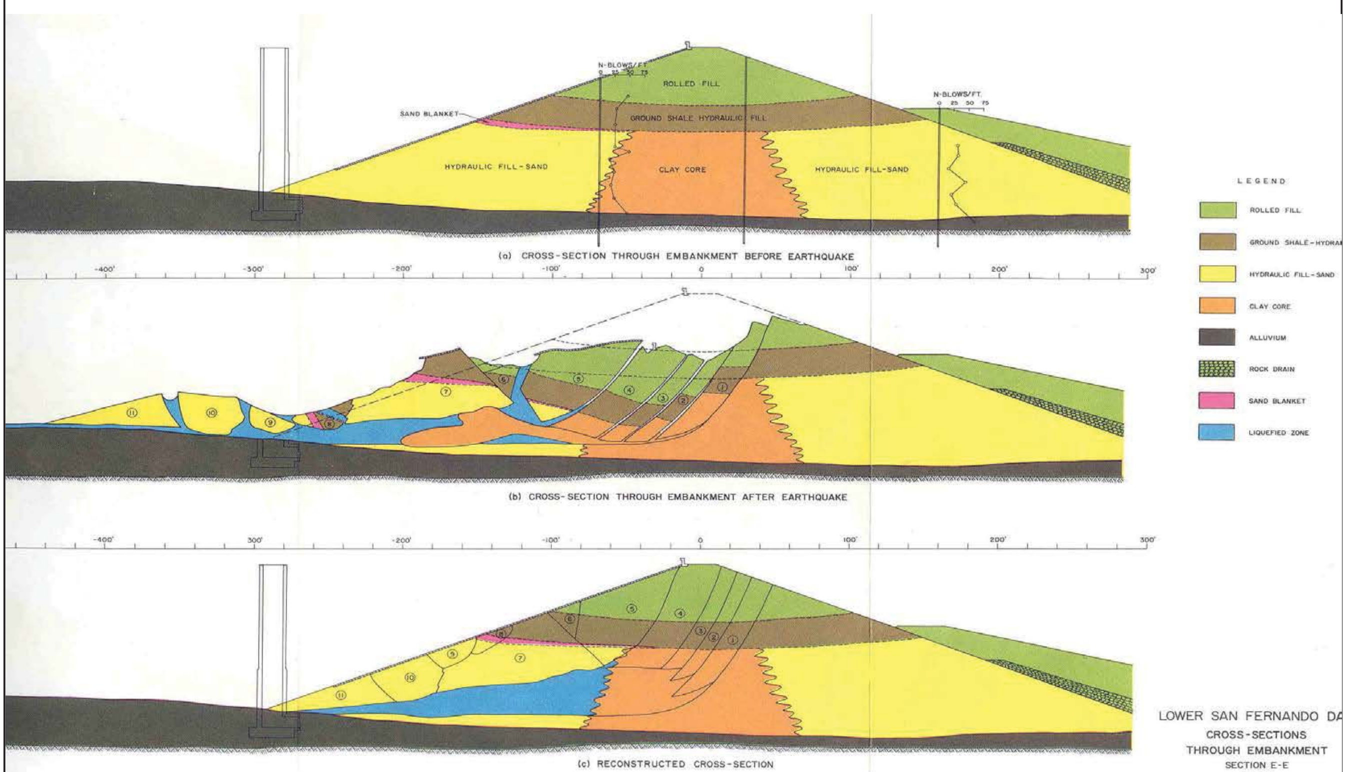

Lower San Fernando Dam Before and After Failure (Harry Seed)

Courtesy of Professor T. L. Youd

Consequences of Liquefaction

- Sand boils
- Flow failure
- **Lateral spread**
- Ground oscillation
- Loss of bearing strength
- Ground settlement

Courtesy of Professor T. L. Youd

LATERAL SPREAD

Before earthquake

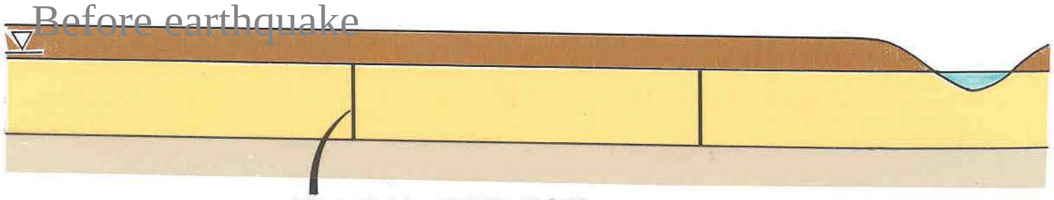

INITIAL SECTION

Courtesy of Professor T. L. Youd

After earthquake

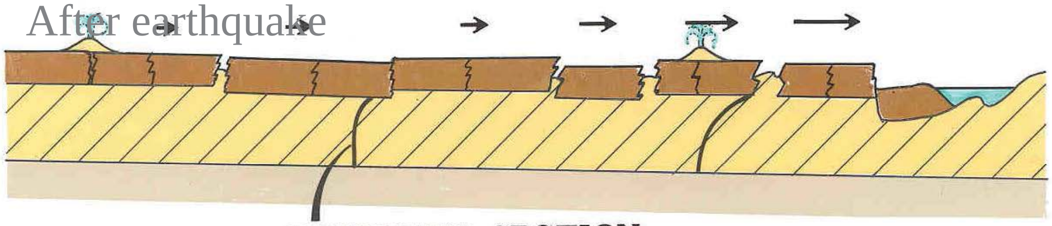

DEFORMED SECTION

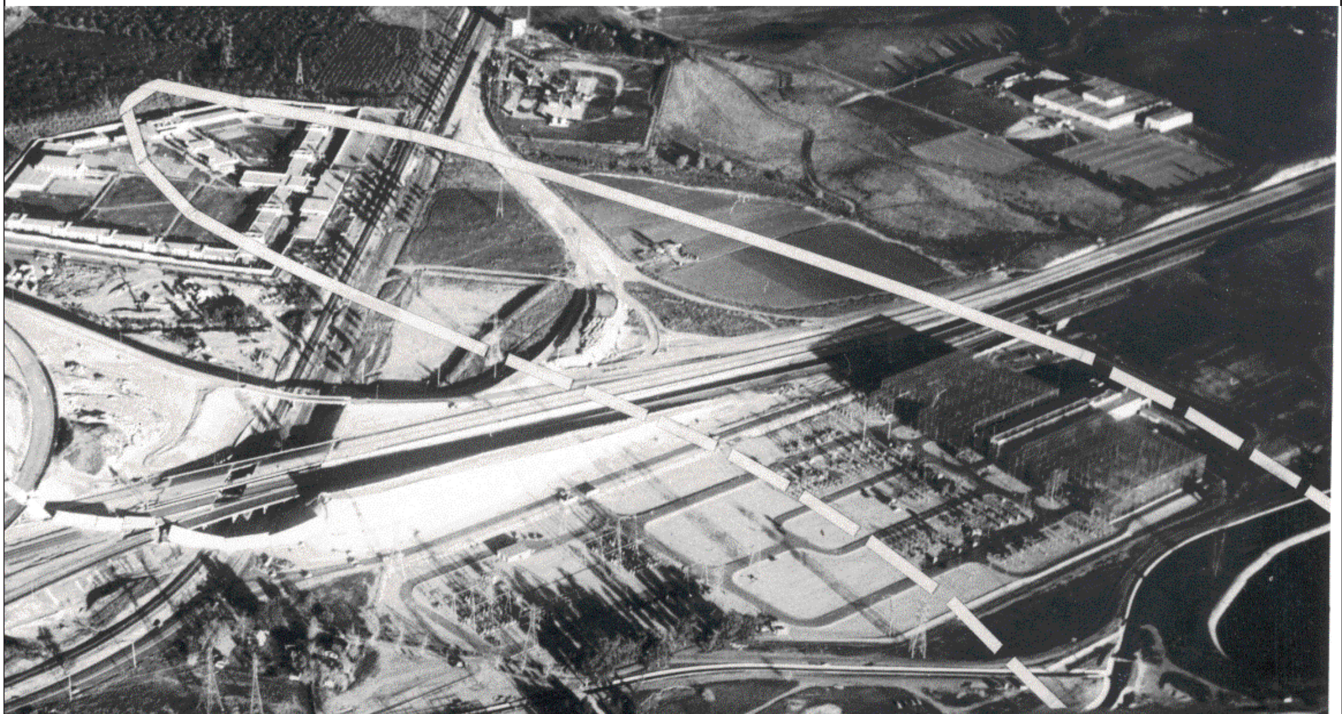

Aerial View of San Fernando Juvenile Hall Lateral Spread Area after 1971 San Fernando, Calif. Earthquake

Courtesy of Professor T. L. Youd

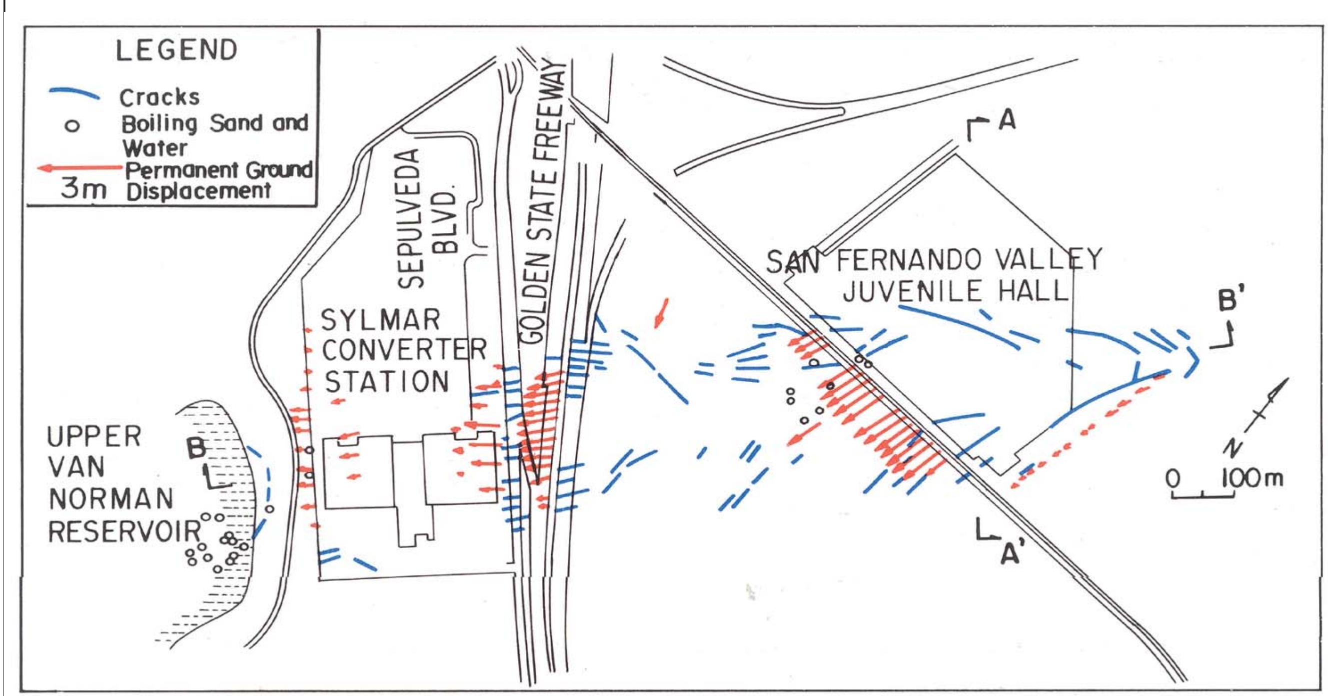

Fissures and Ground Displacements Generated by the San Fernando Juvenile Hall Lateral Spread; 1971 San Fernando, Calif. Earthquake

Courtesy of Professor T. L. Youd

San Fernando Valley Juvenile Hall Damaged by Lateral Spread During 1971 San Fernando, Calif. Earthquake

Courtesy of Professor T. L. Youd

San Fernando Valley Juvenile Hall Damaged by Lateral Spread During 1971 San Fernando, Calif. Earthquake

Courtesy of Professor T. L. Youd

San Fernando Valley Juvenile Hall Damaged by Lateral Spread During the 1971 San Fernando, Calif. Earthquake

Courtesy of Professor T. L. Youd

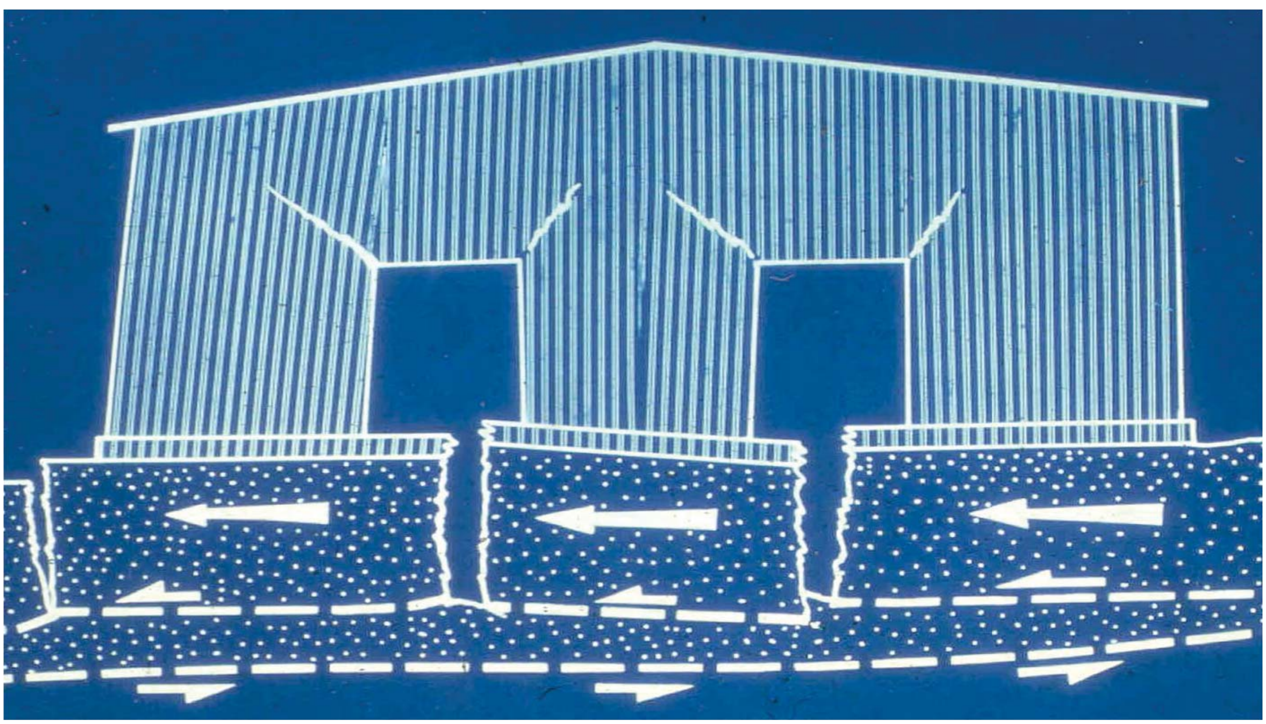

Diagrammatic View of Building Damage Caused by San Fernando Valley Juvenile Hall Lateral Spread

Courtesy of Professor T. L. Youd

Wall around San Fernando Valley Juvenile Hall Was Pulled Apart by Lateral Spread during 1971 Earthquake

Courtesy of Professor T. L. Youd

Craters and Flooding Due to Pipeline Breaks, San Fernando Juvenile Hall Lateral Spread

Courtesy of Professor T. L. Youd

Water Pipeline Break Caused by Displ. of San FernandoValley Juvenile Hall Lateral Spread

Courtesy of Professor T. L. Youd

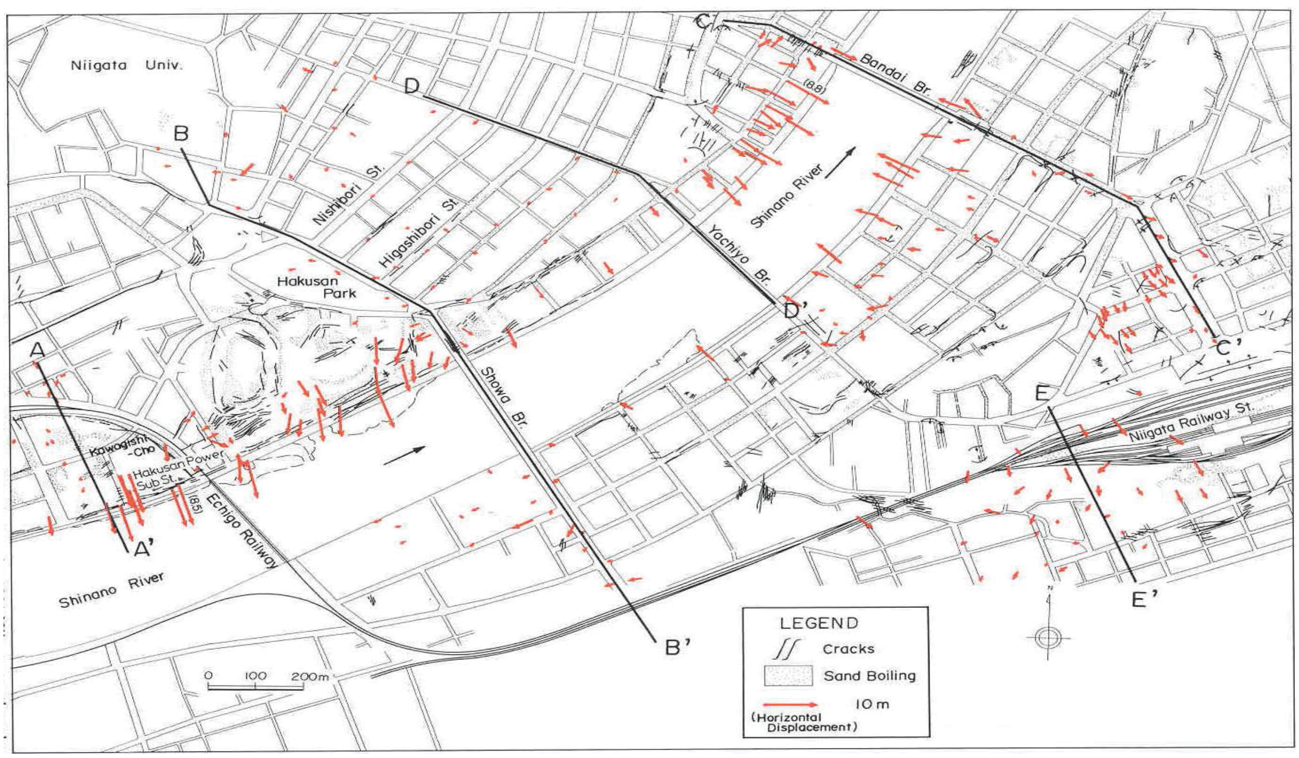

Vectors of Lateral Spread Displacement, 1964 Niigata, Japan Earthquake

Courtesy of Professor T. L. Youd

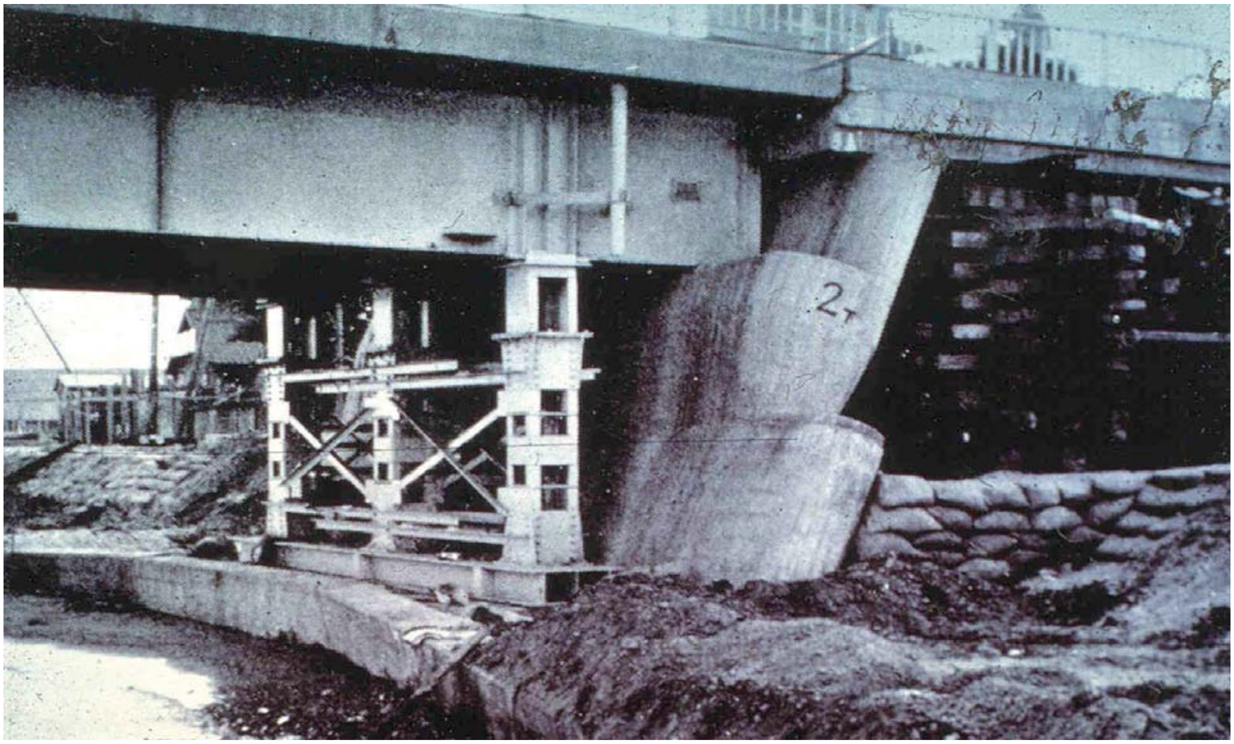

Bridge Pier Displaced Toward Shinano River During 1964 Niigata, Japan Earthquake

Courtesy of Professor T. L. Youd

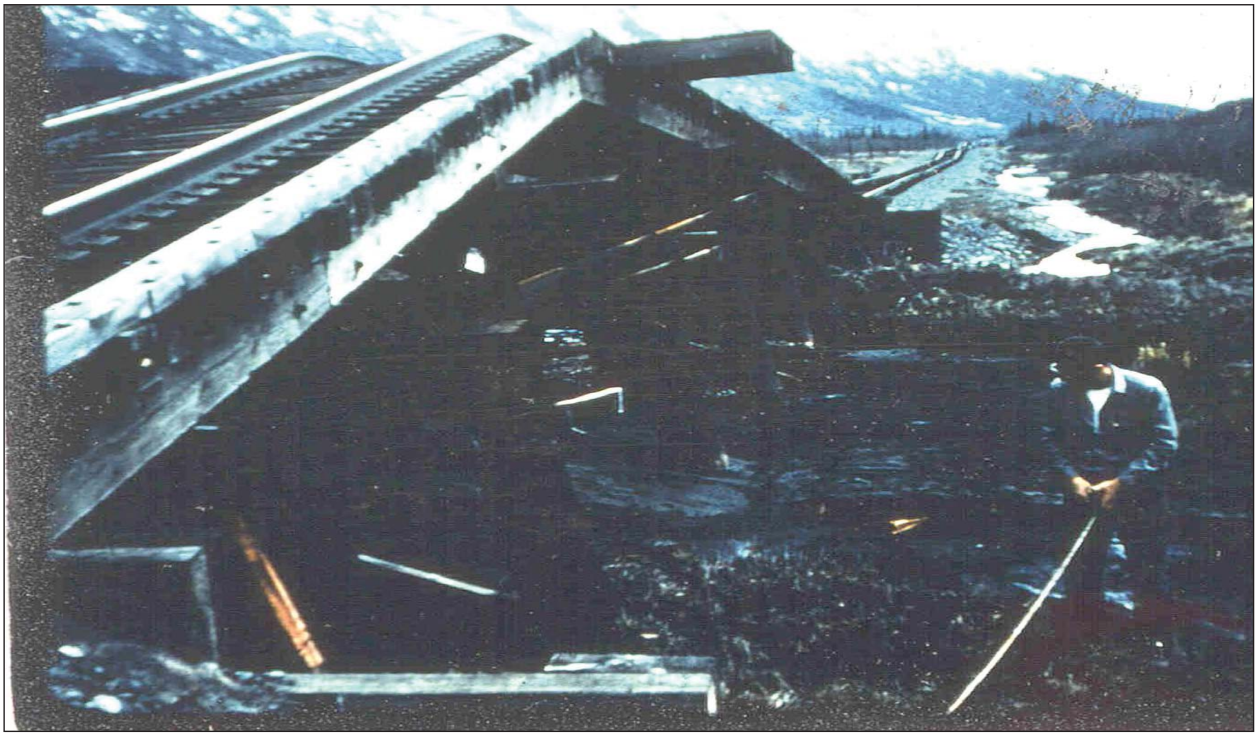

Buckled Railroad Bridge Caused by Lateral Spread During the 1964 Alaska Earthquake

Courtesy of Professor T. L. Youd

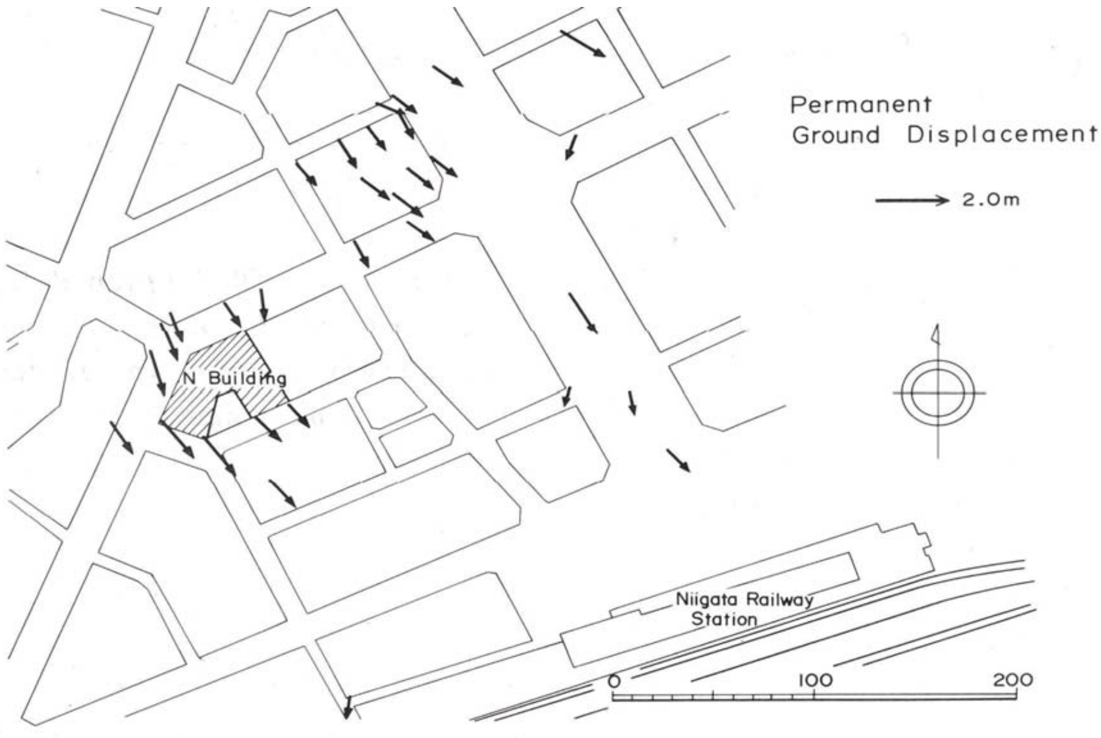

Measured Lateral Spread Displacement around N Building following the 1964 Niigata, Japan Earthquake

Courtesy of Professor T. L. Youd

Fractured Piles Beneath Building Caused by Lateral Spread (1964 Niigata, Japan Earthquake)

Courtesy of Professor T. L. Youd

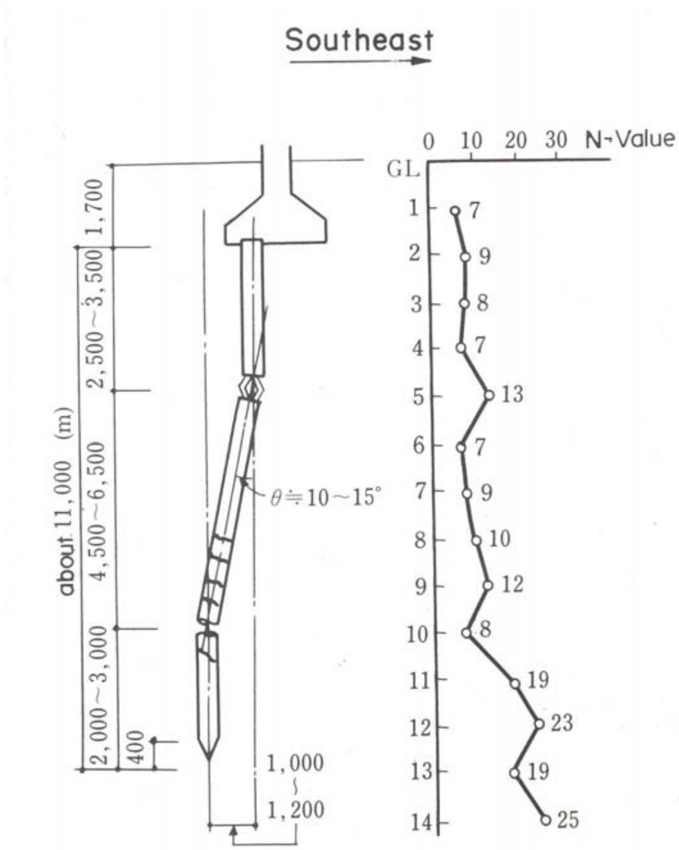

Diagrams of Post Earthquake Pile Configuration and Standard Penetration Resistance versus Depth in Sandy Soil

Courtesy of Professor T. L. Youd

Lateral Spread Pervasively Displaced Quay Walls Seaward Around perimeters of Port and Rokko Islands Decimating Port Facilities

Courtesy of Professor T. L. Youd

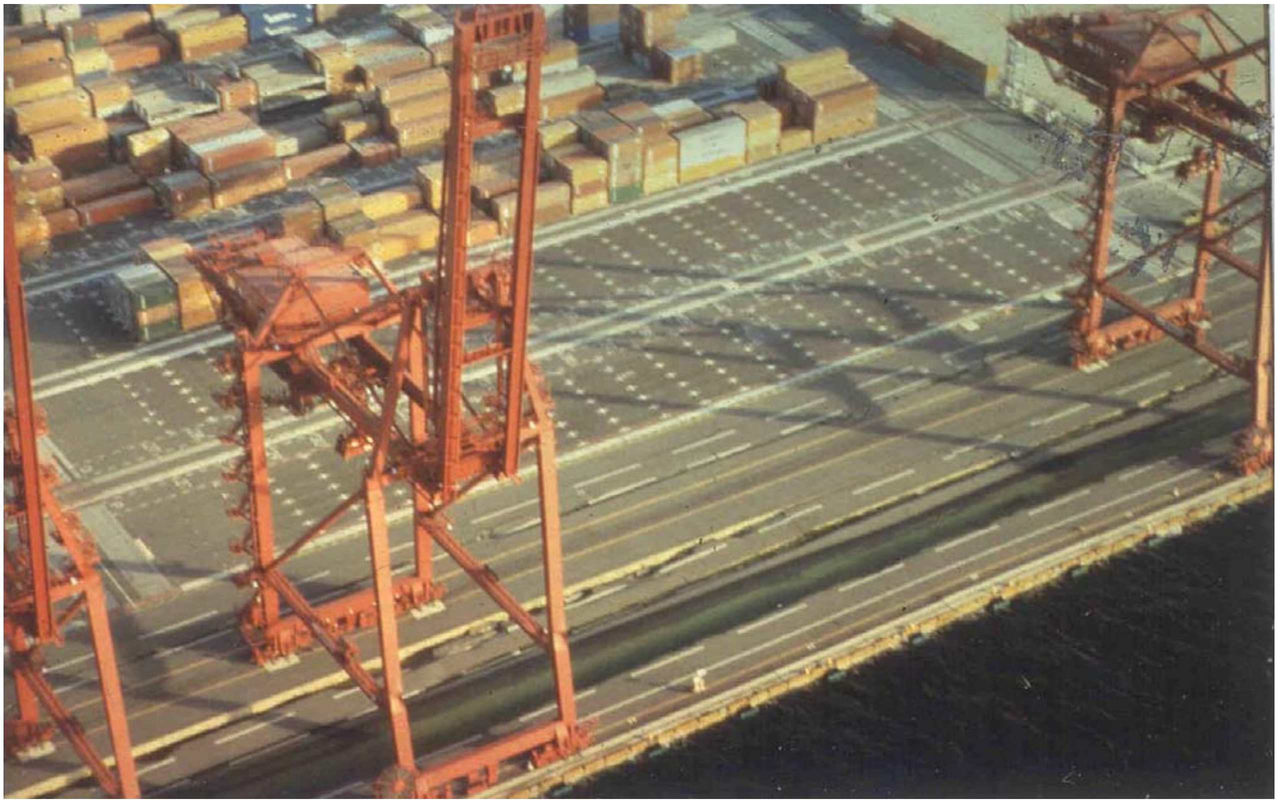

Crane Legs Pulled Apart and Buckled by Lateral Spread Displacement

Courtesy of Professor T. L. Youd

Consequences of Liquefaction

- Sand boils
- Flow failure
- Lateral spread
- **Ground oscillation**
- Loss of bearing strength
- Ground settlement

Courtesy of Professor T. L. Youd

GROUND OSCILLATION

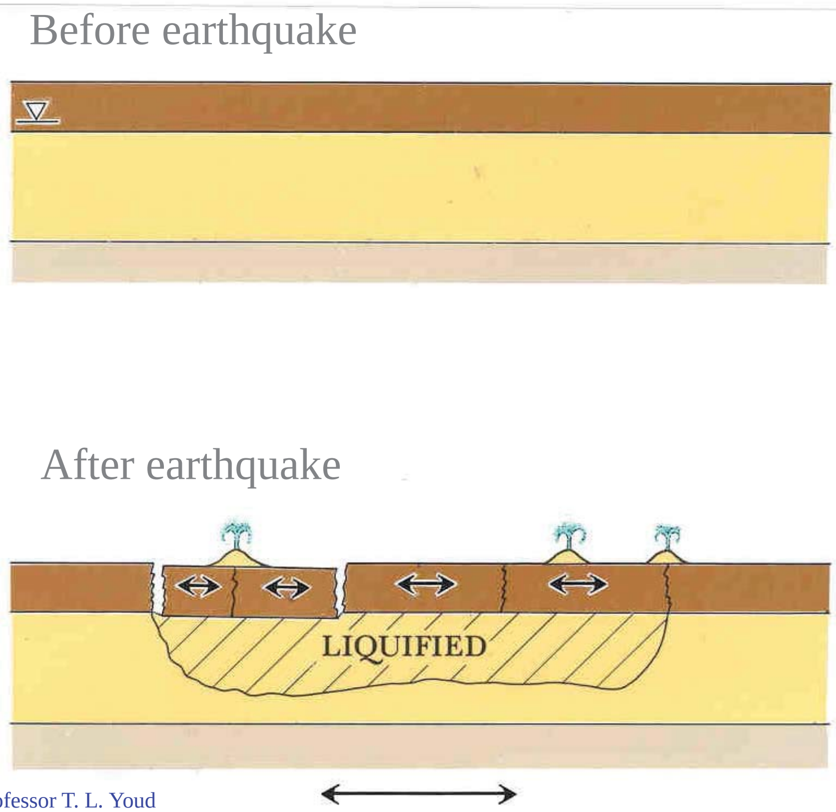

Courtesy of Professor T. L. Youd

Walk and Curb Damage Caused by Ground Oscillation (1989 Loma Prieta, Calif. Earthquake)

Courtesy of Professor T. L. Youd

Pavement and Curb Damage Caused by Ground Oscillation during 1989 Loma Prieta, Calif. Earthquake

Courtesy of Professor T. L. Youd

Consequences of Liquefaction

- Sand boils
- Flow failure
- Lateral spread
- Ground oscillation
- **Loss of bearing strength**
- Ground settlement

Courtesy of Professor T. L. Youd

LOSS OF BEARING STRENGTH

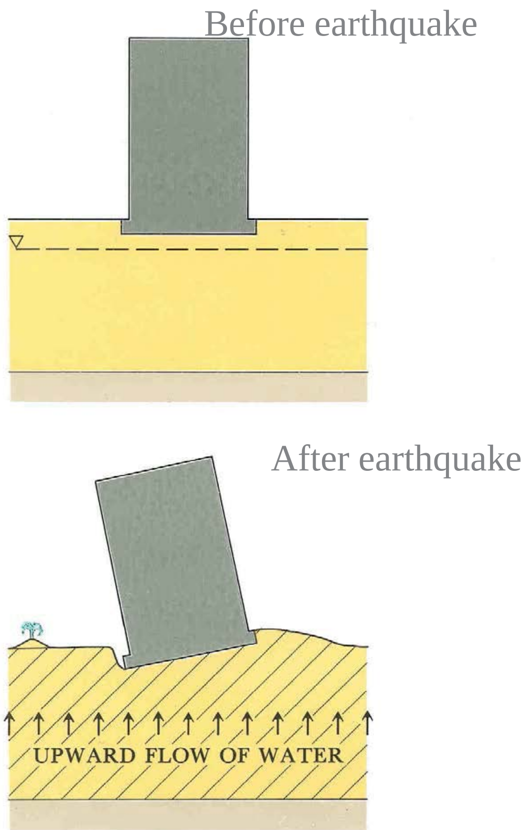

Courtesy of Professor T. L. Youd

Tipped Buildings Caused by Liquefaction-Induced Loss of Bearing Strength,1964 Niigata, Japan Earthquake

Courtesy of Professor T. L. Youd

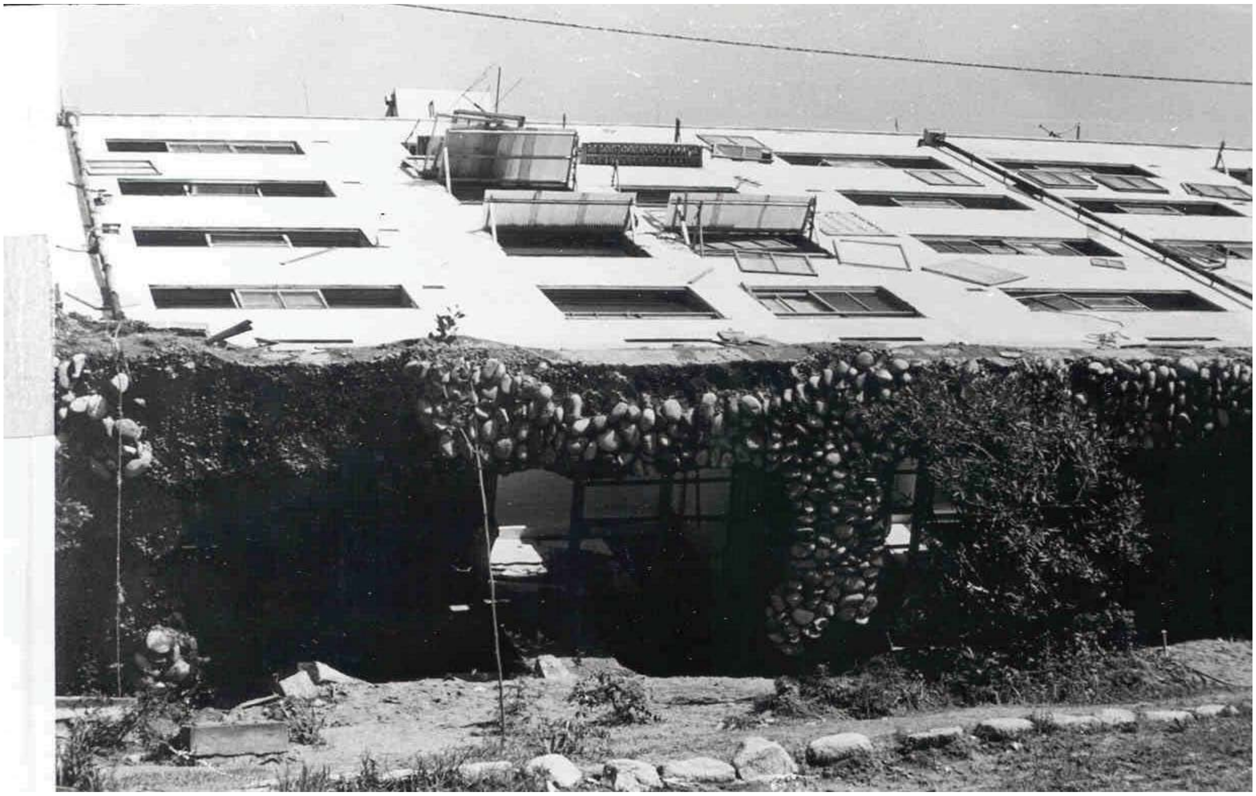

Tipped Buildings Caused by Liquefaction-Induced Loss of Bearing Strength, 1964 Niigata, Japan Earthquake

Courtesy of Professor T. L. Youd

Tipped Buildings Caused by Liquefaction-Induced Loss of Bearing Strength,1964 Niigata, Japan Earthquake

Courtesy of Professor T. L. Youd

Tipped Building in Adapazari, Turkey Caused by Liquefaction-Induced Loss of Bearing Strength during 1999 Koaceli, Turkey Earthquake

Courtesy of Professor T. L. Youd

Building Settlement in Adapazari, Turkey Caused by Liquefaction-Induced Loss of Bearing Strength during 1999 Koaceli, Turkey Earthquake

Courtesy of Professor T. L. Youd

Oil Tank that Buoyantly Floated to Ground Surface through Liquefied Soil during 1983 Hokkaido-Nansei-Oki, Japan Earthquake

Courtesy of Professor T. L. Youd

Consequences of Liquefaction

- Sand boils
- Flow failure
- Lateral spread
- Ground oscillation
- Loss of bearing strength
- **Ground settlement**

Courtesy of Professor T. L. Youd

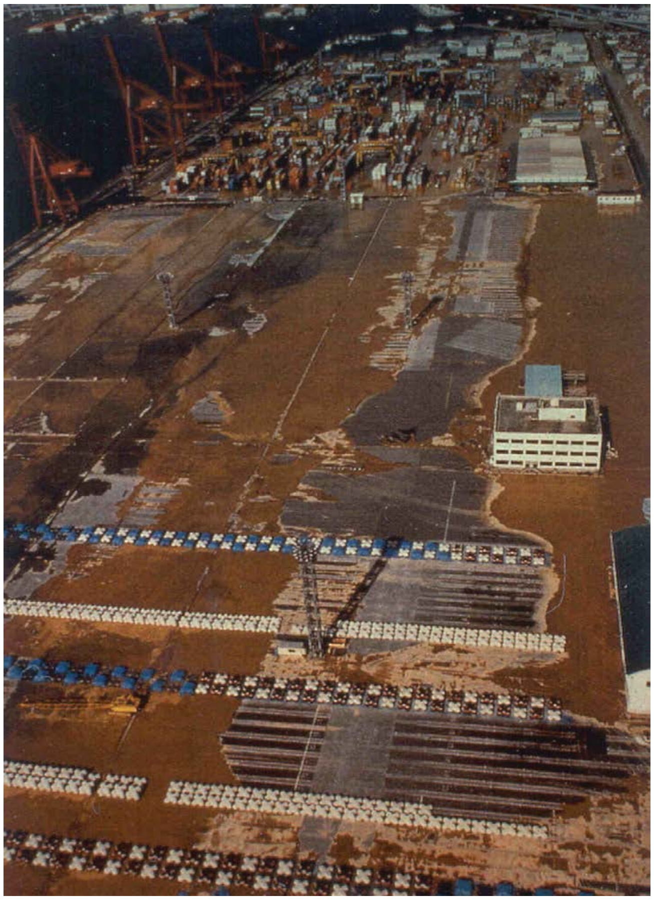

Water and Sand (brown areas) from Sand Boils that Erupted on Rokko Island during 1995 Kobe, Japan Earthquake; the Ground Surface also Subsided 0.5 m to 0.7m

Courtesy of Professor T. L. Youd

Differential Settlement Between Column on Piles and Surrounding Ground on Rokko Island; Settlement due to Liquefaction and Compaction of 12 m of Artificial Fill during 1995 Kobe, Japan Earthquake

Courtesy of Professor T. L. Youd

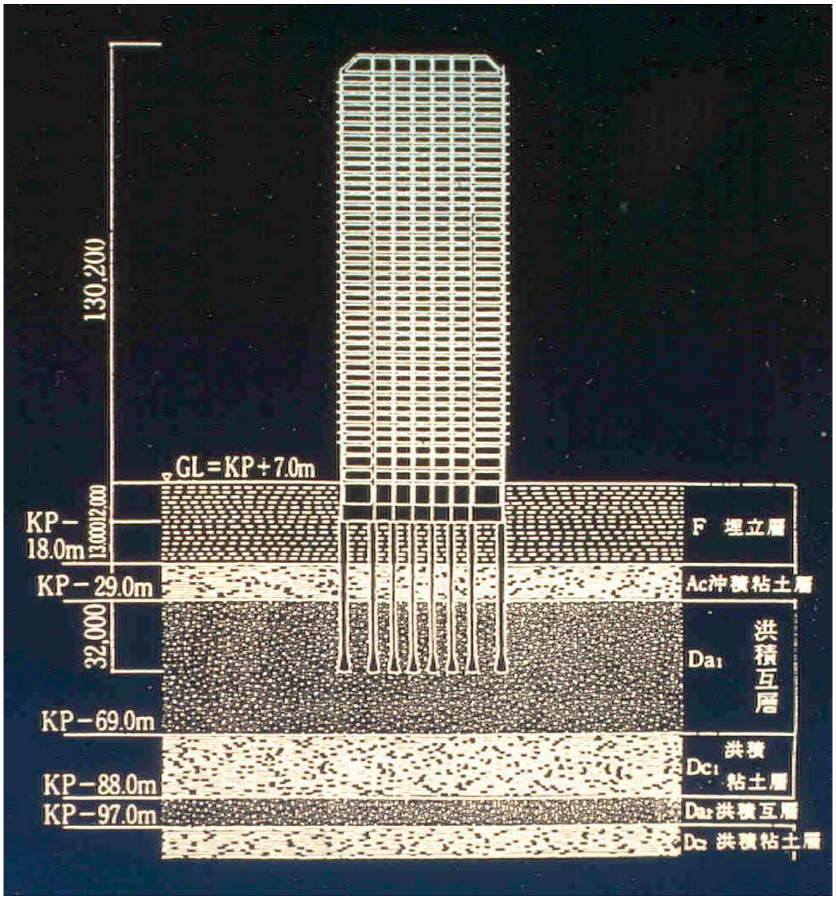

Cross Section Showing Soil Profile and Typical Pile Foundation Configuration for Buildings on Port and Rokko Islands that Were Shaken by the 1995 Kobe, Japan Earthquake

Courtesy of Professor T. L. Youd

Differential Settlement Between Building on Piles and Natural Ground Caused by Liquefaction and Compaction of Artificial Fill during the 1995 Kobe, Japan Earthquake

Courtesy of Professor T. L. Youd

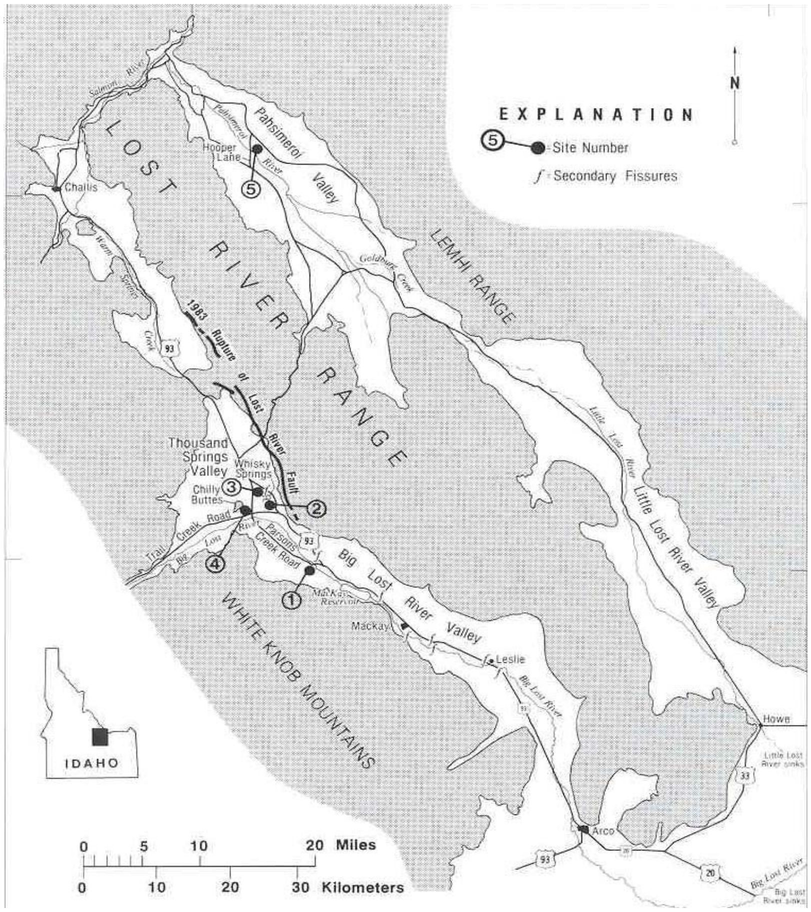

Localities in Idaho Where Liquefaction Occurred During the 1983 Borah Peak Earthquake

Courtesy of Professor T. L. Youd

Whiskey Springs Lateral Spread Generated by the 1983 Borah Peak Earthquake Displaced Highway 93 1 m toward Camera

Courtesy of Professor T. L. Youd

Segment of Highway 93 Displaced 1 m to Left by Whiskey Springs Lateral Spread; 1983 Borah Peak, Idaho Earthquake

Courtesy of Professor T. L. Youd

Buckled Sod at Toe of Whiskey Springs Lateral Spread

Courtesy of Professor T. L. Youd

Buckled Sod at Toe of Whiskey Springs Lateral Spread

Courtesy of Professor T. L. Youd

Sand Boil Deposit and House on Pence Ranch Affected by Liquefaction During 1983 Borah Peak, Idaho Earthquake

Courtesy of Professor T. L. Youd

View of Back of House on Pence Ranch Showing Wall Pulled Away from Foundation because of Lateral Spread; 1983 Borah Peak, Idaho Earthquake

Courtesy of Professor T. L. Youd

Water Tank on Right Buoyantly Rose Due Liquefaction of Subsurface Soils at Pence Ranch; 1983 Borah Peak Earthquake

Courtesy of Professor T. L. Youd

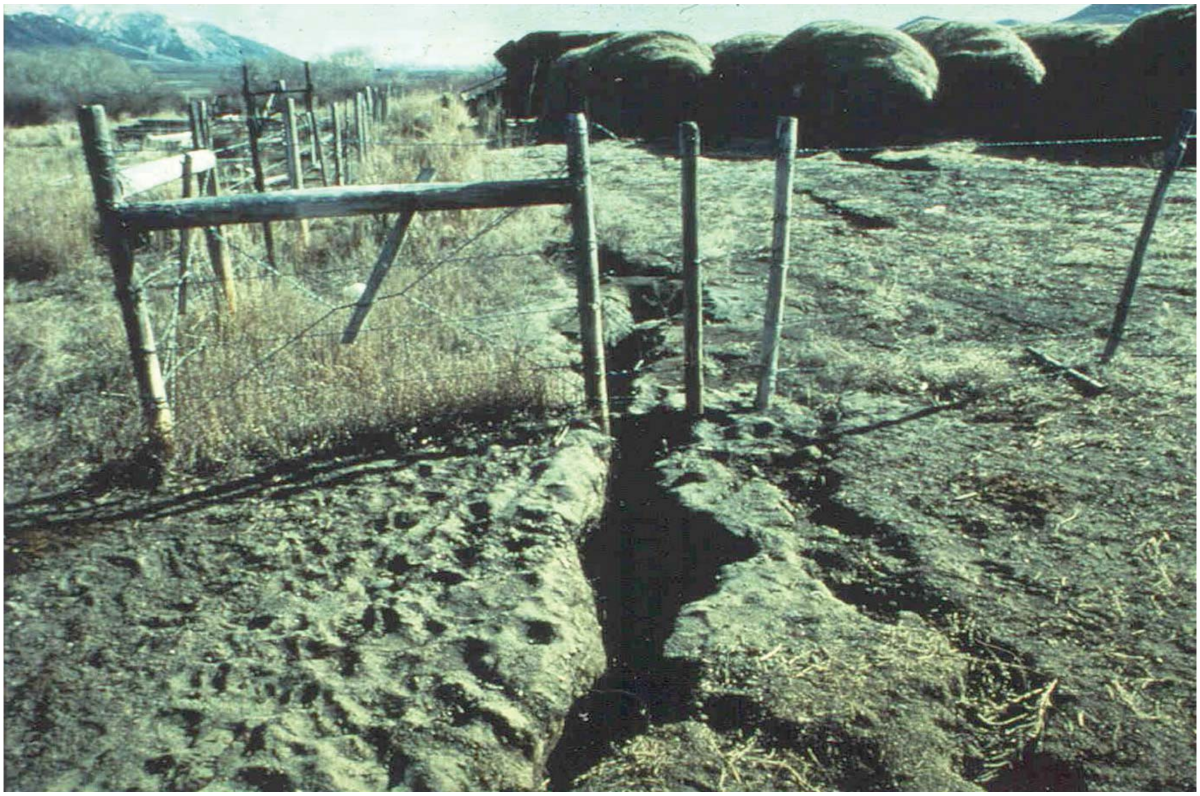

Fence on Pence Ranch Pulled Apart by 0.45 m Due to Lateral Spread During 1983 Borah Peak, Idaho Earthquake

Courtesy of Professor T. L. Youd

Gravel Sample Taken from Layer that Liquefied beneath Pence Ranch

Courtesy of Professor T. L. Youd

Sand Boil That Erupted In Pahsimeroi Valley During 1983 Borah Peak Earthquake

Courtesy of Professor T. L. Youd

Site Liquefaction

Stress-Strain Response
Stress-Strain Models
Site Response
Lateral Deformation

Nonlinear soil response

(Shear stress τ and shear strain γ)

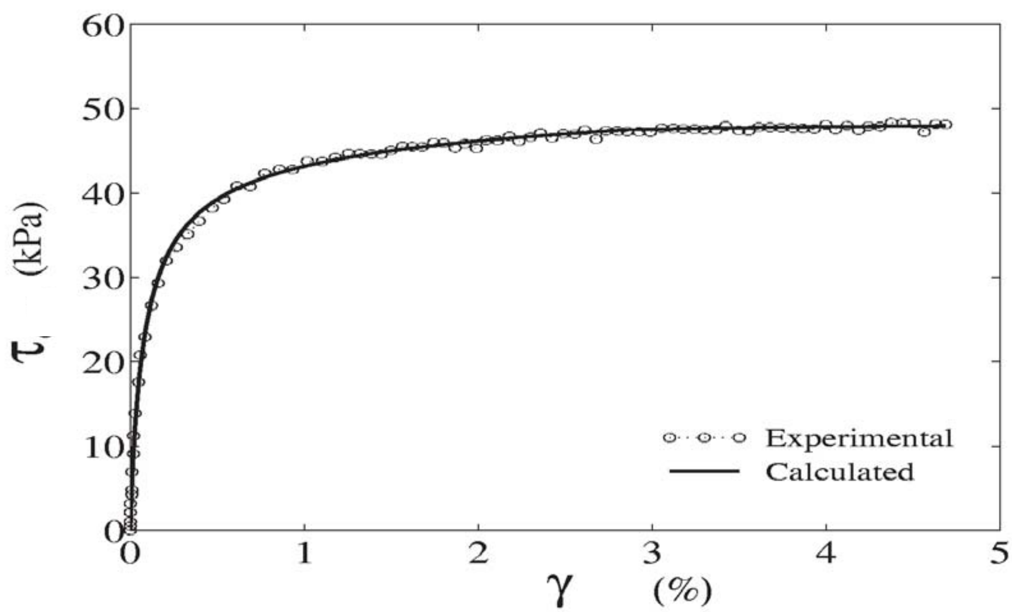

The above nonlinear shear stress-strain relationship is sometimes called the *backbone* shear stress-strain relationship.

Among the typical equations used to represent this backbone behavior is the *Hyperbolic relationship*

$\tau = G \gamma / (1 + \gamma/\gamma_r)$

where G = Low strain shear modulus (G_{max})

and γ_r is a constant that is used to match the observed level of nonlinear response.

This relationship reaches a maximum shear stress τ_{max} of $G\gamma_r$ at infinite shear strain. As such, it is common to cap this relationship at a value of $R\tau_{max}$ where R is generally in the range of 0.8 or higher.

Cyclic Stress-strain response

Hysteresis response is commonly observed, with *Masing-type* behavior often adopted to reproduce hysteretic damping. This damping mechanism is strain-level dependent and frequency-independent, both being desirable features that mimic data from experimentation.

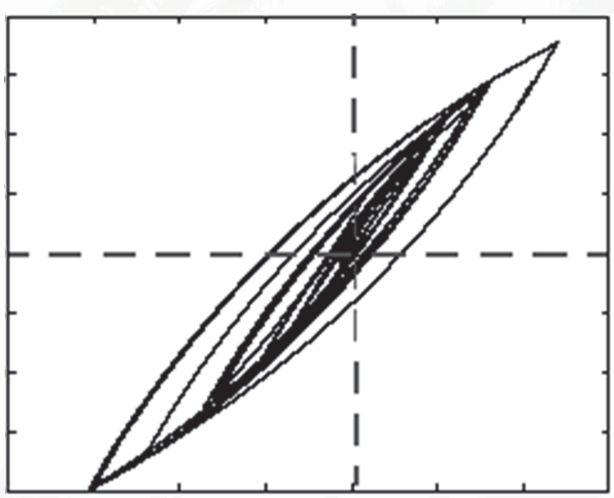

Confinement dependence

Shear stiffness and strength may or may not be significantly dependent on confinement.

If behavior is not confinement dependent, a *cohesion* intercept (c) describes shear strength, and

$R\tau_{max}$ is then equated to this value of cohesion (c)

If behavior is confinement dependent, then the shear strength

$R\tau_{max} = c + p' \sin\phi$ where ϕ is the friction angle and p' is confinement described by (for level ground scenarios)

$p' = (\sigma'_v + \sigma'_h)/2$

where σ'_v is *vertical effective stress* and σ'_h is horizontal effective stress ($\sigma'_v = \sigma_v - u$, with u = hydrostatic water pressure)

Shear-volume strain coupling (for confinement dependent soils with c=0)

During small-strain cyclic loading, upon shearing a loose (high void ratio) soil, volume gradually decreases.

If the soil is saturated with water, and the rate of loading is rapid (i.e., preventing water from exiting the soil skeleton), this tendency for volume decrease translates into the soil particles partially floating in the water, which then carries this additional soil granules weight (in the limit, this is termed "*undrained behavior*").

The fraction of soil self weight carried by the water becomes "*excess pore-water pressure*" known as u_e gradually reducing the effective confinement p' (and therefore the shear strength). If u_e reaches σ'_v, no effective confinement remains and the soil is "Liquefied" or reaches "Liquefaction" (at which point, $r_u = 1$, where r_u is known as the *excess pore-pressure ratio* $= u_e / \sigma'_v$).

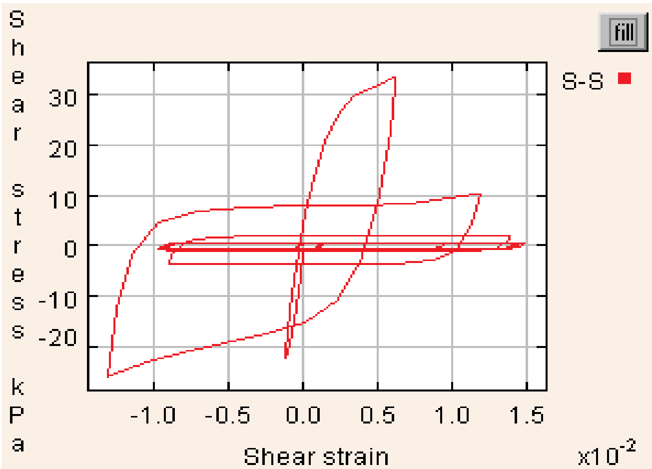

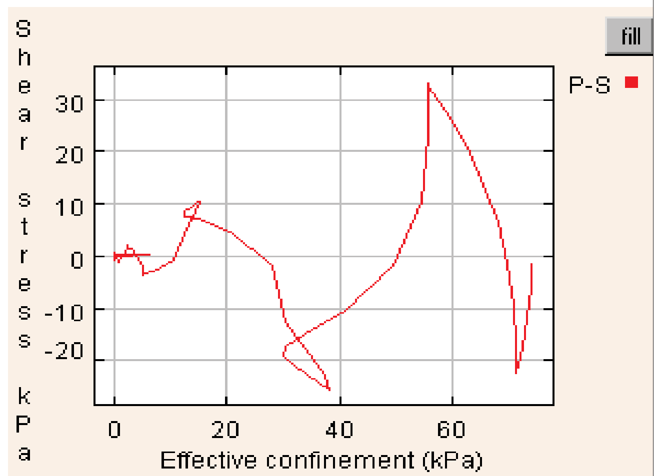

Shear-volume strain coupling (for confinement dependent soils with c=0), .. continued

If the applied cyclic strains are large enough, then the cyclic volume decrease at lower strains turns into a volume increase at larger strains. For the undrained scenario, this becomes a tendency for volume decrease (u_e buildup) followed by a tendency for volume increase (which momentarily reduces u_e). Examples of this behavior are presented below

Note: If the rate of loading is slow enough to permit some level of water exiting the soil skeleton, this allows excess pore-pressure to dissipate and the pore-pressure goes back towards the original hydrostatic value, thus allowing confinement to stay close to its original value. This will tend to occur for higher permeability sands/gravels that are capable of fast/very-fast excess pore-pressure dissipation.

Cyclic Torsional Tests (after Ishihara 1985)

Medium Fuji river sand (Dr=47%)

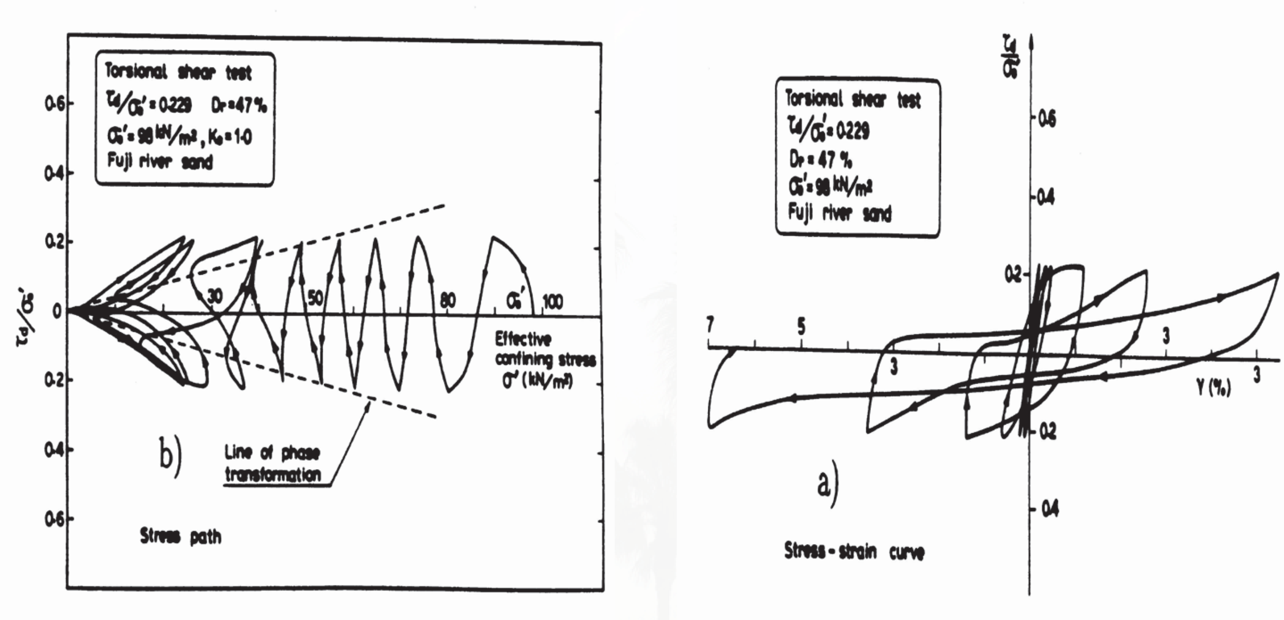

Cyclic Torsional Tests (after Ishihara 1985)

Dense Fuji river sand (Dr=75%)

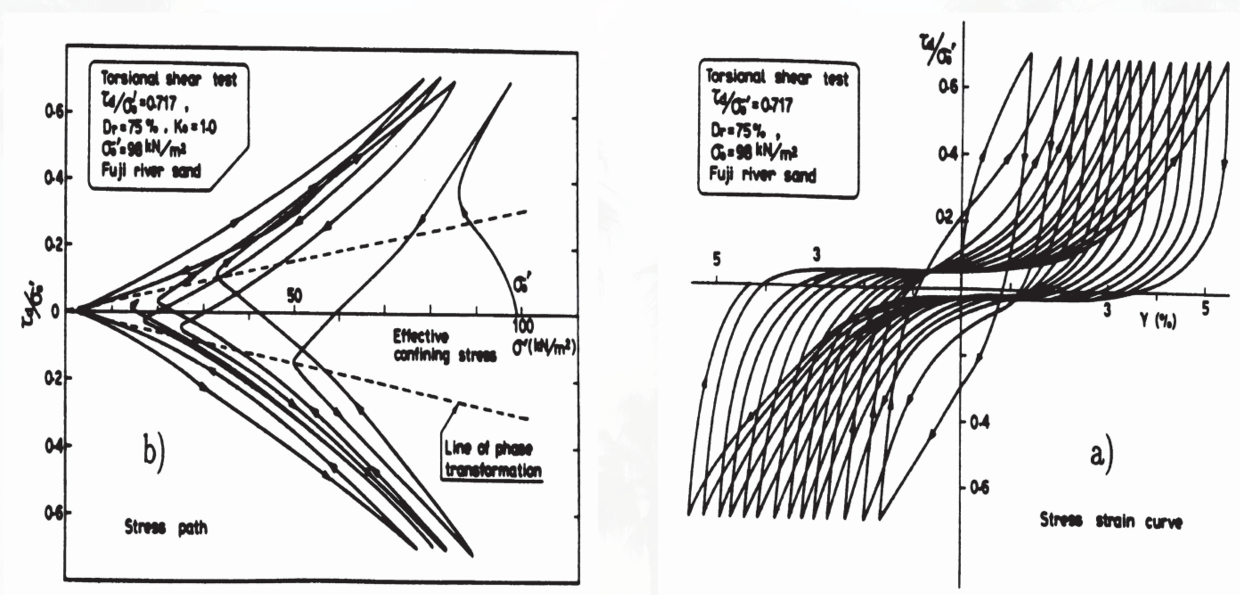

Back-calculated soil response at Wildlife site during 1987 Superstition Hills earthquake (Zeghal and Elgamal 1994)

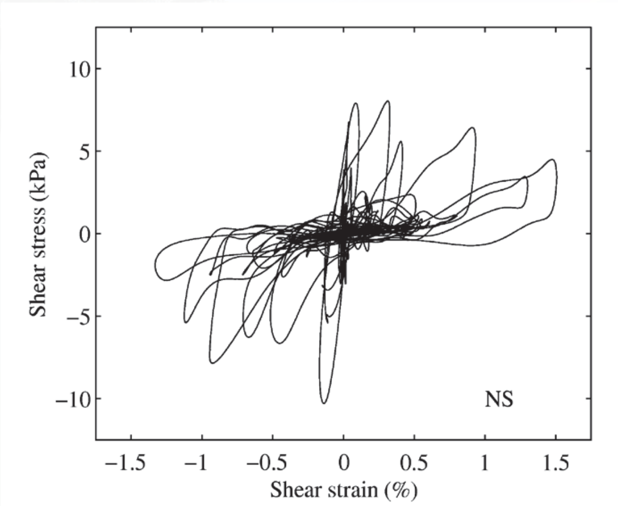

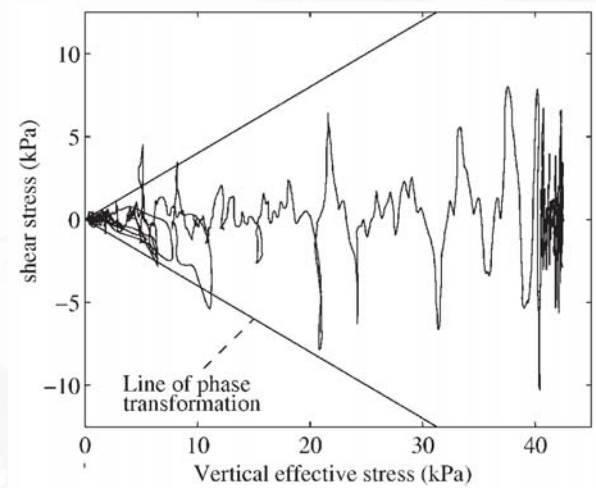

Shear stress - shear strain

Effective stress path

Mildly sloping ground and accumulation of lateral deformations

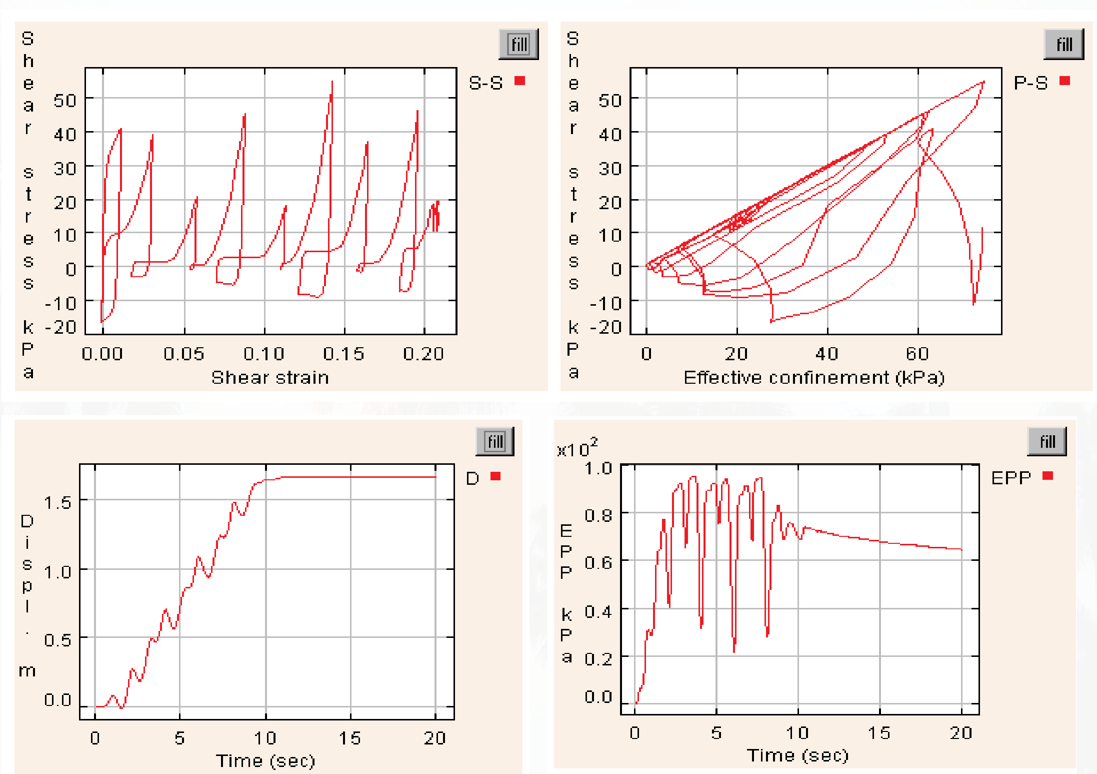

Elements of liquefaction stress-strain model

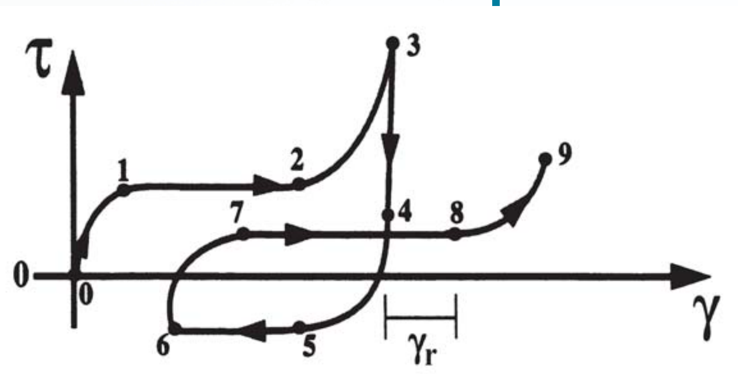

Parra 1996, Yang 2000

Shear Stress-Strain

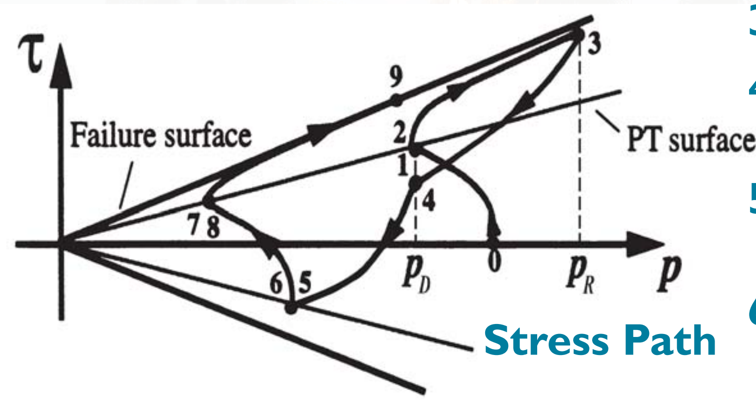

Stress Path

Stage:

0 - 1: Contractive phase

1 - 2: Perfectly plastic phase

2 - 3: Dilative phase

3 - 4: Unloading phase

4 - 5: Contractive phase (opposite)

5 - 6: Perfectly plastic phase (opposite)

6 - 9: Logic of 0 - 3

Simulation of a stress-controlled cyclic simple shear test

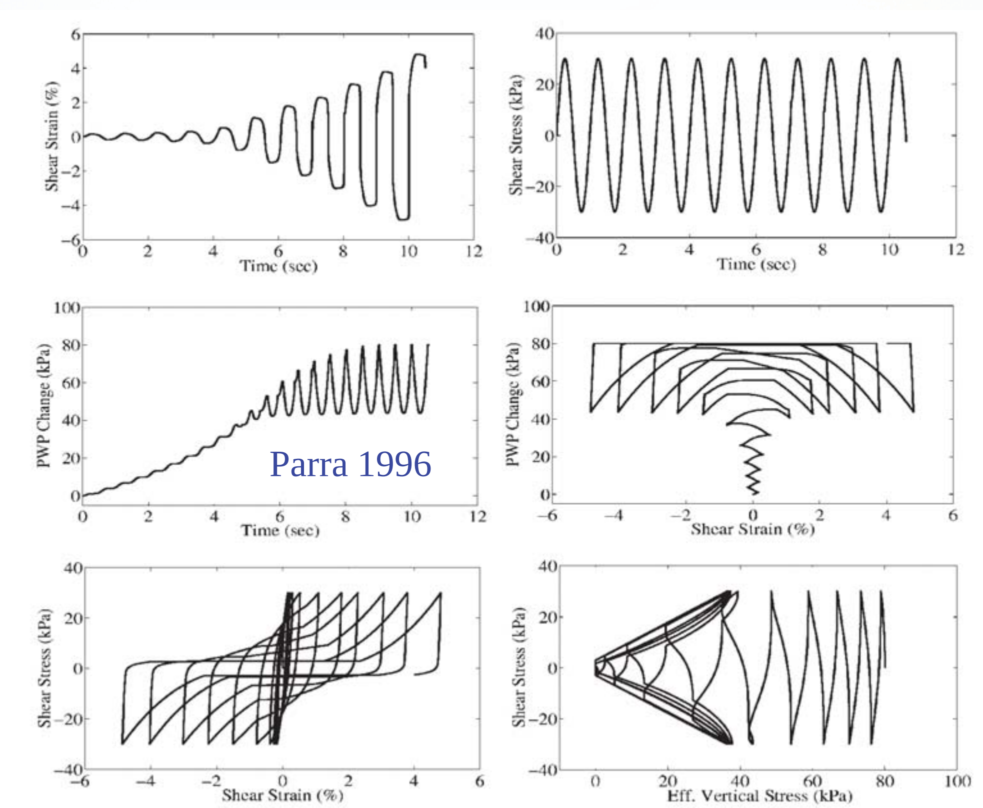

Simulation of a strain-controlled cyclic simple shear test

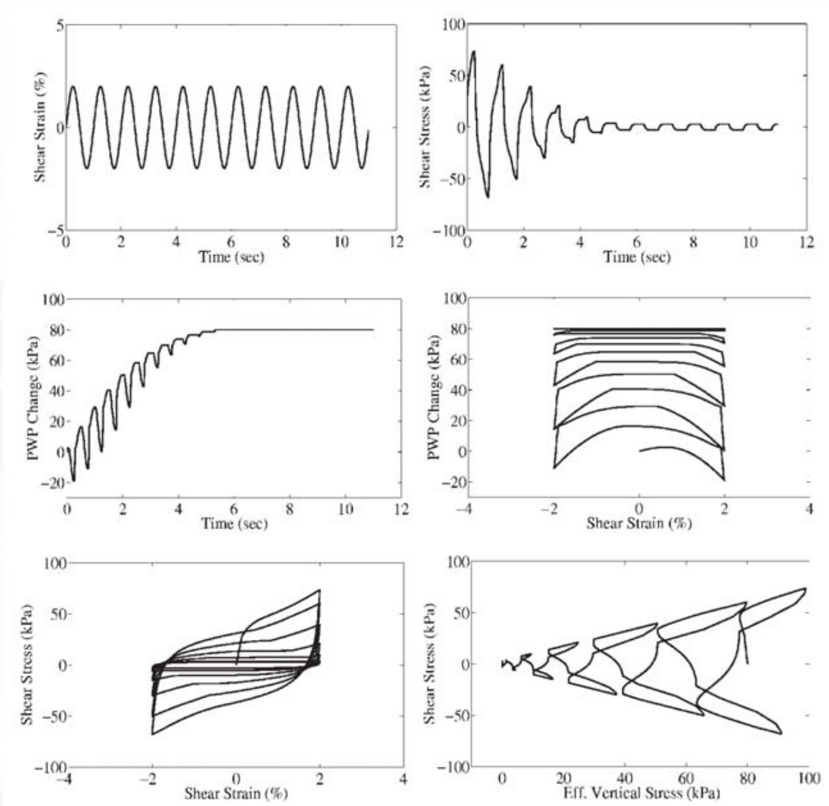

Parra 1996

Simulation of a stress-controlled cyclic triaxial test with an imposed static driving shear stress

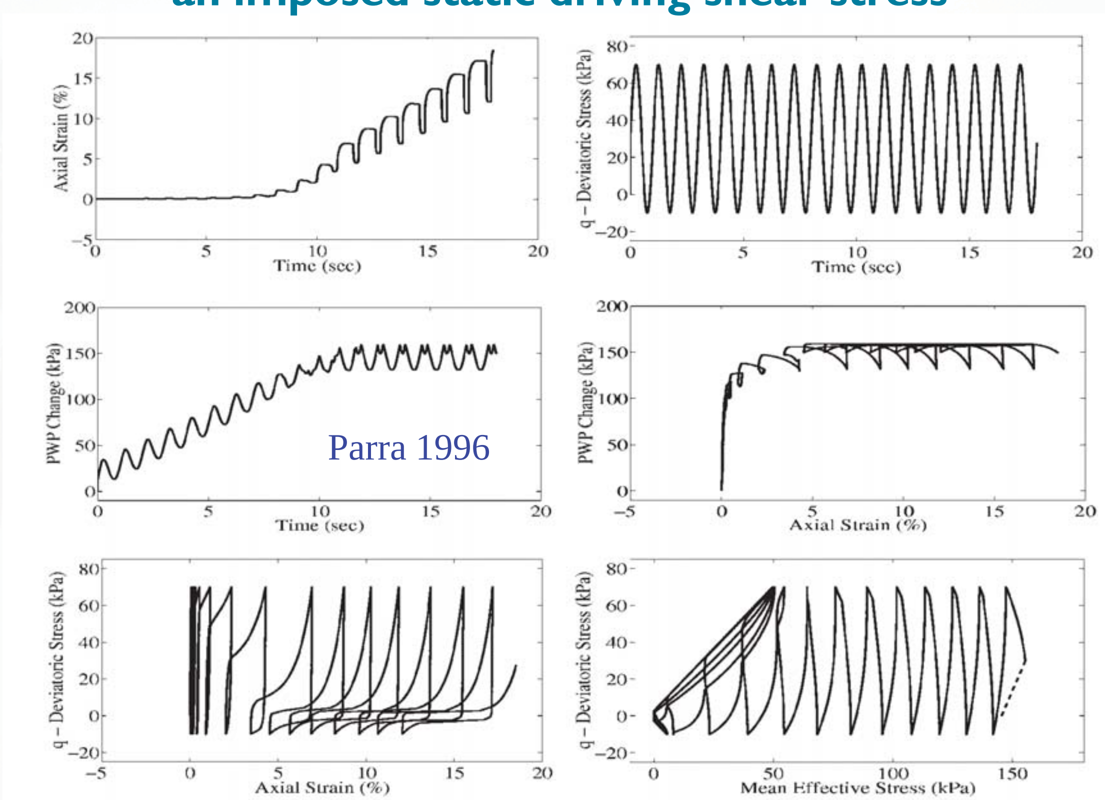

Model response under cyclic loading for different soil types

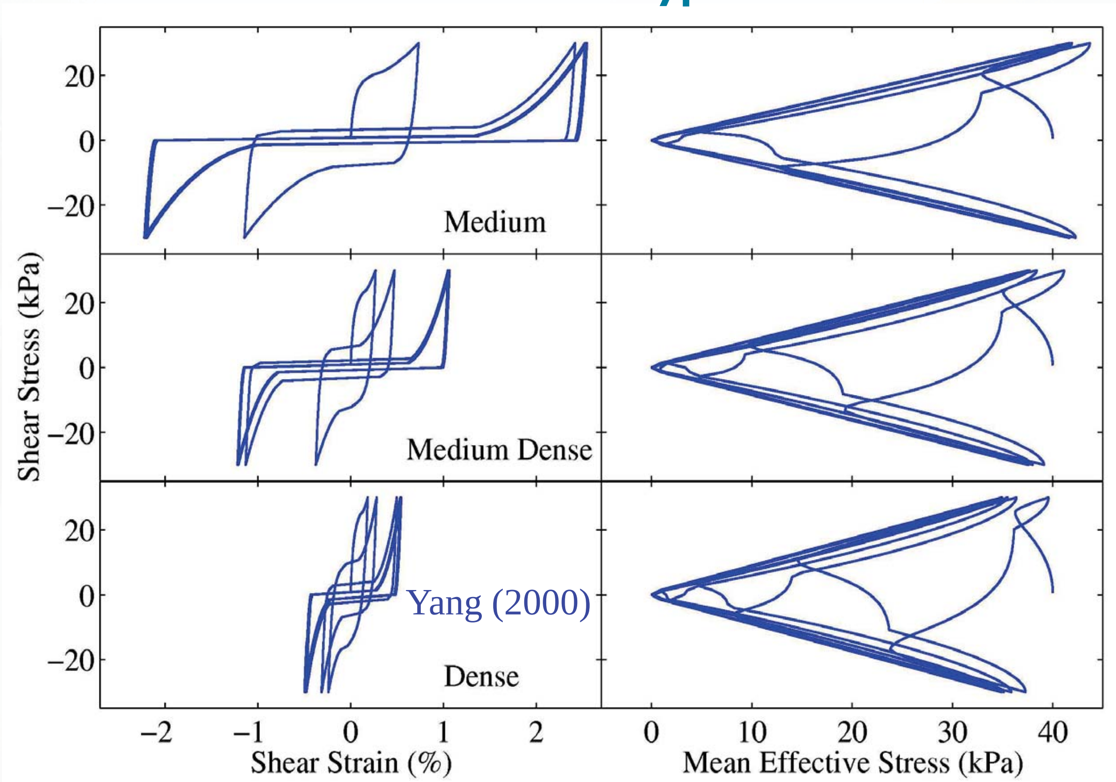

Model response under cyclic loading with a driving shear stress imposed for different soil types

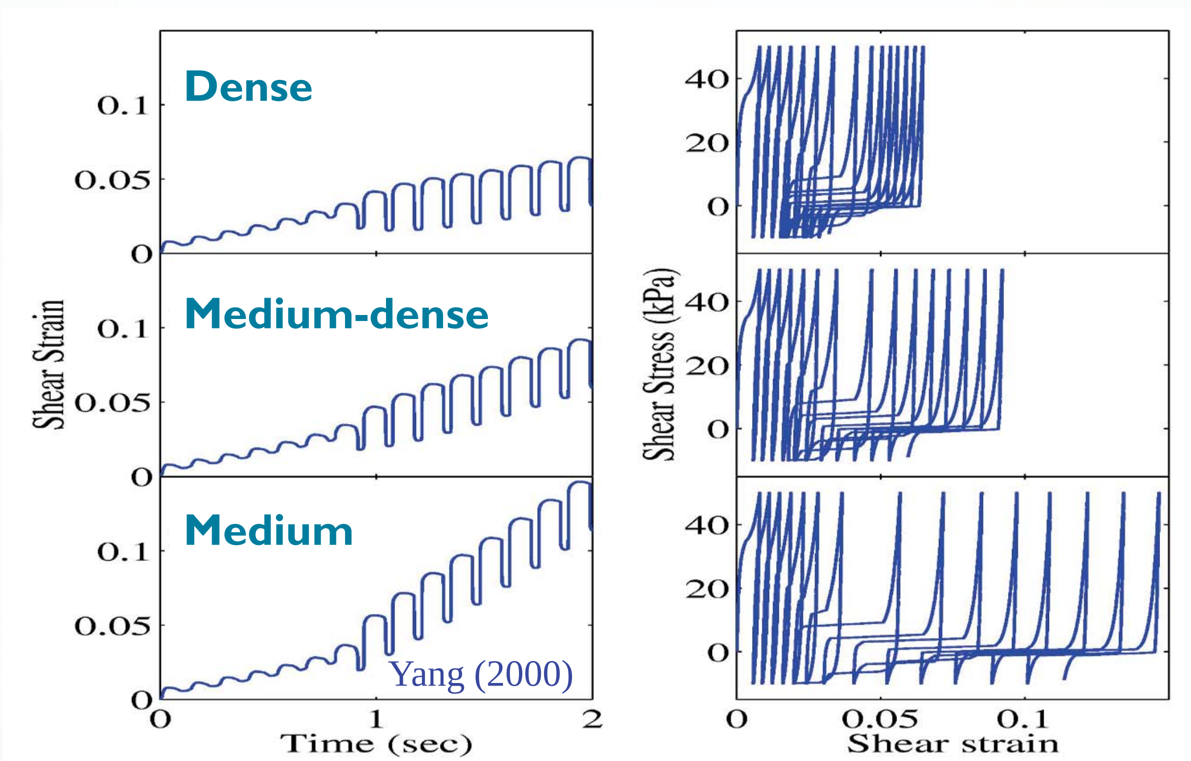

Suggested Cyclic Strain Levels During Liquefaction

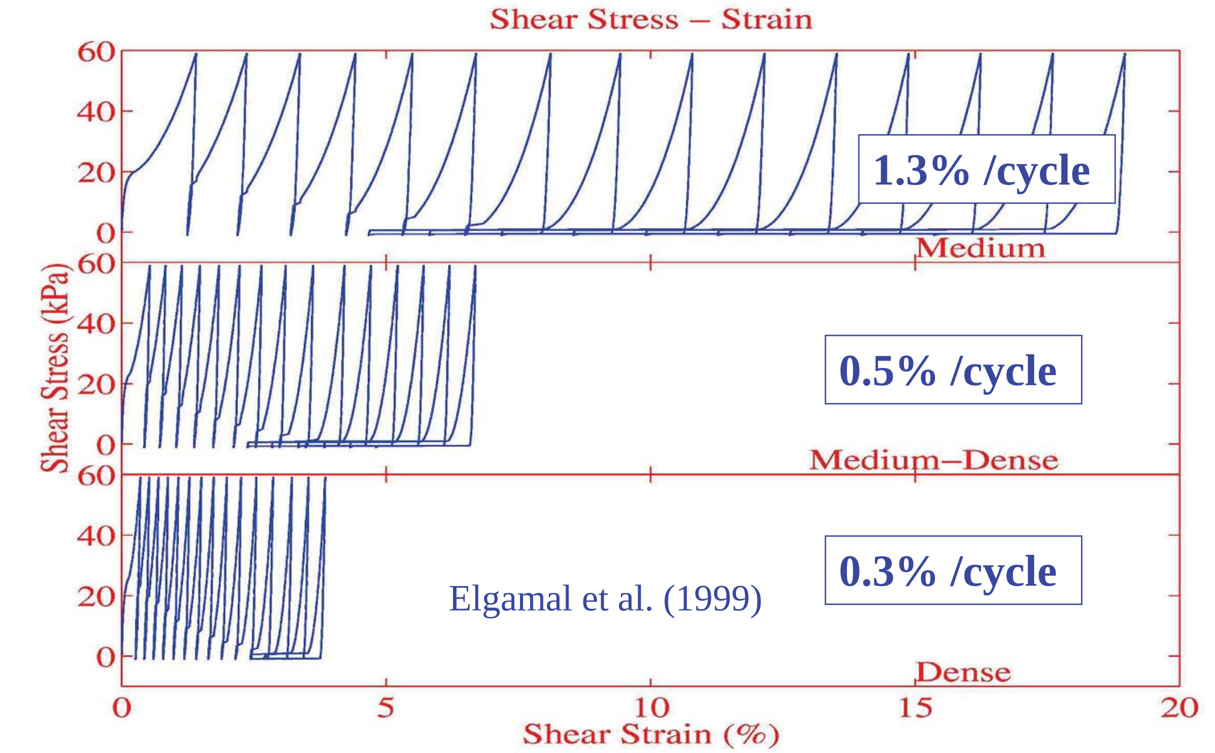

The above soil constitutive model is incorporated in a solid-fluid fully coupled Finite Element program: CYCLIC

http://cyclic.ucsd.edu

Fluid Saturated Porous Media
Simplified u-p Formulation (Chan 1988)

Assumptions

Soil is fully saturated.

Constant fluid density with respect to space.

Constant porosity with respect to time.

Fluid is compressible and solid grains are incompressible.

Fluid velocity gradient is small and all convective terms are negligible.

Fluid acceleration relative to solid phase is negligible.

Soil is considered a continuum.

Isothermal process.

Parra 1996, Yang 2000, Elgamal et al. 1999

Notation

u_i = Displacement of solid phase

p = Pore fluid pressure

w_i = Displacement of the fluid relative to solid phase

ρ = Mass density of the mixture

ρ_f = Mass density of the fluid

g_i = Acceleration of gravity

Q = Bulk modulus of the mixture

R_i = Viscous drag force exerted on the fluid by the solid

k_{ij} = Permeability tensor

Definition of strain

$$d\varepsilon_{ij} = \frac{1}{2}(du_{i,j} + du_{j,i})$$

Definition of effective stress

$$\sigma'_{ij} = \sigma_{ij} + \delta_{ij} p$$

Constitutive relation

$$d\sigma'_{ij} = D_{ijkl} d\varepsilon_{kl}$$

Fluid equilibrium and mass conservation

$$\boxed{\frac{\dot{p}}{Q} + \dot{\varepsilon}_{ii} - k_{ij}(p_{,i} + \rho_f \ddot{u}_i - \rho_f g_i)_{,j} = 0}$$

Mixture equilibrium

$$\boxed{\sigma_{ij,j} - \rho(\ddot{u}_i - g_i) = 0}$$

Chan (1988)

Above two equations constitute a strong form of simplified u-p formulation.

Finite element implementation

$$\mathbf{M}\ddot{\mathbf{u}} + \int_{\Omega} \mathbf{B}^T \boldsymbol{\sigma}' d\Omega - \mathbf{Q}\mathbf{p} - \mathbf{f}^{\mathrm{m}} = \mathbf{0}$$

$$\mathbf{Q}^T \dot{\mathbf{u}} + \mathbf{H}\mathbf{p} + \mathbf{S}\dot{\mathbf{p}} - \mathbf{f}^{\mathrm{p}} = \mathbf{0}$$

Chan 1988, Parra 1996, Yang 2000

where

- $\mathbf{u}$ = displacement vector
- $\mathbf{p}$ = pore pressure vector
- $\mathbf{M}$ = mass matrix
- $\mathbf{B}$ = strain-displacement matrix
- σ' = effective stress vector
- $\mathbf{Q}$ = discrete gradient operator
- $\mathbf{H}$ = permeability matrix
- $\mathbf{S}$ = compressibility matrix
- $\mathbf{f}^{\mathrm{m}}$ = force vector for the mixture
- $\mathbf{f}^{\mathrm{p}}$ = force vector for the fluid phase

Typical 9-4-node element employed in

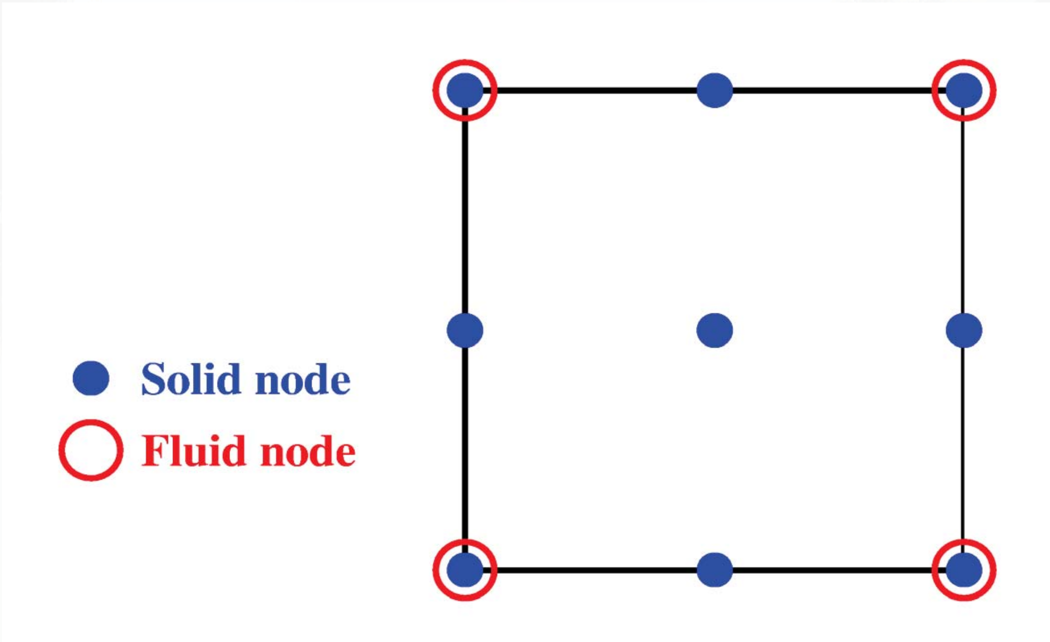

Chan 1988, Parra 1996, Yang 2000

CYCLIC simulation: effect of permeability gradient

Without clay cap Yang (2000) **With clay cap**

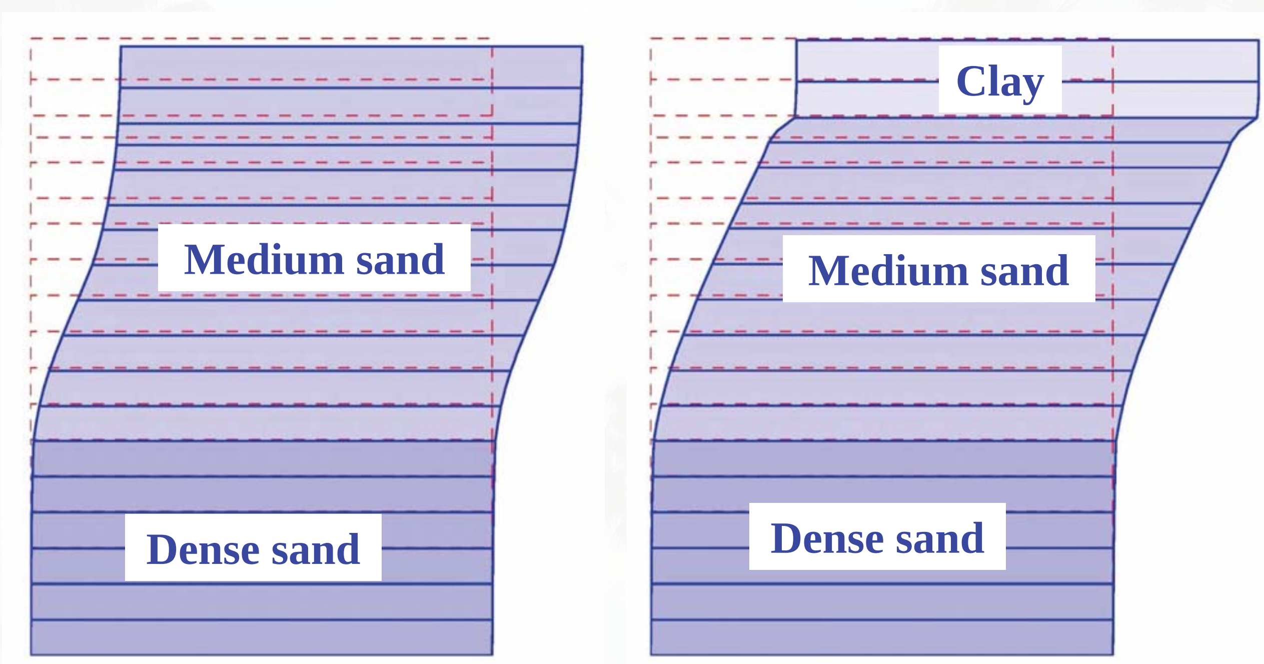

Hydraulic fill liquefaction (Adalier and Elgamal 1992)

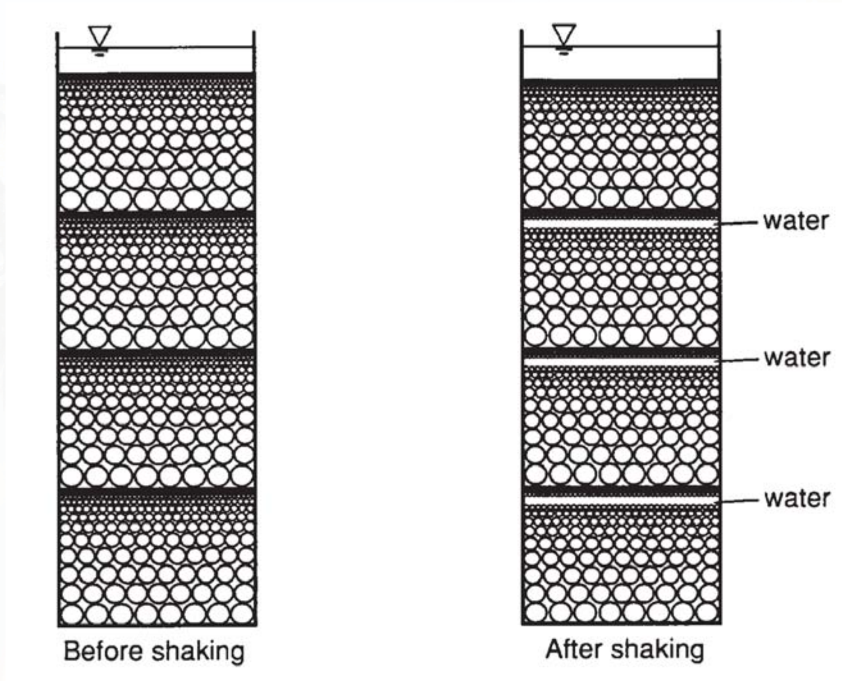

Example *Cyclic 1D* Simulations

- 10 m soil profile height.
- 10 elements.
- Water table at ground surface.
- Rigid base.
- Inclination and material definition see the table:

box	1	2	3	4
Material	Cohesionless medium	Cohesionless medium	Cohesionless medium	Cohesionless medium, with clay cap
Permeability	sand	sand	gravel	gravel
Inclination	level	4^o	4^o	4^o

Example *Cyclic 1D* Simulations

Input motion is composed of 10 cycles of sinusoidal motion at a frequency of 1 Hz and amplitude of 0.2 g.

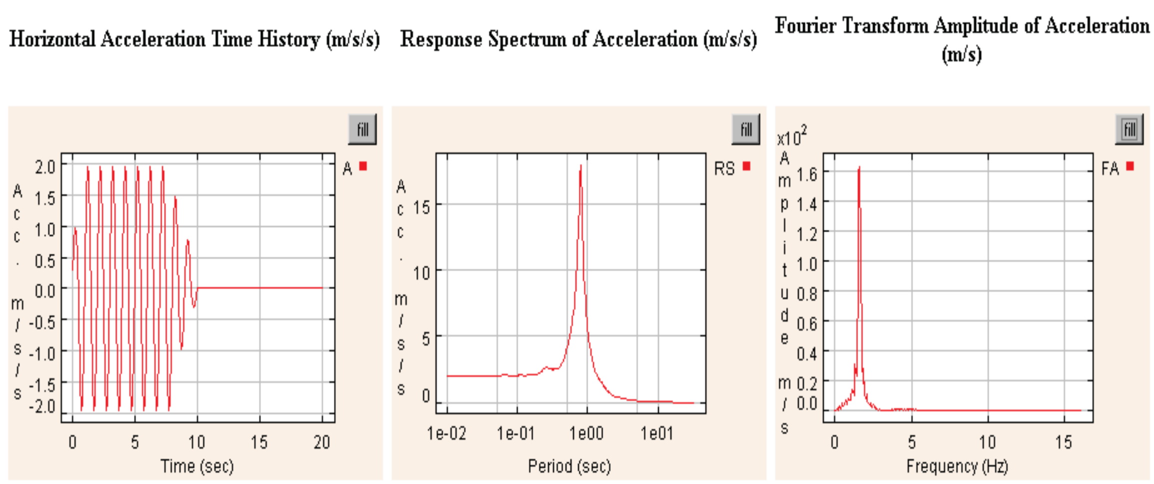

Cohesionless (Dr = medium, sand permeability, level

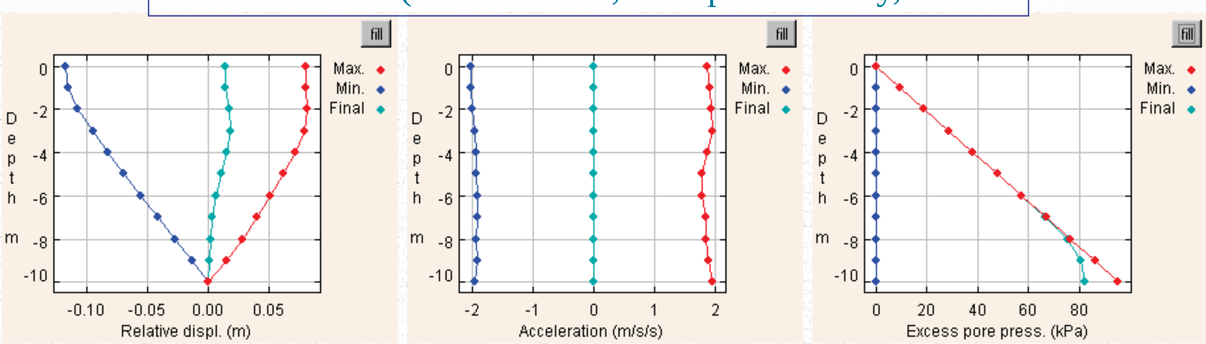

Horizontal Displacement (Relative to the base, m) | **Horizontal Acceleration (m/s/s)** | **Excess Pore Pressure (kPa)**

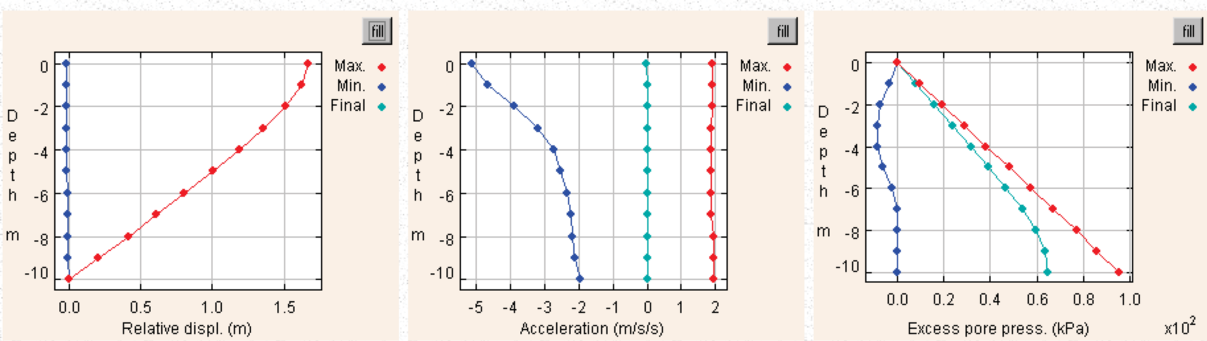

Cohesionless medium, sand permeability, 4° inclination

Cohesionless medium, sand permeability, level

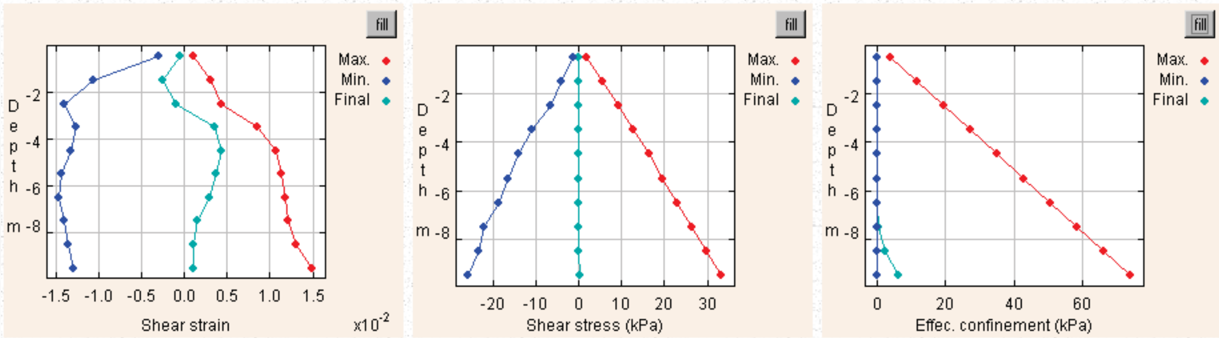

Shear strain **Shear stress (kPa)** **Effective confinement (kPa)**

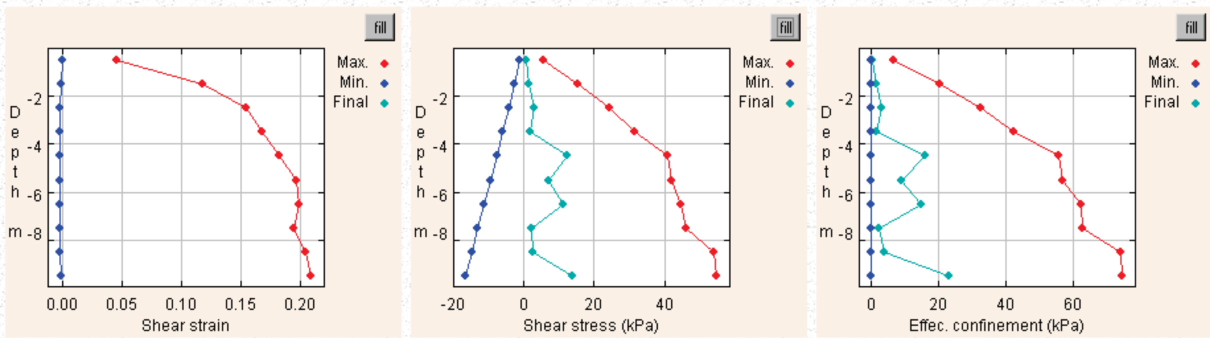

Cohesionless medium, sand permeability, 4º inclination

Cohesionless medium, sand permeability, level

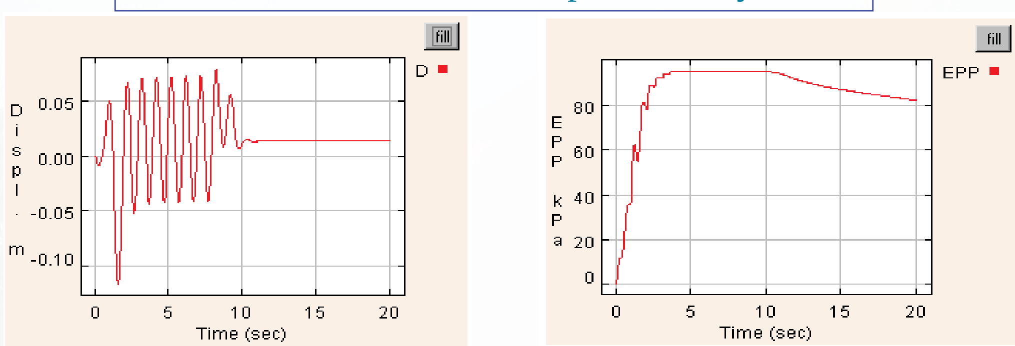

Surface Horizontal Displacement (Relative to the base, m)

Base Excess Pore Pressure (kPa)

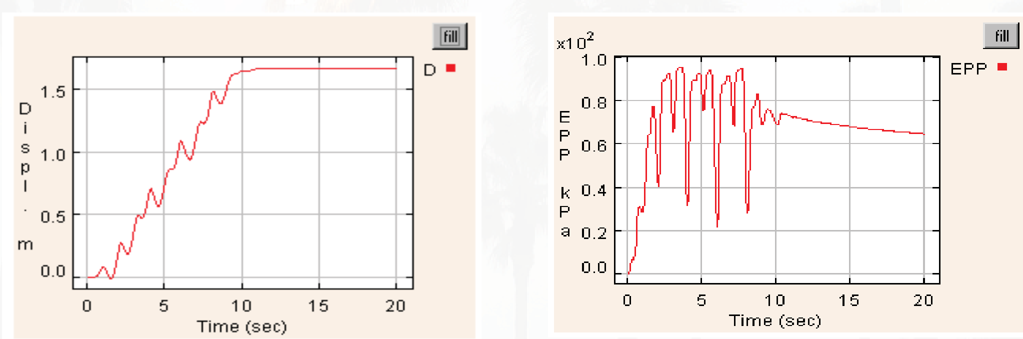

Cohesionless medium, sand permeability, 4º inclination

Cohesionless medium, sand permeability, level

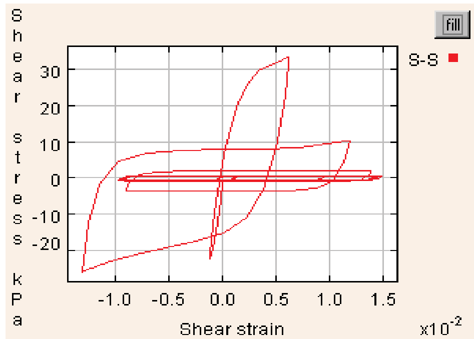

Shear stress-strain near base

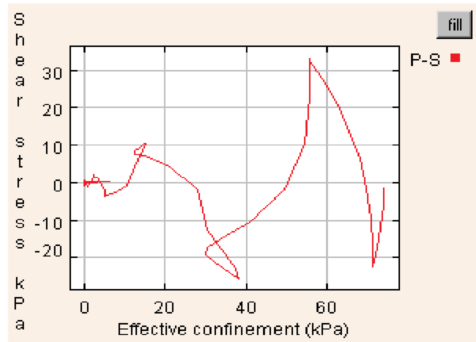

Effective stress path near base

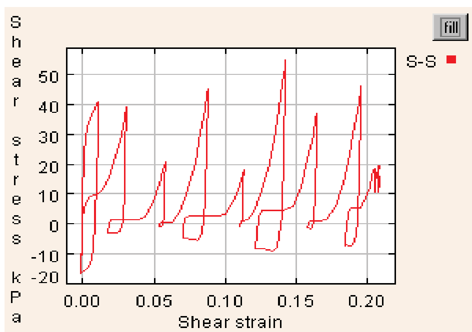

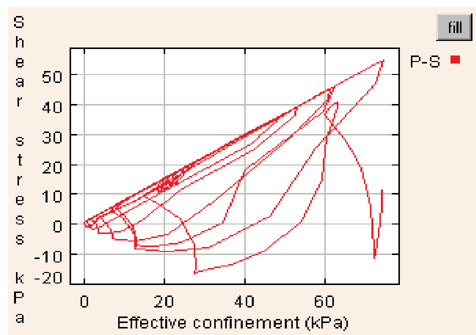

Cohesionless medium, sand permeability, 4º inclination

Cohesionless medium, sand permeability, level

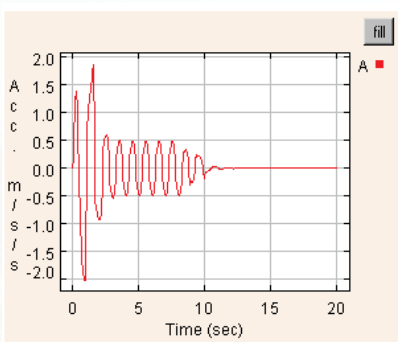

Surface horizontal acceleration (m/s/s)

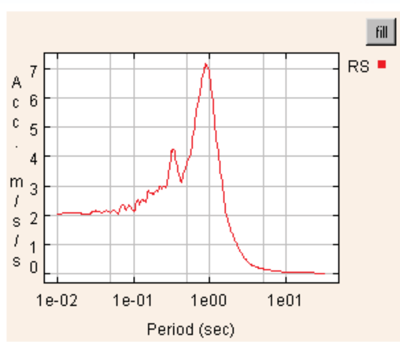

Acceleration response spectrum (5% damping)

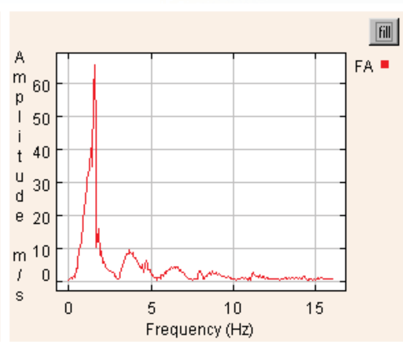

Acceleration Fourier transform amplitude

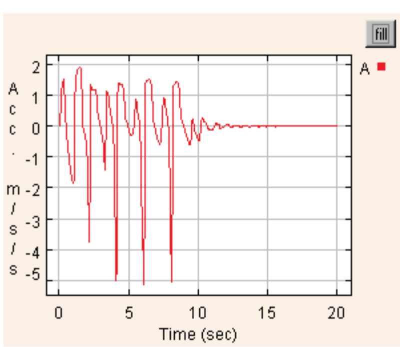

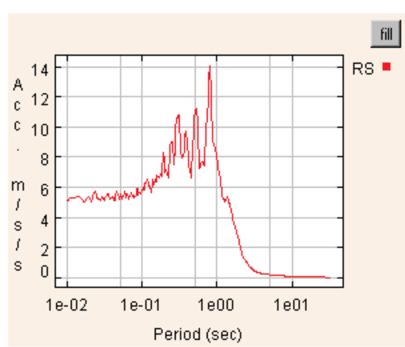

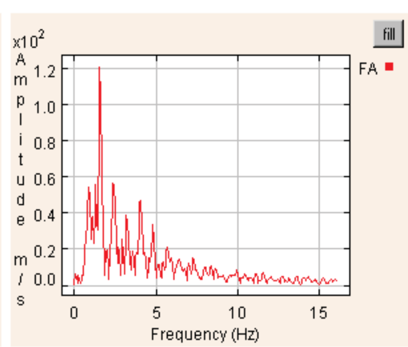

Cohesionless medium, sand permeability, 4º inclination

Cohesionless medium, gravel permeability, 4° inclination

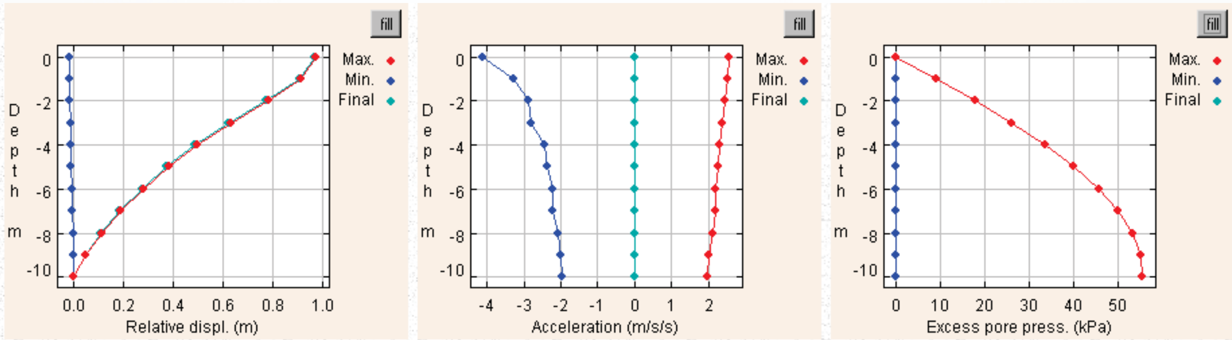

Horizontal Displacement (Relative to the base, m) | **Horizontal Acceleration (m/s/s)** | **Excess Pore Pressure (kPa)**

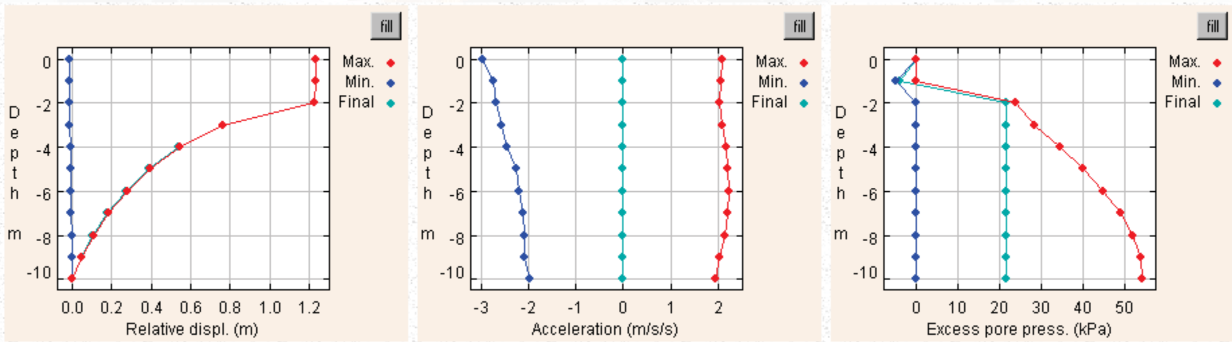

Cohesionless medium, gravel permeability, 4° inclination, with a clay cap

Cohesionless medium, gravel permeability, 4° inclination

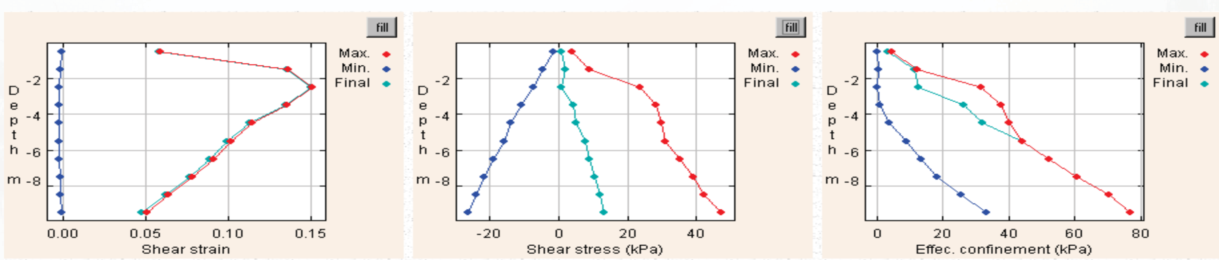

Shear strain | **Shear stress (kPa)** | **Effective confinement (kPa)**

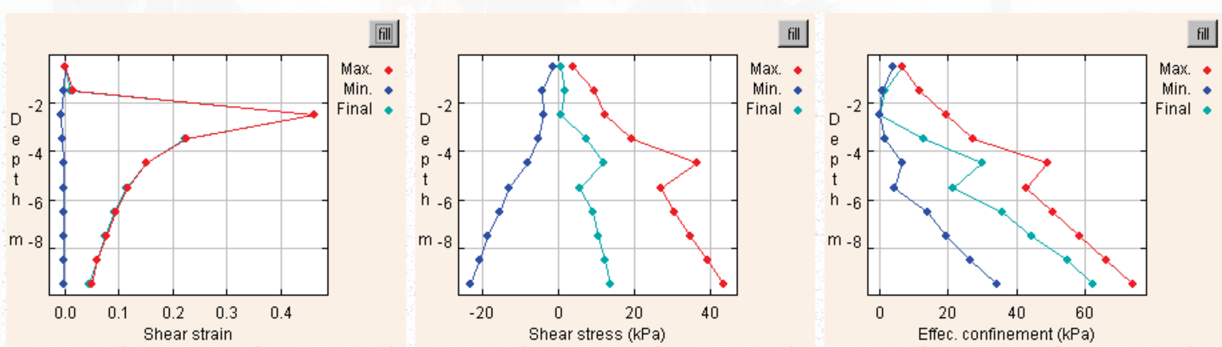

Cohesionless medium, gravel permeability, 4° inclination, with a clay cap

Cohesionless medium, gravel permeability, 4° inclination

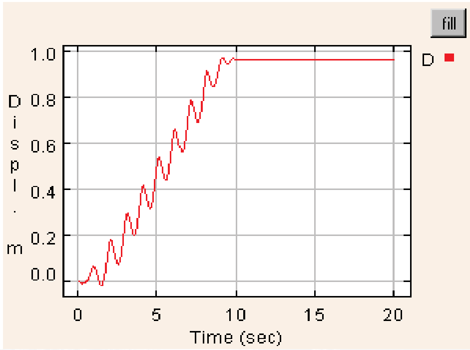

Surface Horizontal Displacement (Relative to the base, m)

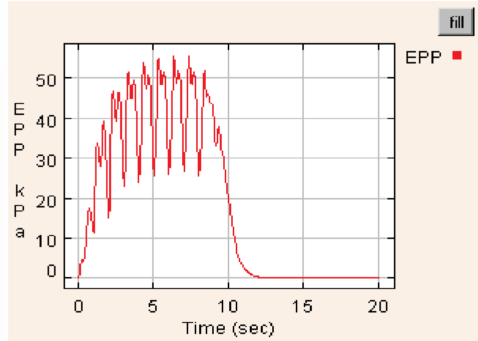

Base Excess Pore Pressure (kPa)

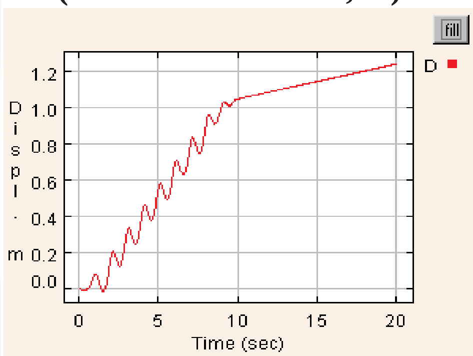

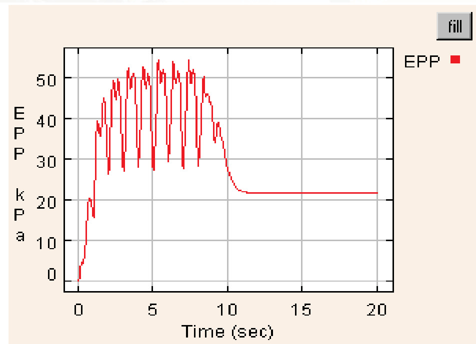

Cohesionless medium, gravel permeability, 4° inclination, with a clay cap

Cohesionless medium, gravel permeability, 4° inclination

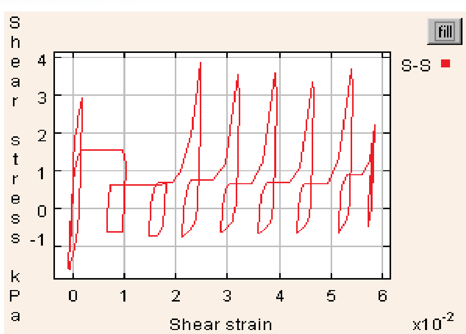

Shear stress-strain near surface

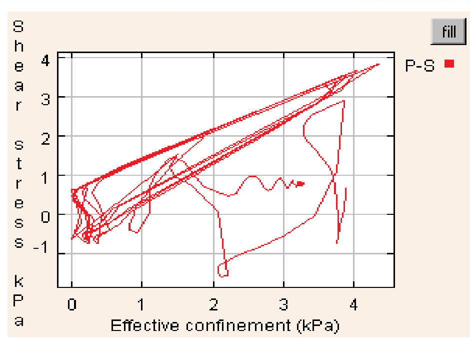

Effective stress path near surface

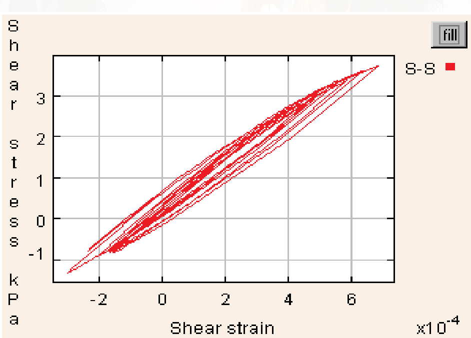

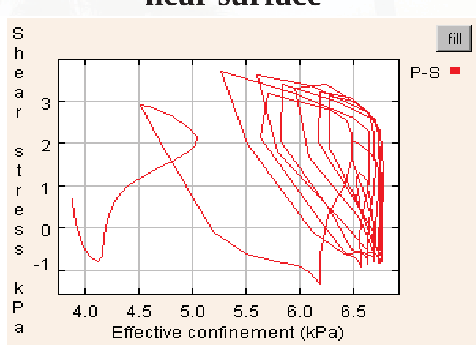

Cohesionless medium, gravel permeability, 4° inclination, with a clay cap

Cohesionless medium, gravel permeability, 4º inclination

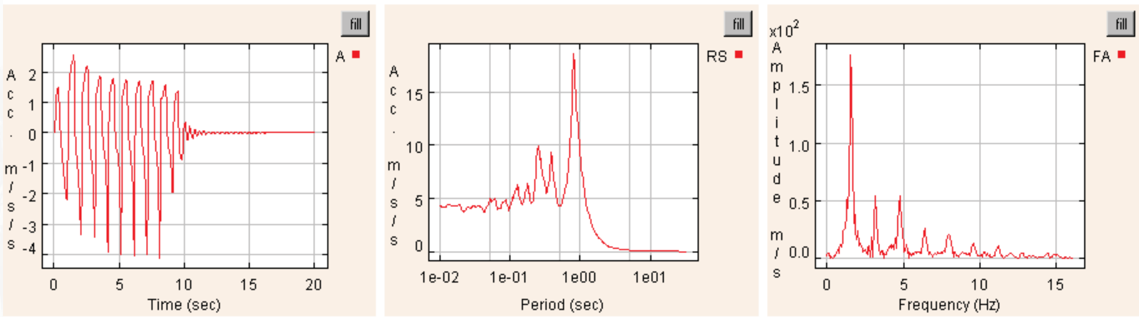

Surface horizontal acceleration (m/s/s) | **Acceleration response spectrum (5% damping)** | **Acceleration Fourier transform amplitude**

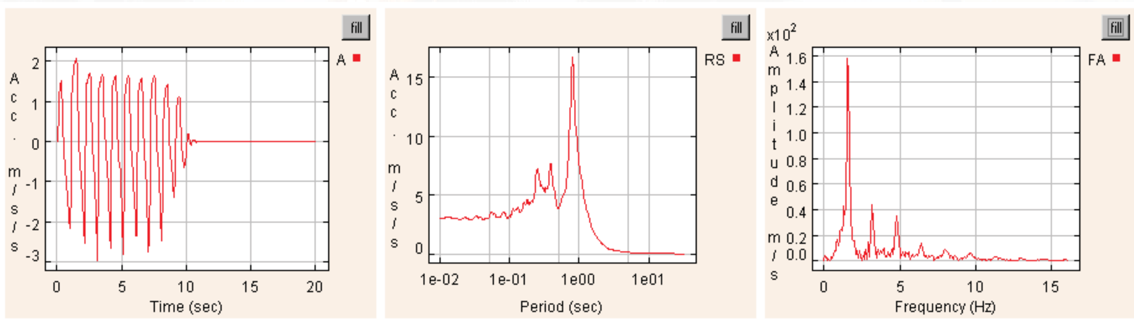

Cohesionless medium, gravel permeability, 4º inclination, with a clay cap

Insightful simulation scenarios using Cyclic1D

Using the computer code Cyclic1D http://cyclic.ucsd.edu , or http://www.soilquake.net/ :

a) Run the **default** case (10 m saturated cohesionsless medium, sand permeability soil, and 0.2g 1Hz base sinusoidal acceleration for 10 cycles of loading). Inspect the results and on this basis, discuss the observed liquefaction mechanisms (generation of excess pore pressure, stress-strain histories at different depths, changes in effective vertical stress versus shear stress, and the resulting form of acceleration at and near ground surface.

b) Repeat the above upon changing to soil to the cohesionless medium, gravel permeability soil. Pay particular attention to the main changes that occurred on account of the now higher soil permeability (gravel permeability versus sand permeability). Note also the changes that occur after the end of base excitation (computations continue for 10 more seconds after the base shaking ends).

c) Repeat the above upon changing to soil to the cohesionless dense, sand permeability soil. Pay particular attention to the main changes that occurred on account of the now dense soil characteristics of stress-strain response (e.g., lower tendency for excess pore-pressure u_e buildup and so forth).

Insightful simulation scenarios using Cyclic1D (continued)

d) Repeat case a) above, upon changing the site inclination angle to 1.5 degrees (i.e., mild site inclination, imposing a small driving shear stress). Pay particular attention to the main changes that occurred on account of the now imposed driving shear stress. Discuss change in relative ground surface displacement and the displacement profile, compared to the corresponding zero inclination scenario of case a). Note and discuss the changes in shear stress-strain, excess pore-pressure histories, and shear stress versus effective confinement.

Important note: If you get the message below, it might be on account of selecting and inclination angle that results in excessive lateral deformations (upon liquefaction), precluding/hampering the possibility of convergence of the analysis (at some particular time step during the computations). Simply, the available shear strength is inadequate to sustain the inclination-imposed driving shear force (upon liquefaction and degradation of soil strength). A similar outcome would also result from imposing a high inclination when a very weak soil layer (low inadequate shear strength) is specified (in this case convergence would not be possible right from the start).

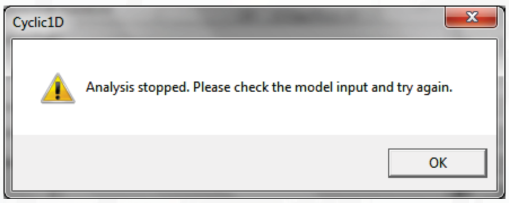

For Liquefaction-induced lateral-spreading countermeasures, see: **http://cyclic.ucsd.edu/openseespl**
Elgamal, Ahmed, Lu, Jinchi, and Forcellini, Davide, "Mitigation of Liquefaction-Induced Lateral Deformation in a Sloping Stratum: Three-dimensional Numerical Simulation," Journal of Geotechnical and Geoenvironmental Engineering, ASCE, Vol. 135, No. 11, November, 1672-1682, 2009.

Gravel Drain/Stone column Ground Modification

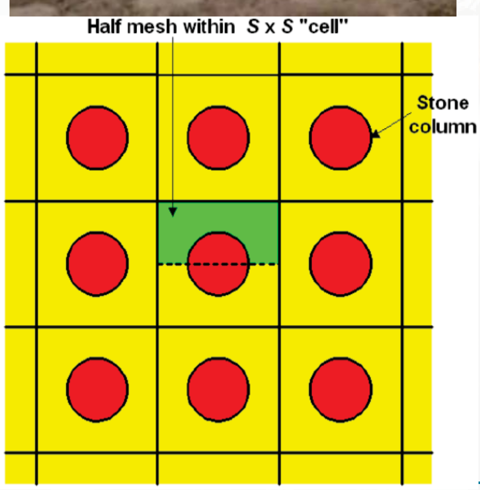

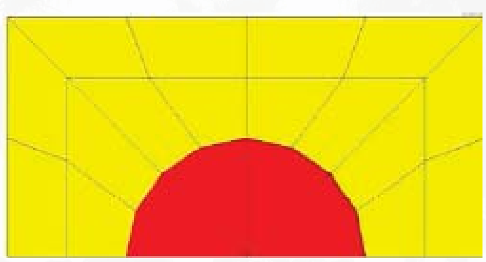

Schematic view of stone column or pile layout

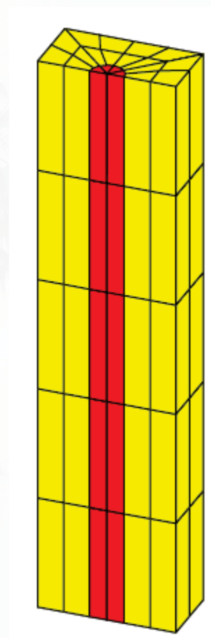

3D isometric view (10m thick soil stratum with ½ mesh employed due to symmetry)

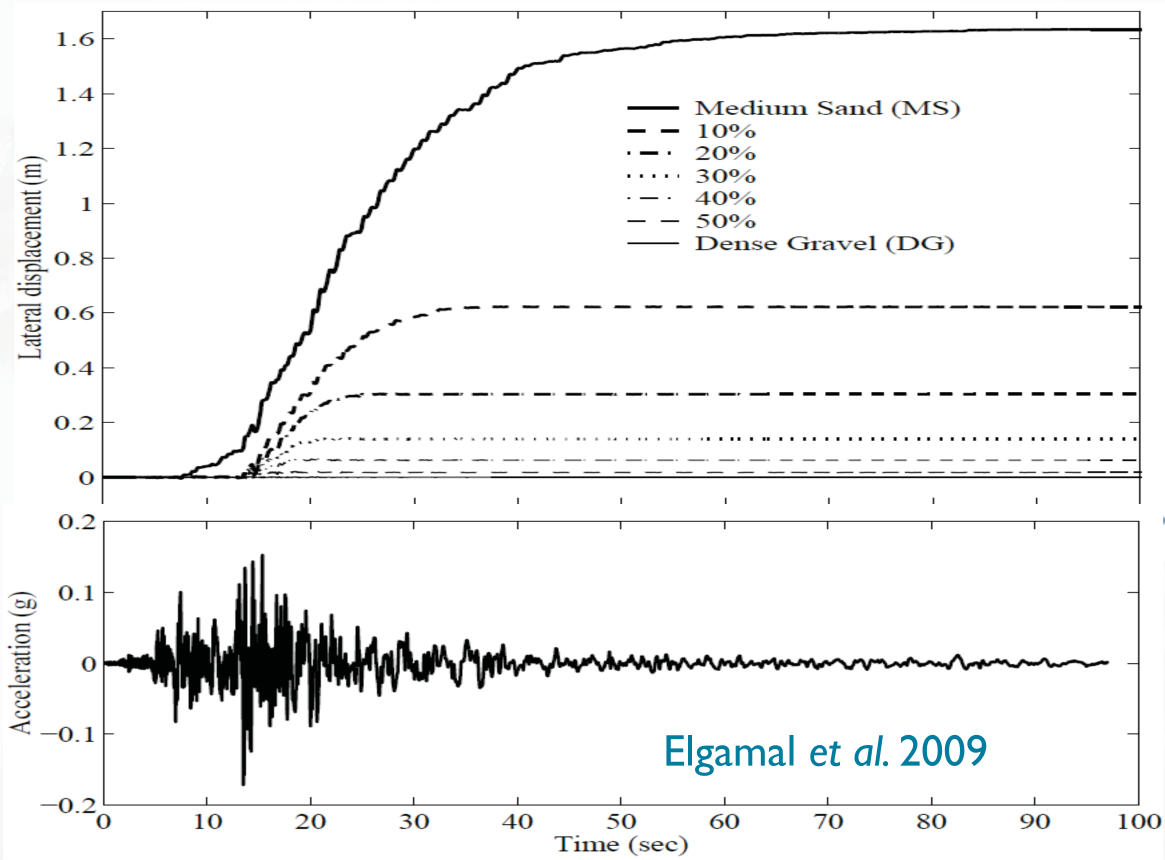

Medium Sand (MS)
10%
20%
30%
40%
50%
Dense Gravel (DG)
Lateral displacement (m)
Acceleration (g)
Time (sec)
Elgamal *et al.* 2009

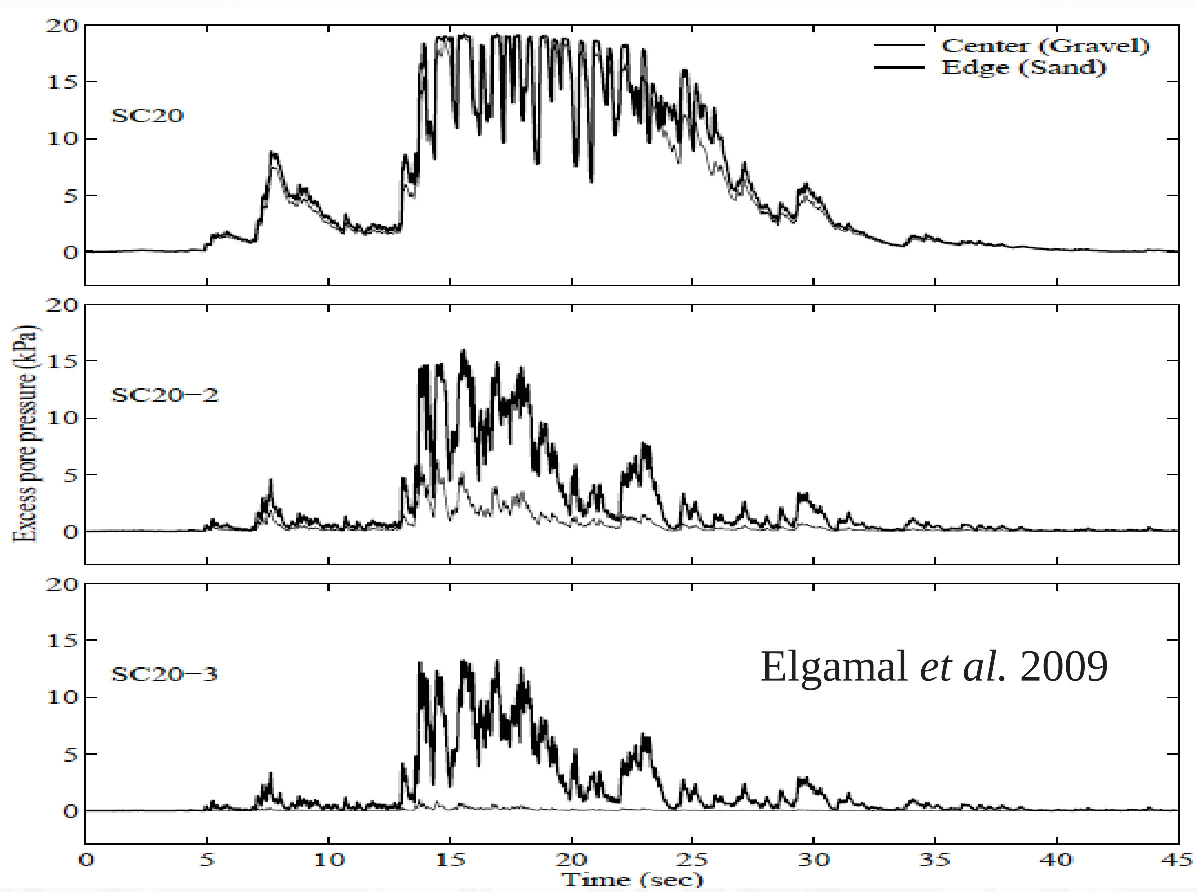

Center (Gravel)
Edge (Sand)
SC20
SC20−2
SC20−3
Excess pore pressure (kPa)
Time (sec)
Elgamal *et al.* 2009

References

Adalier, K. and Elgamal, A. -W. (1992). "Post-liquefaction Behavior of Soil Systems," *Report*, Department of Civil Engineering, Rensselaer Polytechnic Institute, Troy, NY.

Arulmoli, K., Muraleetharan, K. K., Hossain, M. M., and Fruth, L. S. (1992). "VELACS: Verification of Liquefaction Analyses by Centrifuge Studies, Laboratory Testing Program, Soil Data Report," *Report, The Earth Technology Corporation, Project No. 90-0562*, Irvine, California.

Chan, A. H. C. (1988). "A Unified Finite Element Solution to Static and Dynamic Problems in Geomechanics," *Ph.D. dissertation*, University College of Swansea, U. K.

Elgamal, A. -W., Zeghal, M., and Parra, E. (1996). "Liquefaction of Reclaimed Island in Kobe, Japan," *Journal of Geotechnical Engineering*, ASCE, Vol. 122, No. 1, pp. 39-49.

Elgamal, A., Yang, Z., Parra, E., and Dobry, R. (1999). "Modeling of Liquefaction- Induced Shear Deformations," *Proceedings, Second International Conference on Earthquake Geotechnical Engineering*, Lisbon, Portugal, 21-25 June, Balkema.

Florin, V.A. and Ivanov, P.L. (1961). "Liquefaction of saturated sandy soils," *Proceedings, 5th International Conference on Soil Mechanics and Foundation Engineering*, Paris, Vol. 1, pp. 107-111.

Ishihara, K. (1985). "Stability of Natural Deposits During Earthquakes," Theme Lecture, *Proceedings, 11th International Conference on Soil Mechanics and Foundation Engineering*, San Francisco, Vol. 2, pp. 321-376.

Parra, E. (1996). "Numerical Modeling of Liquefaction and Lateral Ground Deformation Including Cyclic Mobility and Dilation Response in Soil Systems," *Ph.D. Thesis*, Dept. of Civil Engineering, RPI, Troy, NY.

Scott, R.F. (1986). "Solidification and consolidation of a liquefied sand column," *Soils and Foundations*, Vol. 26, No. 4, pp.23-31.

Yang, Z. (2000). "Numerical Modeling of Earthquake Site Response Including Dilation and Liquefaction," *Ph.D. Dissertation*, Dept. of Civil Engineering and Engineering Mechanics, Columbia University, New York, NY.

Yang, Z., Elgamal, A., Abdoun, T., and Lee, C-J. (2001). "A Numerical Study of Lateral Spreading Behind a Caisson Type Quay Wall," *proceedings, 4th International Conference on Recent Advance in Geotechnical Earthquake Engineering and Soil Dynamics*, San Diego, California, March 26-31.

Youd, T.L. (1977). "Packing changes and liquefaction susceptibility," *Journal of the Geotechnical Engineering Division*, ASCE, Vol. 103, No. GT8, pp. 918-923.

Zeghal, M. and Elgamal, A. -W. (1994). "Analysis of Site Liquefaction Using Earthquake Records," *Journal of Geotechnical Engineering*, ASCE, Vol. 120, No. 6, pp. 996-1017.

Additional References

Adalier, K., A. -W. Elgamal, and G. R. Martin, "Foundation Liquefaction Countermeasures for Earth Embankments," Journal of Geotechnical and Geo-environmental Engineering, ASCE, Vol. 124, No. 6, 500-517, June, 1998. (Experimental)

Gunturi, V. R., A.-W. Elgamal and H.–T. Tang, "Hualien Seismic Down hole Data Analysis," Engineering Geology, Elsevier Science B.V., 50, 9-29, 1998. (In-situ azimuthal anisotropy)

Zeghal, M., A. -W. Elgamal, X. Zeng, and K. Arulmoli, "Mechanism of Liquefaction Response in Sand-Silt Dynamic Centrifuge Tests," Soil Dyn & Earthq Eng, Elsevier, 18, 71-85, 1999. (Computational, Layered soil system based on VELACS Experiment)

Zeghal, M., and Ahmed-W. Elgamal, "Site Response and Vertical Seismic Arrays," Progress in Structural Engineering and Materials, Construction Engineering Research Communications Ltd, UK, issue 2:1, January 2000, John Wiley and Sons, Ltd. (In-situ vertical arrays)

Adalier, K. and Elgamal, A., "Seismic Response of Adjacent Dense and Loose Saturated Sand Columns," Journal of Soil Dyn and Earthq Eng, Vol. 22, No. 2, 115-127, 2002. (Experimental)

Elgamal, A., Yang, Z. and Parra, E., "Computational Modeling of Cyclic Mobility and Post-Liquefaction Site Response," Journal of Soil Dynamics and Earthquake Engineering, Volume 22, Issue 4, Pages 259-271, June 2002. (Computational)

Elgamal, A.-W., R. Dobry, E. Parra, and Z. Yang, "Soil Dilation and Shear Deformations During Liquefaction," Proc. 4th Intl. Conf. on Case Histories in Geotechnical Engineering, S. Prakash, Ed., 1238-1259, St. Louis, MO, March 8-15, 1998.
(Extensive compilation of in-situ and experimental data showing cyclic mobility)

Elgamal, A., Tao Lai, Zhaohui Yang, and Liangcai He, "Dynamic Soil Properties, Seismic Downhole Arrays and Applications in Practice," 4th International Conference on Recent Advances in Geotechnical Earthquake Engineering and Soil Dynamics, S. Prakash, Ed., San Diego, California, USA, March 26-31, 2001, Vol. II, 85 pages (85 page, Invited State-of-the-art paper). (Extensive compilation of data and analyses of Downhole seismic arrays)

Zhaohui Yang and Ahmed Elgamal, "Influence of Permeability on Liquefaction-Induced Shear Deformation," Journal of Eng Mechanics, ASCE, 128, 7, July 2002. (Computational)

Ahmed Elgamal, Ender Parra, Zhaohui Yang, and Korhan Adalier, "Numerical Analysis of Embankment Foundation Liquefaction Countermeasures," Journal of Earthquake Engineering, Vol. 6, No. 4, pp. 447-471, 2002. (Computational)

Ahmed Elgamal, Zhaohui Yang, Ender Parra, and Ahmed Ragheb, "Modeling of Cyclic Mobility in Saturated Cohesionless Soils," International Journal of Plasticity, Pergamon, Elsevier Science Ltd., Vol. 19, No. 6, pp. 883-905, June 2003. (Computational, Soil Model)

K. Adalier, A. Elgamal, J. Meneses, and J. I. Baez, "Stone Columns as Liquefaction Countermeasure in Non-Plastic Silty Soils," Soil Dynamics and Earthquake Eng, Elsevier Science Ltd., Volume 23, Issue 7, Pages 571-584, October 2003. (Experimental)

Zhaohui Yang, Ahmed Elgamal, and Ender Parra, "Computational Model for Liquefaction and Associated Shear Deformation," J. Geotechnical and Geoenvironmental Engineering, ASCE, Vol. 129, No. 12, 2003. (Computational, Soil Model)

Zhaohui Yang and Ahmed Elgamal, "Application of Unconstrained Optimization and Sensitivity Analysis to Calibration of a Soil Constitutive Model," Intl. J. Numerical Analytical Methods in Geomechanics, Vol. 27, No. 15, 1277-1297, 2003. (Computational material properties ID)

Korhan Adalier, and Ahmed Elgamal, "Mitigation of liquefaction and associated ground deformations by stone columns," Journal of Engineering Geology, Volume 72, Issues 3-4, Elsevier, April 2004, Pages 275-291. (Experimental, Overview)

Jinchi Lu, Jun Peng, Ahmed Elgamal, Zhaohui Yang, and Kincho H. Law, "Parallel Finite Element Modeling of Earthquake Ground Response and Liquefaction," Journal of Earthquake Engineering and Engineering Vibration, Vol. 3, No.1, June 2004. (Computational)

A. W. Elgamal, T. Lai, V. R. Gunturi, and M. Zeghal, "System Identification of Landfill Seismic Response," Journal of Earthquake Engineering©, Imperial College Press, Vol. 8, #4, pages 545-566, 2004. (Case History material identification)

A. Elgamal and Liangcai He, "Vertical Earthquake Ground Motion Records: An Overview", Journal of Earthquake Eng©, Imperial College Press Vol. 8, November 2004. (Analytical)

Zhaohui Yang, Jinchi Lu, and Ahmed Elgamal, "A Web-based Platform for Live Internet Computation of Seismic Ground Response," Advances in Engineering Software, Elsevier, Vol. 35, pp. 249-259, 2004. (Computational, On-line)

Zhaohui Yang, Ahmed Elgamal, Korhan Adalier, and Michael Sharp, "Earth Dam on Liquefiable Foundation: Numerical Prediction of Centrifuge Experiments," Journal of Engineering Mechanics, ASCE, Volume 130, Issue 10, October 2004. (Experimental/Computational)

Jun Peng , Jinchi Lu, Kincho H. Law, and Ahmed Elgamal, "ParCYCLIC: Finite Element Modeling of Earthquake Liquefaction Response on Parallel Computers," International Journal of Numerical Methods in Geomechanics, Vol. 28, 1207-1232, 2004. (Computational)

Ahmed Elgamal, Zhaohui Yang, Tao Lai, Daniel Wilson, and Bruce Kutter, "Dynamic Response of Saturated Dense Sand in Laminated Centrifuge Container," Journal of Geotechnical and Geo-environmental Engineering, ASCE, Vol. 131, No. 5, May 2005. (Experimental/Computational)

Adalier, Korhan, and Elgamal, Ahmed, "Liquefaction of over-consolidated sand: a centrifuge investigation," Journal of Earthquake Engineering, Vol. 9, Special Issue 1, 127-150, Imperial College Press, 2005. (Experimental)

Elgamal, Ahmed, Lu, Jinchi, and Yang, Zhaohui, "Liquefaction-Induced Settlement of Shallow Foundations, and Remediation: 3D Numerical Stimulation, Journal of Earthquake Engineering, Vol. 9, Special Issue 1, 17-45, Imperial College Press, 2005. (Computational)

Liquefaction Evaluation

Ahmed Elgamal & Zhaohui Yang

Acknowledgements

The Liquefaction Evaluation section is prepared mainly following:

•Kramer, S. L. (1996). "Geotechnical Earthquake Engineering," *Ch 9,* Prentice Hall, 653 pp.
•Bozorgnia, Y. and Bertero, V.V. , Eds. (2004). "Earthquake Engineering: From Engineering Seismology to Performance-Based Engineering," Ch. 4: Geotechnical Aspects of Seismic Hazards, by S. L. Kramer and J. Stewart, CRC Press, 976 pages.
•Youd, T. L., and Idriss, I. M., eds. (1997). NCEER Workshop Proc. on Evaluation of Liquefaction Resistance of Soils, Natl. Center for Earthquake Engineering Research (NCEER), State Univ. of New York at Buffalo, NY.
•Youd ,T.L., I. M. Idriss, R. D. Andrus, I. Arango, G. Castro, J. T. Christian, R. Dobry, W. D. L. Finn, L.F. Harder Jr., M.E. Hynes, K. Ishihara, J. P. Koester, S.S C. Liao, 13 W.F. Marcuson III, G.R. Martin, J.K. Mitchell, Y. Moriwaki, M. S. Power, P.K. Robertson, R.B. Seed and K. H. Stokoe II (2001). "Liquefaction Resistance of Soils: Summary Report from the 1996 NCEER and 1998 NCEER/NSF Workshops on Evaluation of Liquefaction Resistance of Soils," J. of Geotechnical and Geo-environmental Engineering, ASCE, 127, 10, 817-833.
•Martin, G. R., and Lew, M., eds. (1999). Recommended procedures for implementation of DMG Special Publication 117: Guidelines for analyzing and mitigating liquefaction hazards in California, Southern, California Earthquake Center, University of Southern California, Los Angeles, California.

Updates and new additional information can be found in:

•R. B. Seed, K. O. Cetin, R. E. S. Moss, A. M. Kammerer, J. Wu, J. M. Pestana, M. F. Riemer, R.B., Sancio, J.D. Bray, R. E. Kayen, and A. Faris (2003). "Recent Advances in SOIL Liquefaction Engineering: A Unified Consistent Framework," 26th Annual ASCE Los Angeles Geotechnical Spring Seminar, Keynote Presentation, H.M.S. Queen Mary, Long Beach, California, April 30, 2003.

•Idriss, I. M., and Boulanger, R. W. (2004). "Semi-Empirical Procedures for Evaluating Liquefaction Potential During Earthquakes", Invited paper, 11th Intl. Conf. on Soil Dyn. and Eq. Eng ., and 3rd Intl. Conf. on Eq. Geotech. Eng., Jan. 7-9, Berkeley, CA, pp 32-56.

•Idriss, I. M., and Boulanger, R. W. (2008). "Soil Liquefaction during Earthquakes," EERI Monograph, MNO-12, Richmond, CA.

• Bray, J. D., and Sancio, R. B. (2006). "Assessment of the liquefaction susceptibility of fine-grained soils." J. Geotech. Geoenviron. Eng., 132, 9, pp. 1165–1177.

•Boulanger, R. W., and Idriss, I. M. (2007). "Evaluation of cyclic softening in silts and clays," Journal of Geotechnical and Geoenvironmental Engng, 133, 6, June.

Other Main References:

Andrus, R.D. and Stokoe, K.H., II, (2000). "Liquefaction Resistance of Soils From Shear-Wave Velocity," Journal of Geotechnical and Geoenvironmental Engineering, American Society of Civil Engineers, Vol. 126, No. 11, November, pp. 1015-1025.

Ambraseys, N.N. (1988). "Engineering Seismology," *Earthquake Engineering and Structural Dynamics,* Vol. 17, pp. 1-105.

Baziar, M. and Dobry, R (1995). Residual strength and large-deformation potential of loose silty sands, Journal of Geotechnical Engineering, Vol. 121. No. 12, December., 896-906.

Ishihara, K. (1993). "Liquefaction and flow failure during earthquakes," *Geotechnique*, Vol. 43, No. 3, pp. 351-415.

Ishihara, K. and Yoshimine, M. (1992). "Evaluation of settlements in sand deposits following liquefaction during earthquakes," Soils and Foundations, Vol. 32, No. 1, pp. 173-188.

Kavazanjian, E., Jr., N. Matasovic, T. Hadj-Hamou, and P. J. Sabatini, Geotechnical Engineering Circular No. 3 – Design Guidance: Geotechnical Earthquake Engineering for Highways, Design Principles, Volume 1, SA-97-076 (NTIS # PB98-11560).

Kayen, R.E. , and Mitchell, J. K. (1997). Assessment of Liquefaction Potential During Earthquakes by Arias Intensity, Journal of Geotechnical and Geoenvironmental Engineering, Vol. 123, No. 12, December 1997, pp. 1162-1174.

Kramer, S. (1996). "Geotechnical Earthquake Engineering," Prentice Hall, NJ. 653 pp.

Mitchell, J.K. and Tseng, D.-J. (1990). "Assessment of liquefaction potential by cone penetration resistance," *Proceedings, H. Bolton Seed Memorial Symposium*, J.M. Duncan ed., University of California, Berkeley, Vol. 2, pp. 335-350.

Olson, S.M. and Stark, T. D. (2002). "Liquefied strength ration from liquefaction flow failure case histories," Canadian Geotechnical J., 39, 627-647.

Richardson, G. N., Kavazanjian, E., Jr. and Matasovic, N. (1995), "RCRA Substitute D (258) Seismic Design Guidance for Municipal Solid Waste Landfill Facilities," EPA/600/R-95/051, United States Environmental Protection Agency, Cincinnati, Ohio, 143p.

Seed, H.B. and Idriss, I.M. (1971). "Simplified procedure for evaluating soil liquefaction potential," *Journal of the Soil Mechanics and Foundations Division*, ASCE, Vol. 107, No. SM9, pp. 1249-1274.

Seed, H.B., Idriss, I. M., and Arango, I. (1983). "Evaluation of Liquefaction Potential Using Field Performance Data," *Journal of Geotechnical Engineering*, ASCE, Vol. 109, No. 3, pp. 458-482.

Seed, H.B., Tokimatsu, K., Harder, L.F., and Chung, R.M. (1985). "Influence of SPT procedures in soil liquefaction resistance evaluations," *Journal of Geotechnical Engineering*, ASCE, Vol. 111, No. 11, pp. 1016-1032.

Seed, R.B. and Harder, L.F. (1990). "SPT-based analysis of cyclic pore pressure generation and undrained residual strength," *Proceedings, H. Bolton Seed Memorial Symposium*, J.M. Duncan ed., University of California, Berkeley, Vol. 2, pp. 351-376.

Skempton, A. W. (1986). "Standard Penetration Test Procedures and the Effects in Sands of Overburden Pressure, Relative density, Particle Size, Ageing and Overconsolidation," *Geotechnique*, Vo. 36, No. 3, pp. 425-447.

Tokimatsu, K. and Seed, H.B. (1987). "Evaluation of settlements in sand due to earthquake shaking," *Journal of Geotechnical Engineering*, ASCE, Vol. 113, No. 8, pp. 861-878.

Types of liquefaction

1. Flow liquefaction

• Occurs when shear stress required for equilibrium of a soil mass (the static shear stress) is greater than the shear strength (residual strength) of the soil in its liquefied state.

• Potentially very large post-liquefaction lateral deformations are driven by the static shear stress.

Types of liquefaction (cont'd)

2. Cyclic mobility

• Occurs when the static shear stress is less than the shear strength of the liquefied soil.

• Deformations are driven by both cyclic and static shear stresses.

• Deformations develop incrementally during earthquake shaking.

When is the soil liquefied ….

At a given site, typically manifestations include sand boils, large lateral deformation, and significant settlement.

For technical assessments, the "liquefaction" state is reached when the effective confining stress goes down to zero (i.e., the original effective confining stress has gradually decreased and has been become "excess pore-water pressure" known as u_e).

At this state, the value of the "excess pore pressure ratio" r_u is 1.0 where $r_u = u_e / \sigma'_v$ and σ'_v is the initial effective vertical stress.

Also, technically liquefaction may be described by a soil sample building up pore-pressure and reaching a shear strain of 3%-5% or more in a laboratory shear test.

Why does liquefaction occur

If the soil is loose and is being shaken, the particles will settle due to gravity. When the soil is saturated, the pore-water is unable to move of the way quickly enough (because the soil permeability is relatively low), and more and more particles start to partially float in the water (this leads to the excess pore-pressure buildup). Eventually as shaking continues, the particles float in the water temporarily as they settle downwards and reach a new densified and consolidated state.

Soils Susceptible to liquefaction

Most susceptible would be very loose cohesionless soils. The low permeability of non-plastic silts and sands is a disadvantage.

Higher permeability, higher relative density, and higher cohesion (plasticity) reduce the susceptibility.

Notes:

1) Objectionable deformations might still occur if r_u values are high, even if liquefaction does not occur). Looser soils are more vulnerable.

2) As pore pressure builds-up, stratified soil profiles (particularly with permeability contrasts) may cause water to be temporarily trapped under a relatively impervious layer or seam (e.g., a due to alluvial or hydraulic fill construction, or presence of an upper clay stratum), generating a low friction interface and possibly leading to major lateral deformations. This mechanism actually is a driver of what we commonly observe as sand boils where this water escapes upwards through any available high permeability locale (e.g., taking advantage of a crack in the ground, or similar imperfections, …).

Evaluation of Liquefaction Potential and Consequences

I. Is the soil susceptible to liquefaction?

II. If the soil is susceptible, will liquefaction be triggered?

1) Cyclic stress approach (Discussed in notes)

2) Other methods (Refs. on page 2): effective-stress response analysis approach, cyclic strain approach, energy dissipation approach, probabilistic approach.

III. If liquefaction is triggered, how much damage would occur?

- Settlements
- Lateral deformations due to cyclic mobility: a) empirical approach, and b) effective-stress response analysis approach
- Flow Failure (see Kramer 1996).

I. Is the soil susceptible to liquefaction?

1. Historical criteria

The epicentral distance to which liquefaction can be expected, increases with increasing earthquake magnitude.

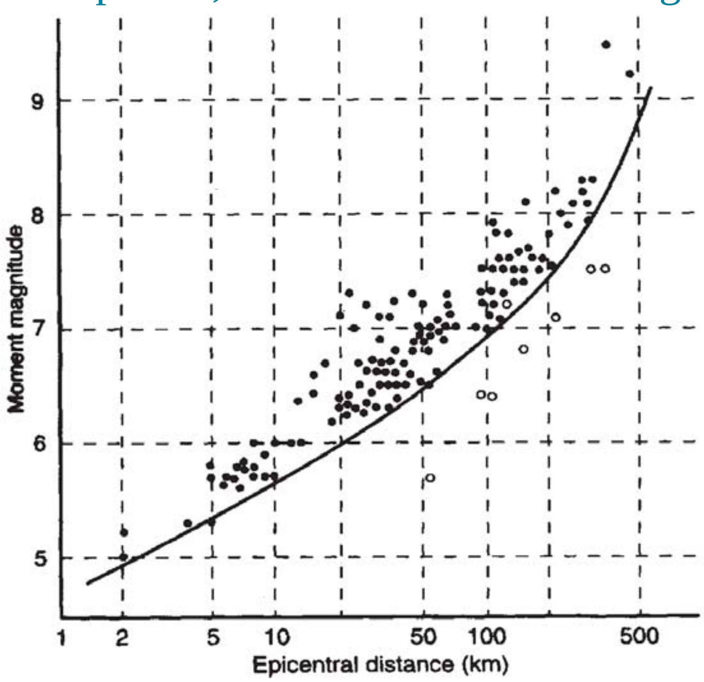

From Kramer (1996)

Figure 9.4 Relationship between limiting epicentral distance of sites at which liquefactio[n has been] observed and moment magnitude for shallow earthquakes. Deep earthquakes (focal depths > 50 km) have produced liquefaction at greater distances. After Ambraseys (1988).

Figure 1.

I. Is the soil susceptible to liquefaction? (cont'd)

2. Geologic criteria

- Depositional environment - Saturated loose fluvial, colluvial, and aeolian deposits are more susceptible to liquefaction.
- Age - Newer soils are more susceptible to liquefaction than older soils.
- Water table - Liquefaction susceptibility decreases with increasing groundwater depth.
- Human-made soils - Uncompacted soils (e.g., hydraulic fill) are more susceptible to liquefaction than compacted soils.

I. Is the soil susceptible to liquefaction? (cont'd)

3. Compositional criteria

- Grain size and plasticity characteristics - Sands, nonplastic silts, and gravelly soils when surrounded by impermeable soils, are susceptible to liquefaction.
- Gradation - Well graded soils are less susceptible to liquefaction than poorly graded soils.
- Particle shape - Soils with rounded particles are more susceptible to liquefaction than soils with angular particles.

I. Is the soil susceptible to liquefaction? (cont'd)

4. Initial stress state criteria (for flow liquefaction)

- A loose soil will be susceptible to flow liquefaction only if the static shear stress exceeds its steady state (or residual) strength.
- Residual strength can be estimated as shown in Figure 2.

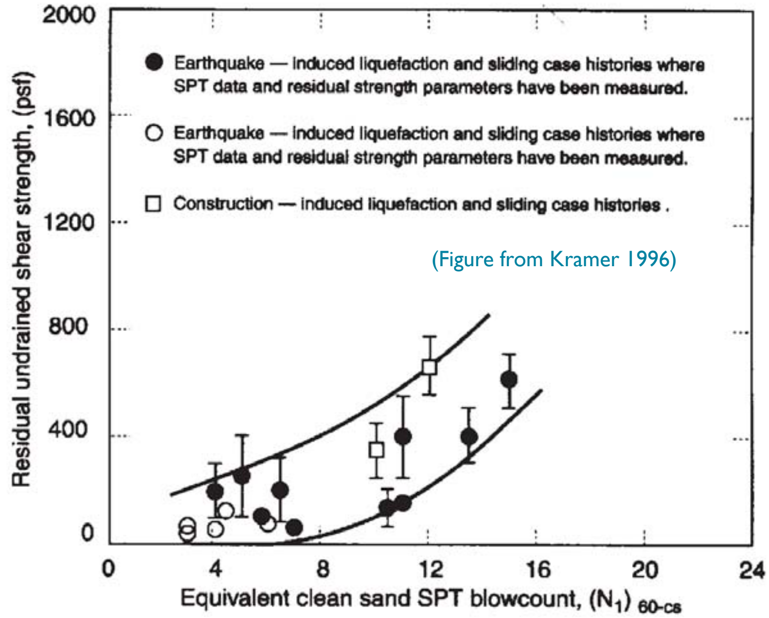

Figure 2. Relationship between residual strength and corrected SPT resistance. (After Seed and Harder, 1990. H. Bolton Seed Memorial Symposium Proceedings, Vol. 2, p. 371. Used by permission of BiTech Publishers, Ltd.)

In Fig. 2 above, $(N_1)_{60-cs} = (N_1)_{60} + N_{corr}$

where N_{corr} may be obtained from the table below. $(N_1)_{60}$ is the number of SPT blow count normalized to an overburden pressure of 1 ton/ft^2 (96 kPa) and corrected to an energy ratio of 60%.

Note: $(N_1)_{60} = C_N N_{60}$ (see below)
$N_{60} = N C_{60}$ (see next page)

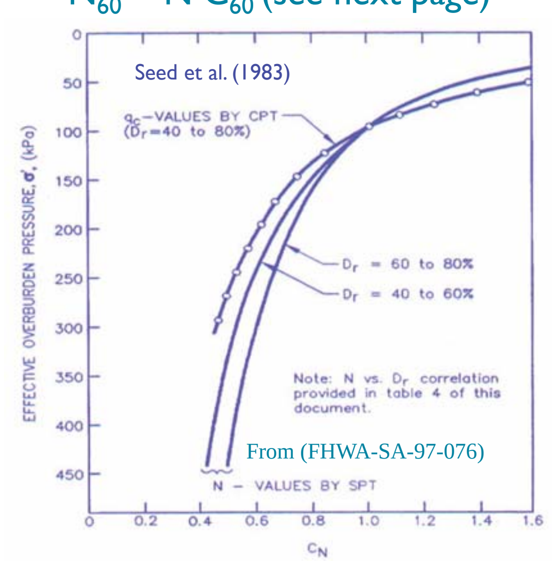

(Table from Kramer 1996)

Table 1. Recommeded Fines Correction for Estimation of Residual Undrained Strength by Seed–Harder and Stark–Mesri Procedures

	N_{corr} (blows/ft)	
Percent Fines	Seed–Harder	Stark–Mesri
0	0	0
10	1	2.5
15	—	4
20	—	5
25	2	6
30	—	6.5
35	—	7
50	4	7
75	5	7

Comment: All recommendations related to "fines" continue to be likely to change in the near future ..

Correction for	Correction Factor	Reference
Nonstandard Hammer Type (DH = doughnut hammer; ER = energy ratio)	C_{HT}=0.75 for DH with rope and pully C_{HT}=1.33 for DH with trip/auto & ER=80	Seed et al. (1985)
Nonstandard Hammer Weight or Height of Fall (H = height of fall in mm; W = hammer weight in kg)	$C_{HW} = \frac{H \cdot W}{63.5 \cdot 762}$	calculated per Seed et al. (1985)
Nonstandard Sampler Setup (standard samples with room for liners, but used without liners)	C_{SS} = 1.10 for loose sand C_{SS} = 1.20 for dense sand	Seed et al. (1985)
Nonstandard Sampler Setup (standard samples with room for liners, and liners are used)	C_{SS} = 0.90 for loose sand C_{SS} = 0.80 for dense sand	Skempton (1986)
Short Rod Length	C_{RL} = 0.75 for rod length 0-3 m	Seed et al. (1983)
Nonstandard Borehole Diameter	C_{BD} = 1.05 for 150 mm borehole diameter C_{BD} = 1.15 for 200 mm borehole diameter	Skempton (1986)

Notes: N = Uncorrected SPT blow count.
$C_{60} = C_{HT} \cdot C_{HW} \cdot C_{SS} \cdot C_{RL} \cdot C_{BD}$
$N_{60} = N \cdot C_{60}$
C_N = Correction factor for overburden pressure.
$(N_1)_{60} = C_N \cdot N_{60} = C_N \cdot C_{60} \cdot N$

C_{60} from Richardson et al. (1995)

From (FHWA-SA-97-076)

II. If the soil is susceptible, will liquefaction be triggered?

(by cyclic stress approach)

Step 1. Calculate equivalent cyclic shear stress induced by a given earthquake (i.e., the "Demand"). Herein, this is dictated by an expected peak acceleration at the site scaled by a factor of 0.65 based on engineering judgment.

$$\tau_{cyc} = 0.65 \frac{a_{max}}{g} \sigma_v \, r_d = CSR \, \sigma'_{v0} \qquad (1)$$

where a_{max} is the peak ground surface acceleration, g the acceleration of gravity, σ_v the total vertical stress, and r_d the value of a stress reduction factor at the depth of interest. r_d may be obtained from Figure 3 below. This equation also defines CSR, the cyclic stress ratio, with σ'_{v0} being the initial vertical effective stress.

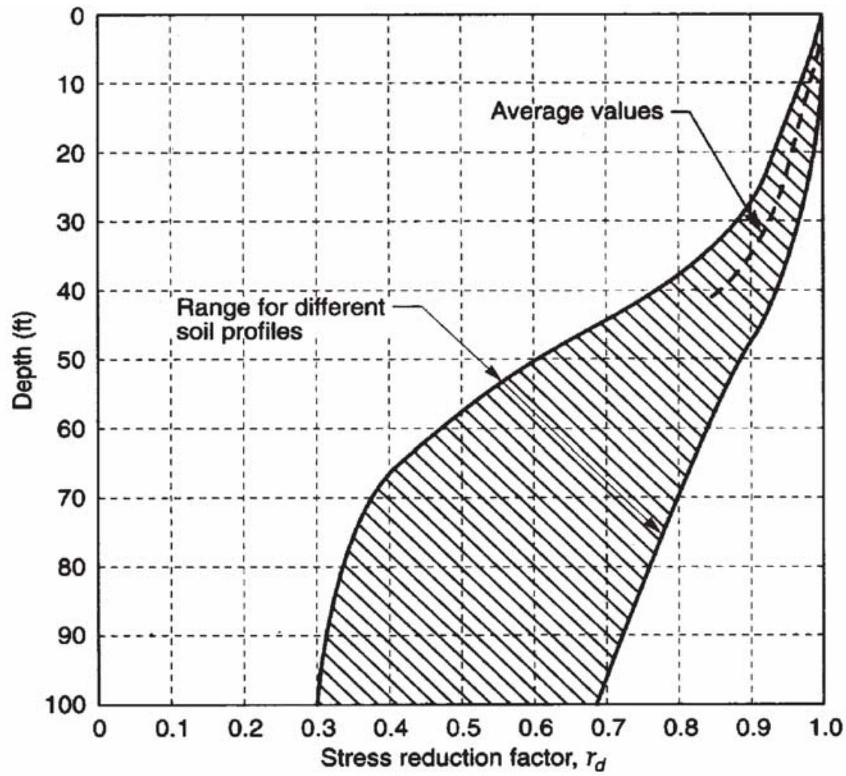

(Figure from Kramer 1996)

Figure 9.25 Reduction factor to estimate the variation of cyclic shear stress with depth
Figure 3. or gently sloping ground surfaces. (After Seed and Idriss, 1971.)

II. If the soil is susceptible, will liquefaction be triggered? (Cont'd)

by cyclic stress approach

Step 2. Calculate the cyclic shear stress required to cause liquefaction

(i.e., the "capacity"):

$$\tau_{cyc,L} = CSR_L\ \sigma'_{v0} \qquad (2)$$

where σ'_{v0} is the initial vertical effective stress, CSR_L is the cyclic stress ratio, and may be obtained based on:

- SPT resistance (Fig. 4 for clean sands, Fig. 5 for silty sands).
- CPT resistance (Fig. 8).

• See also references for Shear wave velocity (Andrus and Stokoe 2000) and Arias Intensity (Kayen and Mitchell 1997) based techniques.

(Figure from Kramer 1996)

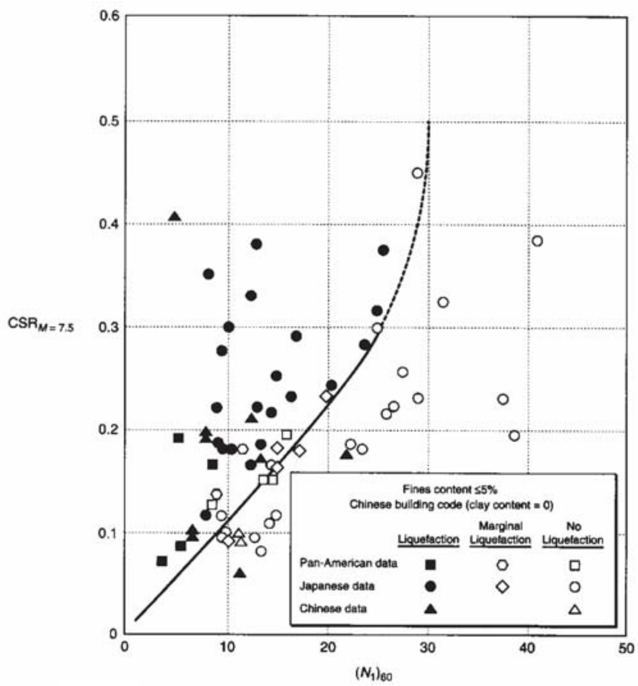

Figure 4. Relationship between cyclic stress ratios causing liquefaction and $(N_1)_{60}$ values for clean sands in $M = 7.5$ earthquakes. (After Seed et al. (1975). Influence of SPT procedures in soil liquefaction resistance evaluations, *Journal of Geotechnical Engineering*, Vol. 111, No. 12. Reprinted by permission of ASCE.)

(Figure from Kramer 1996)

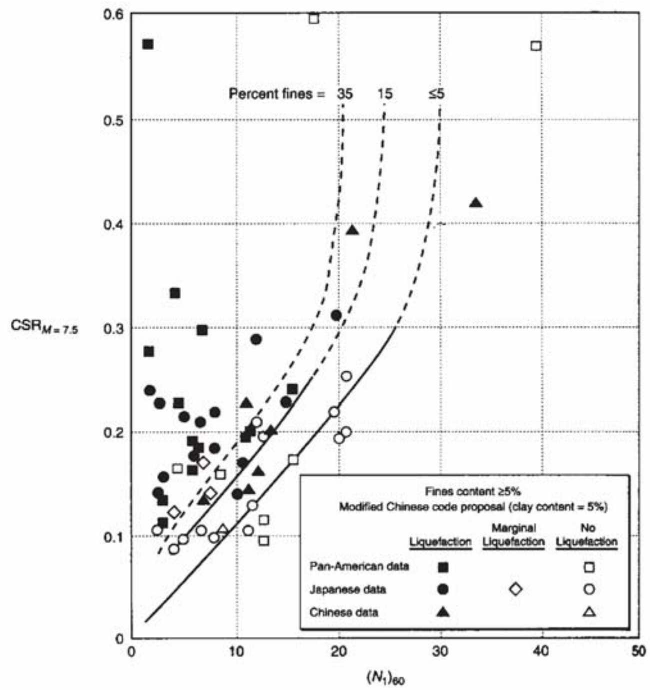

Figure 5. Relationship between cyclic stress ratios causing liquefaction and $(N_1)_{60}$ values for silty sands in $M = 7.5$ earthquakes. (After Seed et al. (1975). Influence of SPT procedures in soil liquefaction resistance evaluations, *Journal of Geotechnical Engineering*, Vol. 111, No. 12. Reprinted by permission of ASCE.)

Note:

1. Use the following table for earthquake magnitudes other than *M*=7.5

Table 2. Magnitude Correction Factors for Cyclic Stress Approach

Magnitude, *M*	$CSR_M/CSR_{M=7.5}$
$5\frac{1}{4}$	1.50
6	1.32
$6\frac{3}{4}$	1.13
$7\frac{1}{2}$	1.00
$8\frac{1}{2}$	0.89

(Table from Kramer 1996)

2. The influence of plasticity could be accounted for by multiplying the CSR_L by the factor (Ishihara 1993):

$$F = \begin{cases} 1.0 & \mathrm{PI} \le 10 \\ 1.0 + 0.022(\mathrm{PI} - 10) & \mathrm{PI} > 10 \end{cases}$$

3. Figs. 4 and 5 are mainly for level-ground sites, and shallow liquefaction. To account for site slope (initial shear stress) and deep liquefaction, modify the CSR_L by:

$$CSR_{\alpha,\sigma} = CSR_L\ K_\alpha\ K_\sigma \qquad (3)$$

where $\alpha = \tau_{h,static} / \sigma'_{v0}$ and K_α and K_σ are correction factors that may be obtained from Figs. 6 and 7 below.

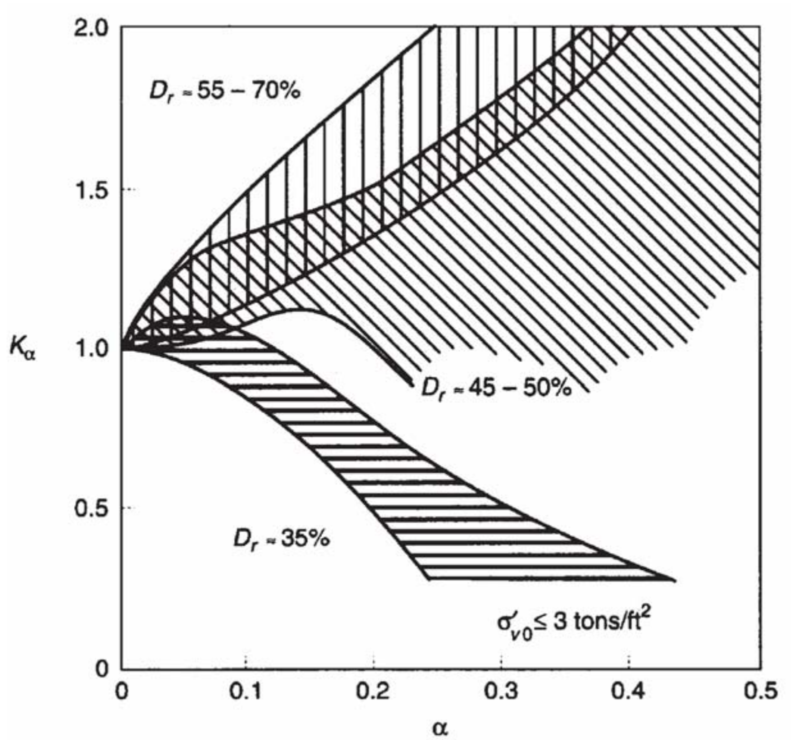

(Figure from Kramer 1996)

Figure 6. Variation of correction factor, K_α, with initial shear/normal stress ratio. (After Seed and Harder, 1990. *H. Bolton Seed Memorial Symposium Proceedings*, Vol. 2, p. 364. Used by permission of BiTech Publishers, Ltd.)

The data in this figure is not accepted fully by all experts

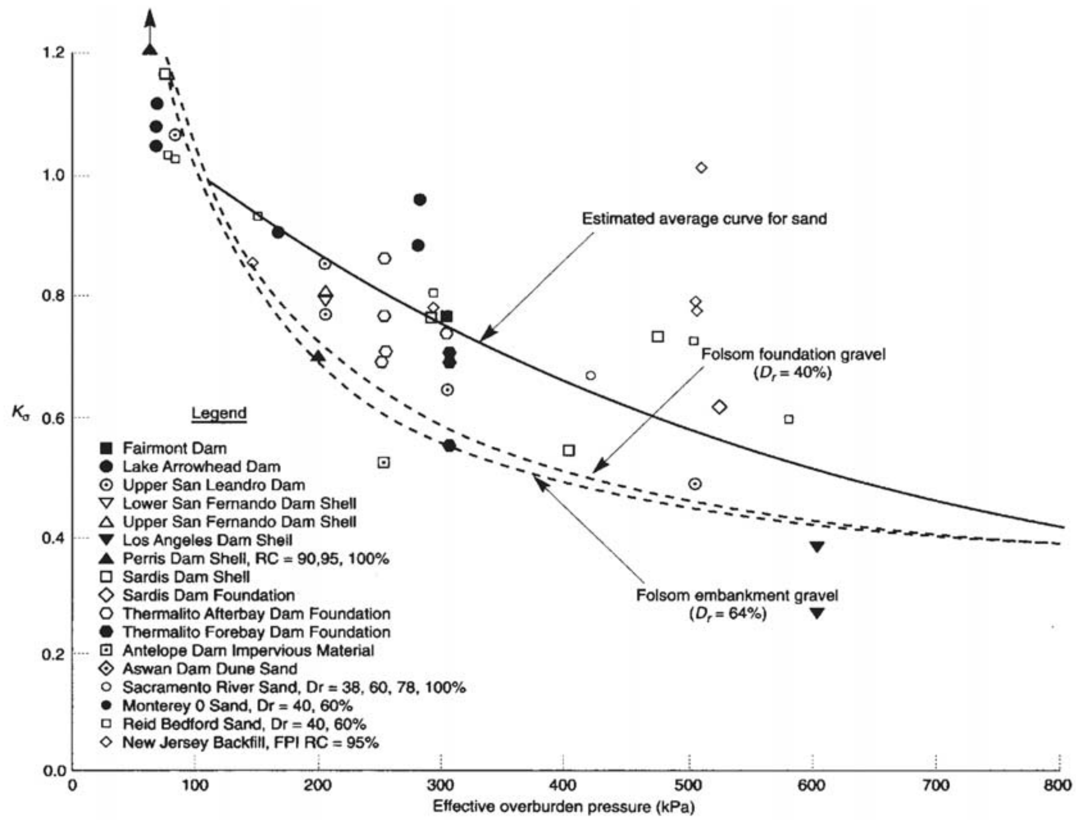

Figure 7.a Variation of correction factor, K_σ, with effective overburden pressure. (After Marcuson et al., 1990. Used by permission of EERI.)

(Figure from Kramer 1996)

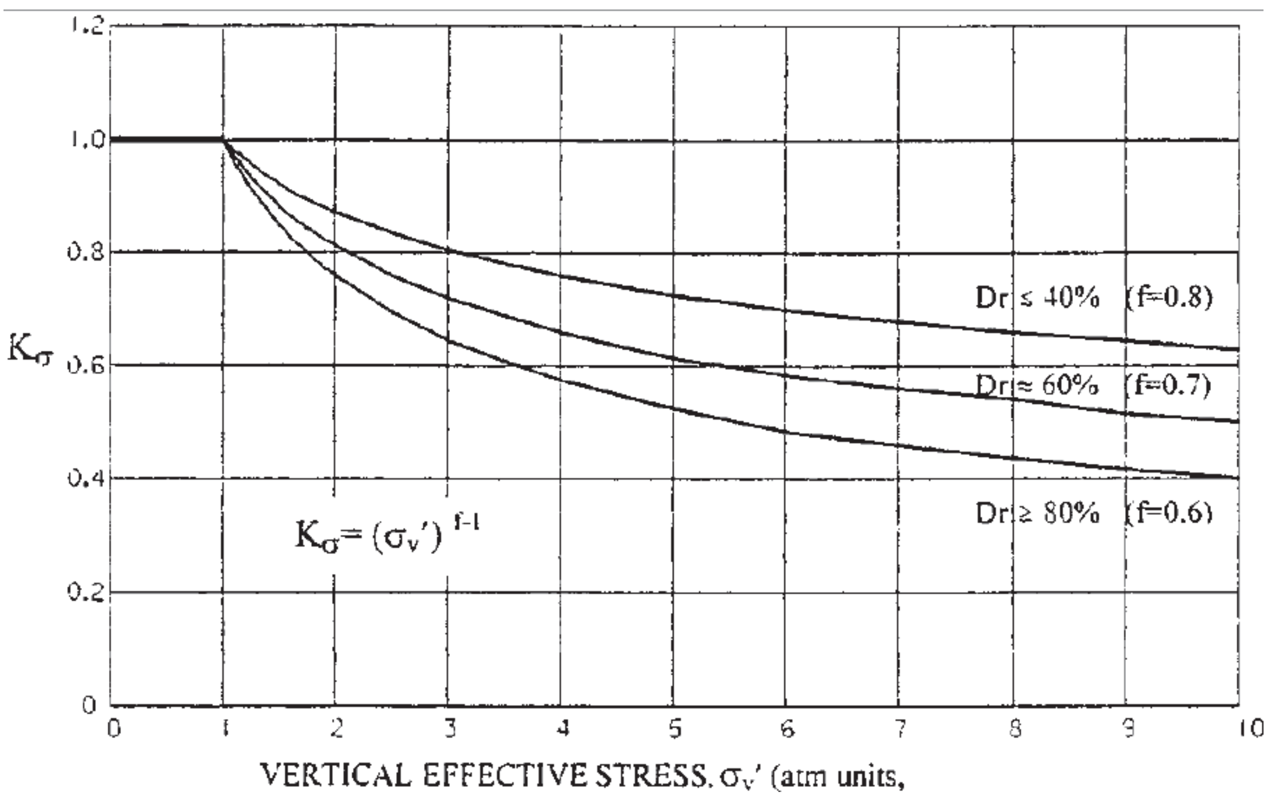

Fig. 7b: Recommended for practice by Youd et al. 2001

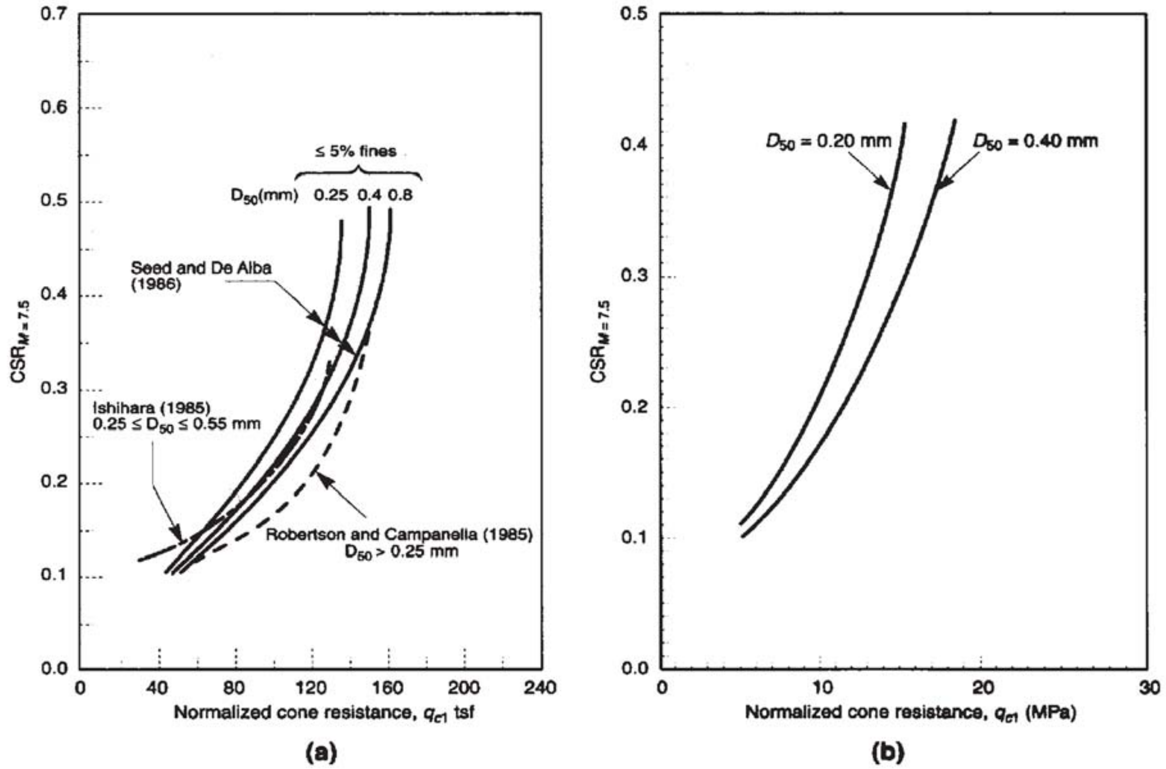

Figure 8. CPT-based liquefaction curves: (a) based on correlations with SPT data; (b) based on theoretical/experimental results. (After Mitchell and Tseng, 1990, H. Bolton Seed Memorial Symposium Proceedings, Vol. 2, p. 347. Used by permission of BiTech Publishers, Ltd.)

(Figure from Kramer 1996)

Note:

1. In Fig. 8, q_{c1} is the tip resistance q_c normalized to a standard effective overburden pressure p_a of 1 ton/ft^2 (96 kPa) by:

$$q_{c1} = q_c \left(\frac{p_a}{\sigma'_{v0}} \right)^{0.5} \qquad \text{or} \qquad q_{c1} = \frac{1.8}{0.8 + \sigma'_{v0}} q_c$$

Where σ'_{v0} is the initial effective overburden pressure.

2. The effects of fines can be accounted for by adding tip resistance increments to the measured tip resistance q_c (Ishihara 1993):

Fines Content (%)	Tip Resistance Increment (tons/ft^2)
≤ 5	0
~ 10	12
~ 15	22
~ 35	40

(Table from Kramer 1996)

3. Use Table 2 for earthquake magnitudes other than M=7.5

II. If the soil is susceptible, will liquefaction be triggered? (cont'd)

by cyclic stress approach

Step 3. Calculate the safety factor against liquefaction.

$$FS_L = \frac{\tau_{cyc,L}}{\tau_{cyc}} = \frac{CSR_L}{CSR} = \frac{CRR}{CSR} \qquad (4)$$

Liquefaction may be triggered if $FS_L < 1$.

Note: CRR above is Cyclic Resistance Ratio

Note:
To more accurately represent the earthquake shaking energy, Youd et al. (2001) suggested including a Magnitude Scaling Factor of the form

$MSF = (7.5/M_w)^n$

where M_w is Moment magnitude, and n = 2.56 for M_w = 7.5 or greater, and up to 3.3 for M_w less than 7.5

As such, $a_{maxM7.5} = a_{max} / MSF$

and

$$\tau_{cycM\,7.5} = 0.65 \frac{a_{\max M\,7.5}}{g} \sigma_v \, r_d = CSR_{M\,7.5}\, \sigma'_{v0}$$

With this adjustment, both *CSR* and *CSR*$_L$ can be compared directly for M=7.5

If liquefaction is triggered, how much Settlement will occur

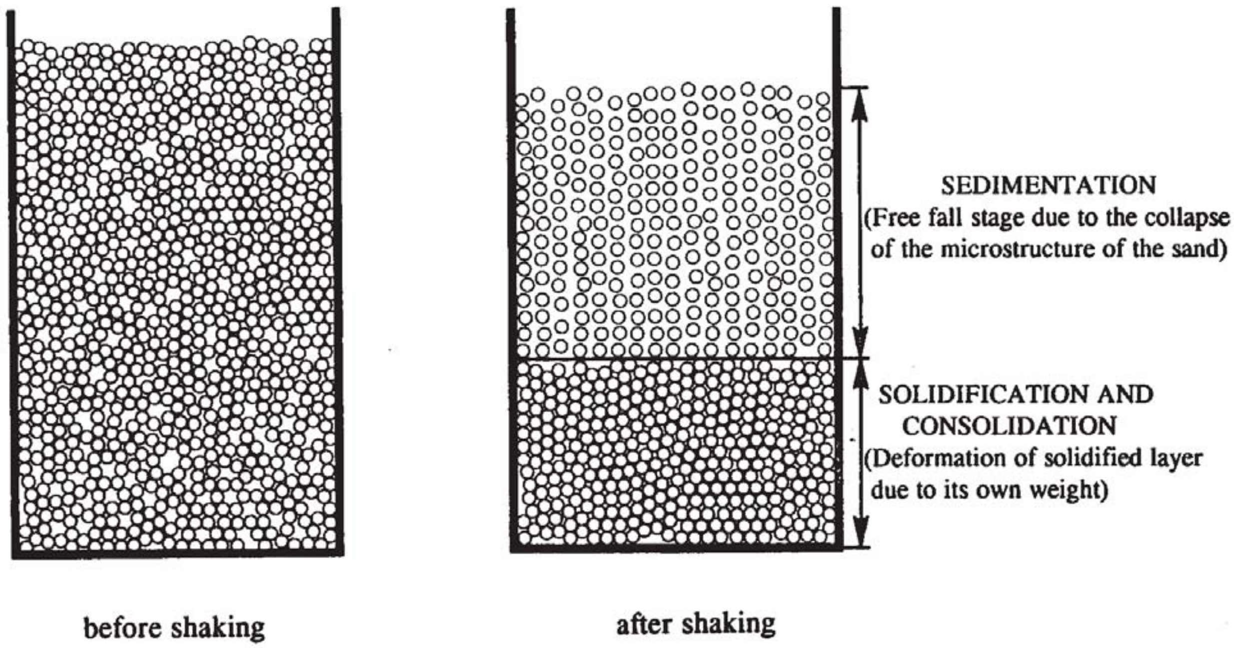

III. If liquefaction is triggered, how much damage would occur?

Settlement by Tokimatsu-Seed method

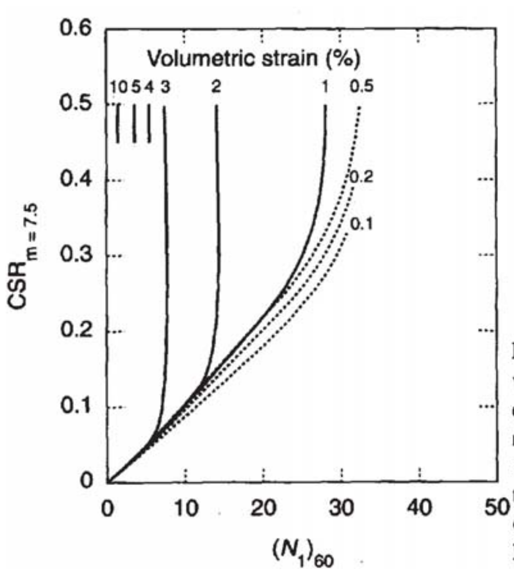

(Figure from Kramer 1996)

Figure 9.53 Chart for estimation of volumetric strain in saturated sands from cyclic stress ratio and standard penetration resistance. (After Tokimatsu and Seed, 1987. Evaluation of settlements in sand due to earthquake shaking, *Journal of Geotechnical Engineering*, Vol. 113, No. 8. Reprinted by permission of ASCE.)

Table 9-2 Magnitude Correction Factors for Cyclic Stress Approach

Magnitude, M	$CSR_M/CSR_{M=7.5}$
$5\frac{1}{4}$	1.50
6	1.32
$6\frac{3}{4}$	1.13
$7\frac{1}{2}$	1.00
$8\frac{1}{2}$	0.89

(Table from Kramer 1996)

To use Fig. 9.53, the *CSR* can be calculated from Equation (1). For earthquake magnitudes other than 7.5, the *CSR* should be modified according to the Table above.

III. If liquefaction is triggered, how much damage would occur?

Settlement by Ishihara-Yoshimine method

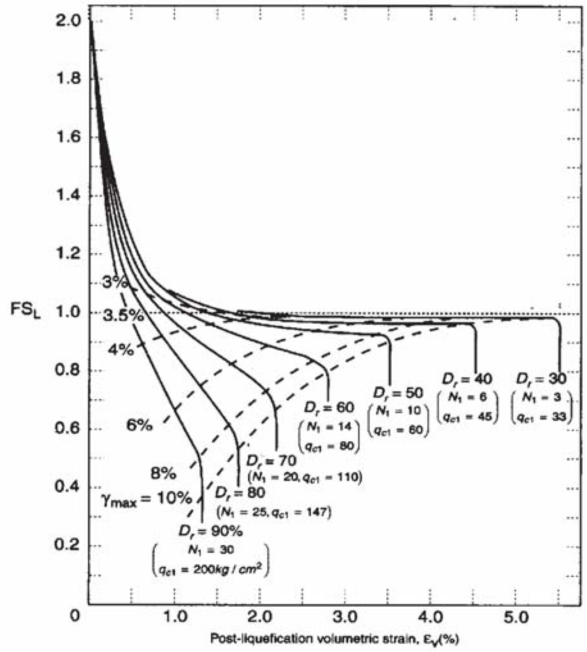

Figure 9.54 Chart for estimating postliquefaction volumetric strain of clean sand as function of factor of safety against liquefaction or maximum shear strain. (After Ishihara and Yoshimine, 1992; used by permission of JSSMFE.)

To use Fig. 9.54, the FS_L can be calculated using Equation (4).

Note $N_1 = 0.833(N_1)_{60}$

(Figure from Kramer 1996)

III. If liquefaction is triggered, how much damage would occur?

Residual Strength (see Fig. 2). In addition, for the residual shear strength S_r, Olson and Stark (2002) proposed:

$S_r/\sigma'_{vo} = 0.03 + 0.0075\ (N_1)_{60}$ plus or minus 0.03

for $(N_1)_{60}$ less or equal to 12

and

$S_r/\sigma'_{vo} = 0.03 + 0.0143\ (q_{c1})$ plus or minus 0.03

for q_{c1} less than or equal to 6.5 Mpa

Earlier, Baziar and Dobry (1995) proposed for loose silty sands:

$S_r = 0.12 - 0.19\ (\sigma'_{vo}\ )$

See Idriss and Boulanger (2008) EERI Monograph for Additional details

Courtesy M. Fraser

Summary of SPT-Based Empirical Method NCEER/NSF Proceedings (Youd et al., 2001)

Step 1 – Discretize boring log into a series of soil layers;

Step 2 – For each soil layer, compute the vertical total stress (σ_{vo}) and vertical effective stresses (σ'_{vo});

Step 3 –Determine Moment Magnitude and Peak Ground Acceleration (a_{max}) for project site;

Step 4 – Compute the Stress reduction coefficient, r_d ;

Step 5 – Compute the Cyclic Stress Ratio, CSR;

Step 6 – Compute $(N_1)_{60}$ the SPT blow count normalized to overburden pressure of 100 kPa (1ton/sq ft) and hammer energy ratio or hammer efficiency of 60%;

Step 7 – Adjust $(N_1)_{60}$ to account for fines content (FC) by calculating the equivalent clean sand value, $(N_1)_{60CS}$;

Step 8 – Calculate the Cyclic Resistance Ratio for Magnitude 7.5 earthquake, $CRR_{7.5}$;

Step 9 – Calculate the Magnitude Scaling Factor, MSF;

Step 10 – Calculate the Factor of Safety (FS) against liquefaction; and

Step 11 – Calculate the volumetric strain / settlement within each liquefied layer.

See Idriss and Boulanger (2008) EERI Monograph for Additional details

Courtesy M. Fraser

SPT-Based Empirical Method – Idriss & Boulanger, 2008

Step 1 – Discretize boring log into a series of soil layers;

Step 2 – For each soil layer, compute the vertical total stress (σ_{vo}) and vertical effective stresses (σ'_{vo});

Step 3 – Determine Moment Magnitude and Peak Ground Acceleration (a_{max}) for project site;

Step 4 – Determine the shear stress reduction coefficient, r_d ;

Step 5 – Compute the Cyclic Stress Ratio, CSR;

Step 6 – Compute $(N_1)_{60}$ the SPT blow count normalized to overburden pressure of 100 kPa (1ton/sq ft) and hammer energy ratio or hammer efficiency of 60%;

Step 7 – Adjust $(N_1)_{60}$ to account for fines content (FC) by calculating the equivalent clean sand value, $(N_1)_{60CS}$;

Step 8 – Calculate the Cyclic Resistance Ratio for Magnitude 7.5 earthquake, $CRR_{7.5}$;

Step 9 – Calculate the Magnitude Scaling Factor, MSF;

Step 10 – Adjust the Cyclic Resistance Ratio for actual earthquake magnitude and overburden stress ($CRR_{M,\sigma'_{vc}}$);

Step 11 – Calculate the Factor of Safety (FS) against liquefaction; and

Step 12 – Calculate the volumetric strain / settlement within each liquefied layer.

Soil Dynamics Short Course

This presentation consists of two parts:

Section 1

Liquefaction of fine grained soils and cyclic softening in silts and clays

Section 2

Empirical relationship for prediction of Lateral Spreading

Liquefaction of fine grained soils and cyclic softening in silts and clays

Main References

Boulanger, R.W., and Idriss, I. M. (2004). "Evaluating the potential for liquefaction or cyclic failure of silts and clays." Rep. UCD/CGM-04/01, Univ. of Calif., Davis, California.

Boulanger, R.W., and Idriss, I. M. (2006). "Liquefaction susceptibility criteria for silts and clays." J. Geotech. Geoenviron. Eng., 132, 11, pp. 1413–1426.

Bray, J. D., and Sancio, R. B. (2006). "Assessment of the liquefaction susceptibility of fine-grained soils." J. Geotech. Geoenviron. Eng., 132, 9, pp. 1165–1177.

Boulanger, R.W., and Idriss, I. M. (2007). "Evaluation of cyclic softening in silts and clays," Journal of Geotechnical and Geoenvironmental Engineering, Vol. 133, No. 6, June.

Idriss, I. M., and Boulanger, R.W. (2008) "Soil Liquefaction during Earthquakes," EERI Monograph, MNO-12, Richmond, CA.

Notation

w_c = Water content = (weight of water / weight of soil) %

LL = Liquid Limit = w_c at which soil starts acting like a liquid

PL = Plastic Limit = w_c at which the soil starts to exhibit plastic behavior

PI = Plasticity Index = *LL* – *PL* =range of w_c when soil exhibits plasticity

e = void ratio = volume of voids / volume of solids

S_u = Undrained shear strength

OCR = Overconsolidation Ratio

Notes:

1. Low *PI* implies low or lack of significant cohesion
2. High *PI* implies presence of high cohesion
3. Higher e implies looser soil samples with lower shear resistance, more susceptibility to liquefaction, and higher potential for post-liquefaction settlement (permanent volumetric strain). For a given soil, these effects are judged more precisely by the Relative Density $D_r = (e_{max}\text{-}e) / (e_{max}\text{-}e_{min})$ %

Highlights

Based on post-earthquake reconnaissance and related soil-testing and analysis:

The “Chinese Criteria” about liquefaction resistance of fine grained soils is not correct. It is based on % clay content with no regard to its plasticity (PI) which makes all the difference.

If relatively non-plastic, saturated fine grained soils can build-up significant excess pore water pressure and liquefy.

Cyclic loading of soft clays degrades strength and softens the shear resistance potentially leading to large objectionable deformations.

Sand-type excess pore-pressure build-up likely for scenarios of w_c / *LL* > 0.85 and PI < or equal 12; being relatively non-plastic soils (some suggest PI < or equal 7) …..These soils exhibit a cyclic mobility-type response …

Clay-type softening behavior likely for soil with w_c / *LL* > 0.8 and 18 > PI > 12 (some suggest PI > 7) …. gradual reduction in shear stiffness and strength …

For PI > 18 soils tested at low confining pressure, potential for loss of shear resistance was minimal, but significant deformation is possible under strong shaking conditions.

Bray and Sancio suggest ***PI*** rather than % ***fines*** to account for higher Liquefaction resistance

A procedure similar to the Liquefaction Cyclic Stress Approach (described earlier) has been developed for cyclic clay softening scenarios (Boulanger + Idriss).

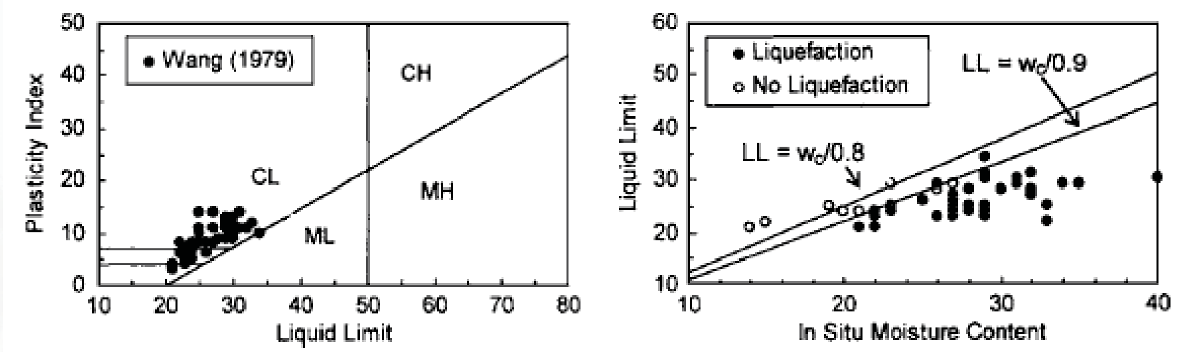

Fig. 2. Data presented by Wang (1979) which led to the development of the Chinese Criteria

Figure from Bray and Sancio (2006) showing Chinese data left of the A-line indicating relatively high plasticity (a key issue that was overlooked when the Chinese Criteria was formulated). Note: CL = Clays of Low Plasticity, CH = Clays of High Plasticity, ML = Silts of Low Plasticity, CH =Silts of High Plasticity.

Seed and Idriss (1982) stated that clayey soils could be susceptible to liquefaction *only if all three* of the following conditions are met: 1) percent of particles less than 0.005 mm <15%, 2) LL < 35, and 3) w_c / *LL > 0.9. Due to* its origin, this standard is known as the **"Chinese criteria."**

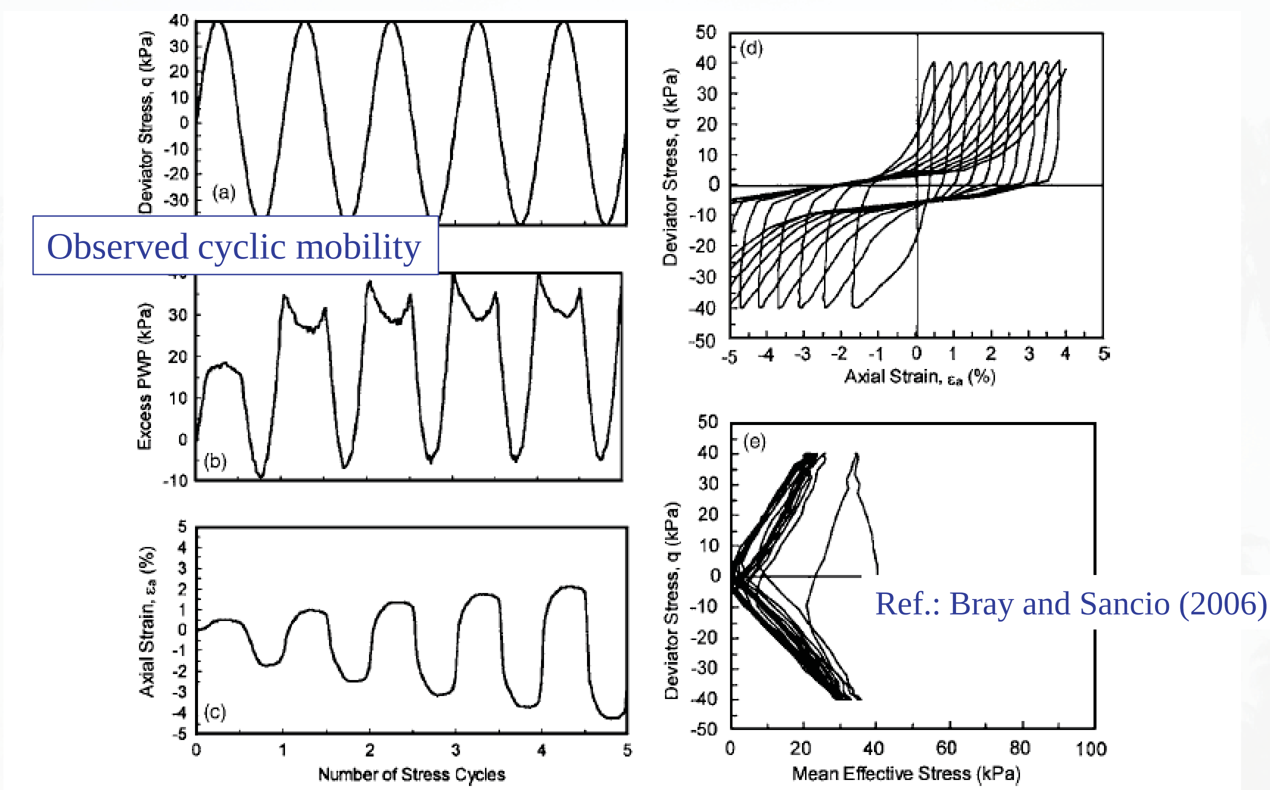

Fig. 5. Results of a slow cyclic triaxial test (loading frequency of 0.005 Hz) on Specimen F7-P3A (ML, PI=0, e=0.76): (a) deviator stress versus number of load cycles; (b) excess pore water pressure versus number of load cycles; (c) axial strain versus number of load cycles; (d) deviator stress versus axial strain; and (e) deviator stress versus mean effective confining stress

Observed cyclic mobility response in fine grained soils

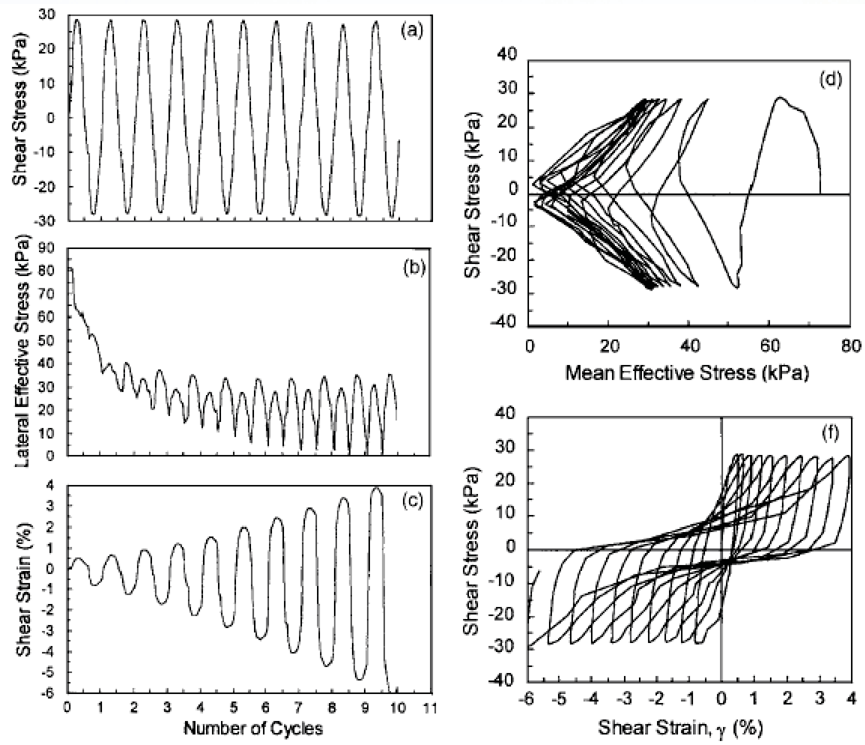

Fig. 9. Results of a cyclic simple shear test (f=1 Hz) on Specimen G4-P3 (ML, PI=0, e=0.83): (a) shear stress versus number of load cycles; (b) lateral effective stress versus number of load cycles; (c) shear strain versus number of load cycles; (d) shear stress versus mean effective stress; and (e) shear stress versus shear strain

Ref.: Bray and Sancio (2006)

Influence of *PI* on observed deformation

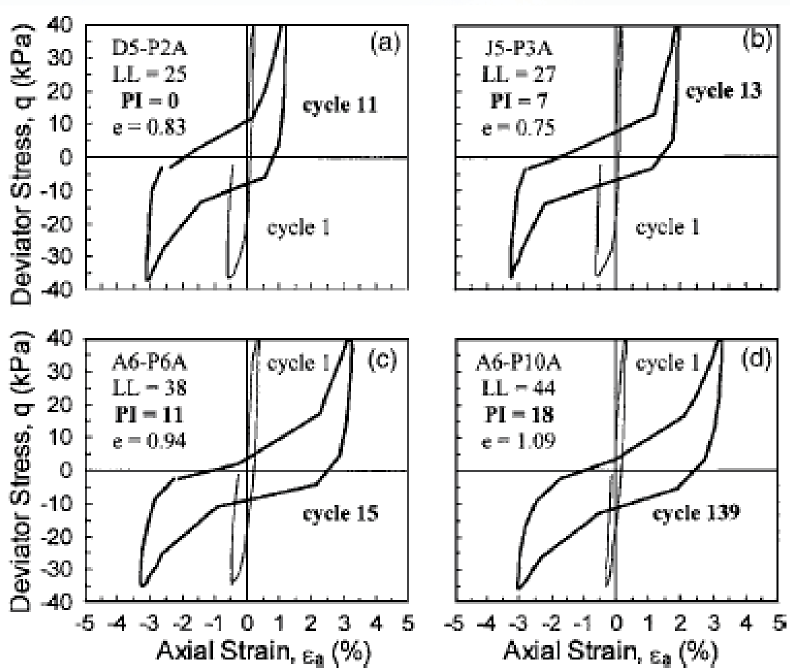

Fig. 6. Stress-strain relationship for the first cycle of loading (fine line) and the cycle at which −3% axial strain is reached (thick line) for four specimens of increasing plasticity. The tests were performed on soils initially isotropically consolidated to an effective stress of 50 kPa.

Ref.: Bray and Sancio (2006)

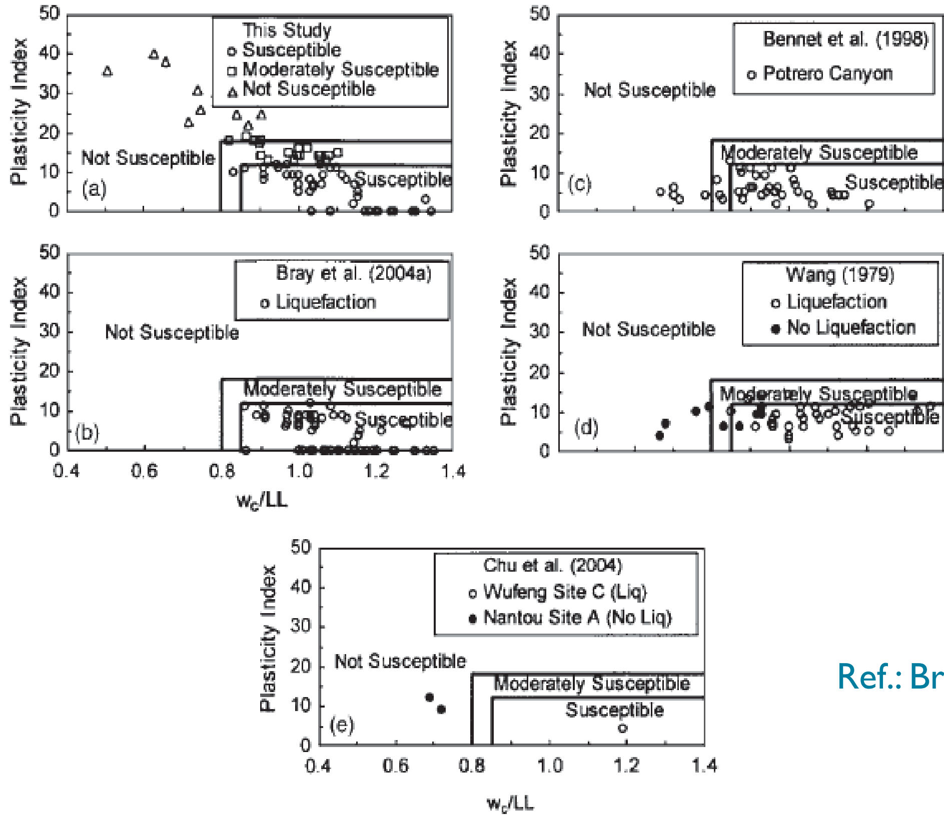

Ref.: Bray and Sancio (2006)

Fig. 13. Graphical representation of the proposed liquefaction susceptibility criteria: (a) isotropically consolidated CTX testing data from this study; (b) field data from Bray et al. (2004a); (c) Potrero Canyon field data from Bennett et al. (1998); (d) field data from Wang (1979); and (e) field data from Chu et al. (2004)

Cyclic reduction of shear stiffness and strength in Saturated clay

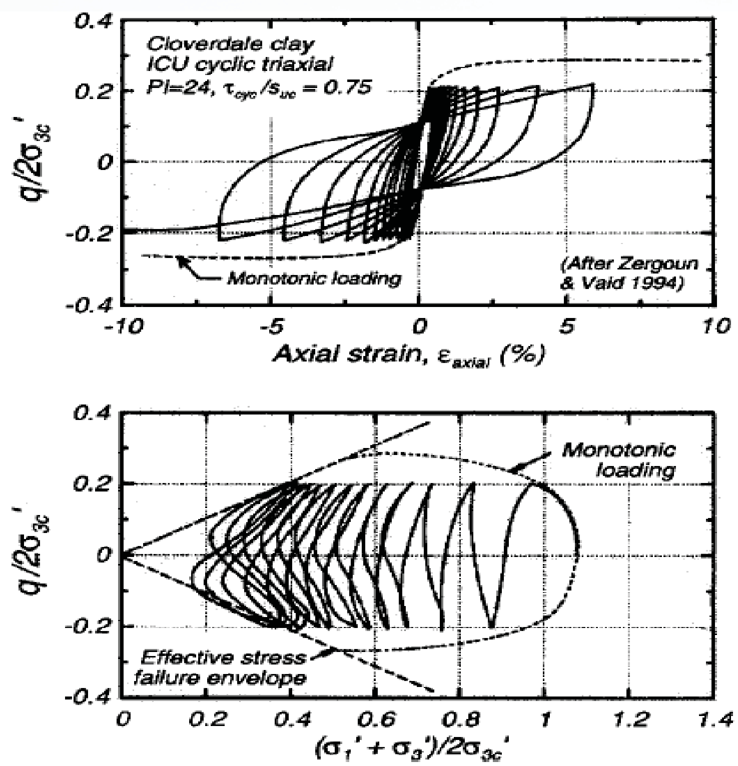

Fig. 4. Stress-strain response and effective stress paths for Cloverdale clay during undrained slow cyclic loading (adapted from Zergoun and Vaid 1994, used with permission)

Ref.: Boulanger and Idriss (2007)

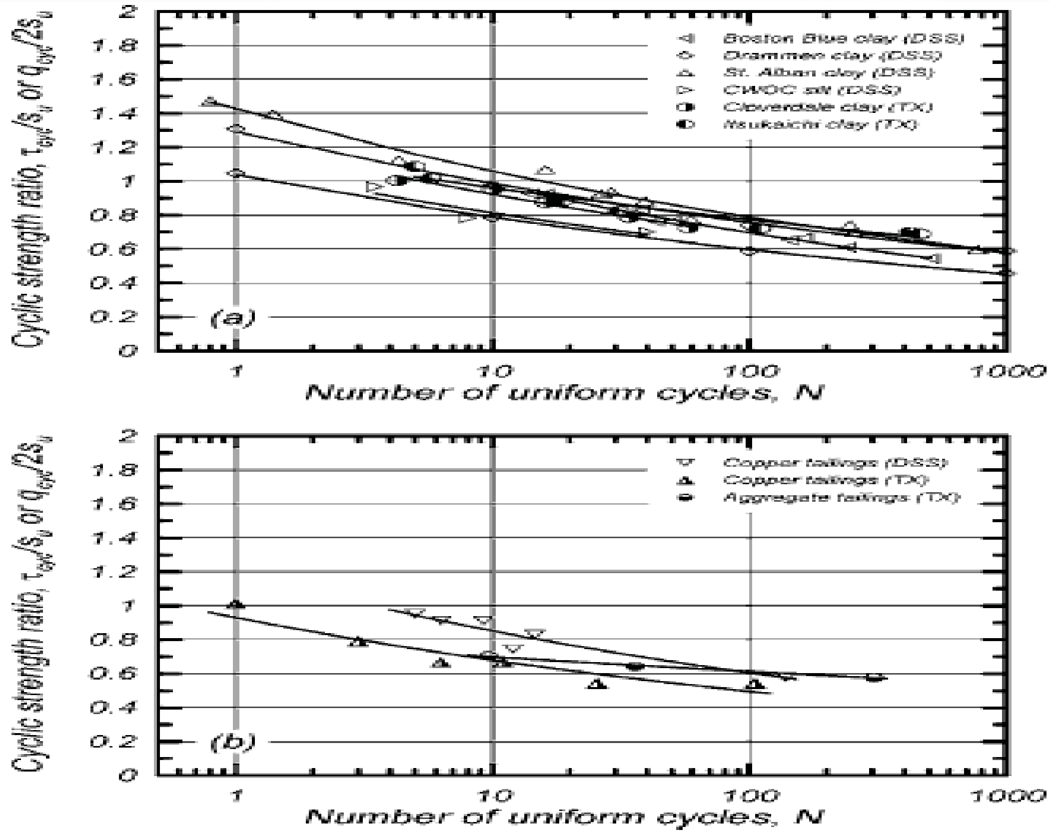

Fig. 1. Cyclic strength ratios to cause cyclic failure versus number of uniform loading cycles at a frequency of 1 Hz: (a) natural soils; (b) tailings materials

Ref.: Boulanger and Idriss (2007) 3% shear strain

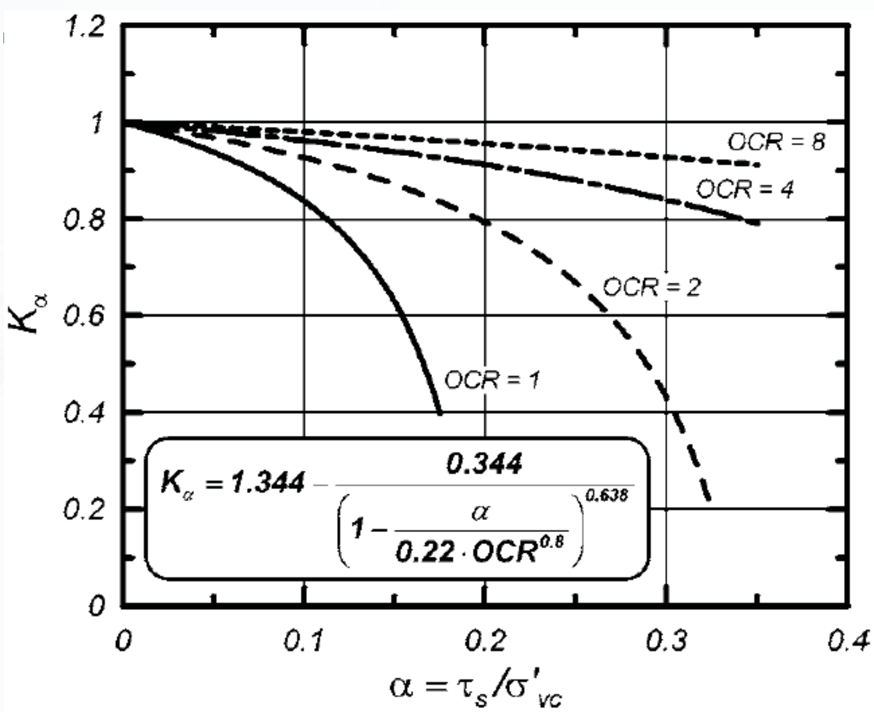

Slope shear stress impacts NC clay (OCR = 1) as acting stress nears shear strength (minimal impact on highly OC clays

Ref.: Boulanger and Idriss (2007)

Fig. 6. K_α versus α for clay at various OCR

$$CRR_{M=7.5} = 0.18 \cdot OCR^{0.8} \cdot K_\alpha$$

See Boulanger and Idriss (2007) for full details

UNIFIED SOIL CLASSIFICATION INCLUDING IDENTIFICATION AND DESCRIPTION

Major division	Subdivision	FIELD IDENTIFICATION PROCEDURES (excluding particles larger than 3 inches and basing fractions on stimated weights)	GROUP SYMBOLS	TYPICAL NAMES	INFORMATION REQUIRED FOR DESCRIBING SOILS		LABORATORY CLASSIFICATION CRITERIA
COARSE GRAINED SOILS More than half of materials is <u>larger</u> than No. 200 sieve size	GRAVELS More than half of coarse fraction is larger than No. 4 sieve size (For visual classification, the 1/4" size may be used as equivalent for the No. 4 sieve size) — CLEAN GRAVELS (Little or no fines)	Wide range in grain size and substantial amounts of all intermediate particle sizes	GW	Well graded gravels, gravel-sand mixtures, little or no fines	Give typical name; indicate approximate percentage of sand and gravel, max. size; angularity, surface condition, and hardness of the coarse grains; local or geological name and other pertinent descriptive information, and symbol in parentheses	Use grain size curve in identifying the fractions as given under field identification. Determine percentages of gravel and sand from grain size curve. Depending on percentage of fines (fraction smaller than No. 200 sieve size) coarse grained soils are classified as follow: Less than 5% GW, GP, SW, SP. More than 12% GM, GC, SM, SC. 5% to 12% <u>Borderline</u> cases requiring use of dual symbols	$C_u = \frac{D_{60}}{D_{10}}$ Greater than 4; $C_c = \frac{(D_{30})^2}{D_{10} \times D_{60}}$ between one and 3
		Predominantly one size or a range of sizes with same intermediate sizes missing	GP	Poorly graded gravels, gravel-sand mixtures, little or no fines			Not meeting all gradation requirements for GW
	GRAVELS WITH FINES (Appreciable amount of fines)	Non-plastic fines (for identification procedures see ML below)	GM	Silty gravel, poorly graded gravel-sand silt mixtures	For undisturbed soils add information on stratification, degree of compactness, cementation, moisture conditions and drainage characteristics		Atterberg limits above "A" line with PI greater than 7 — Above "A" line with PI between 4 and 7 are <u>borderline</u> cases requiring use of dual symbols
		Plastic fines (for identification procedures see CL below)	GC	Clayey gravels, poorly graded gravel-sand clay mixtures			Atterberg limits below "A" line or PI greater than 7
	SANDS More than half of coarse fraction is smaller than No. 4 sieve size — CLEAN SANDS (Little or no fines)	Wide range in grain sizes and substantial amount of all intermediate particle sizes	SW	Well graded sands, gravelly sands, little or no fines			$C_u = \frac{D_{60}}{D_{10}}$ Greater than 6; $C_c = \frac{(D_{30})^2}{D_{10} \times D_{60}}$ between one and 3
		Predominantly one size or a range of sizes with some intermediate sizes missing	SP	Poorly graded sand, gravelly sands, little or no fines	EXAMPLE: <u>Silty sand</u> gravelly; about 20% hard, angular gravel particle $\frac{1}{2}$ - in maximum size; rounded and subangular sand grains coarse to fine; about 15% non-plastic fines with low dry strength; well compacted and moist in place; alluvial sand; (SM)		Not meeting all gradation requirements for SW
	SANDS WITH FINES (Appreciable amount of fines)	Non-plastic fines (for identification procedures see CL below)	SM	Silty sand, poorly graded sand-silt mixtures			Atterberg limits below "A" line or PI less than 4 — Above "A" line with PI between 4 and 7 are <u>borderline</u> cases requiring use of dual symbols
		Plastic fines (for identification procedures see CL below)	SC	Clayey sand, poorly graded sand-clay mixtures			Atterberg limits above "A" line with PI greater than 7

(The No. 200 sieve size is about the smallest particle visible to the naked eye)

Major division	Subdivision	DRY STRENGTH (CRUSHING CHARACTERISTICS)	DILATANCY (REACTION TO SHAKING)	TOUGHNESS (CONSISTENCY NEAR PLASTIC LIMIT)	GROUP SYMBOLS	TYPICAL NAMES	INFORMATION REQUIRED FOR DESCRIBING SOILS
FINE GRAINED SOILS More than half of materials is <u>smaller</u> than No. 200 sieve size	IDENTIFICATION PROCEDURES ON FRACTION SMALLER THAN No 40 SIEVE SIZE						
	SILTS AND CLAYS Liquid limit less than 50	None to slight	Quick to slow	None	ML	Inorganic silts and very fine sands, rock flour, silty or clayey fine sand with slight plasticity	Give typical name; indicate degree and character of plasticity, amount and maximum size of coarse grains; color in wet condition, odor, if any, local or geologic name, and other pertinent descriptive information, and symbol in parentheses
		Medium to high	None to very slow	Medium	OL	Inorganic clays of low to medium plasticity, gravelly clays, sandy clays, silty clays, lean clays	
		Slight to medium	Slow	Slight	MN	Organic silts and organic silt-clays of low plasticity	For undisturbed soils add information on structure, stratification, consistency in undisturbed and remolded strates, moisture and drainage conditions
	SILTS AND CLAYS Liquid limit greater than 50	Slight to medium	Slow to none	Slight to medium	OL	Inorganic silt, micaceous or diatomaceus fine sandy or silty soils, elastic silts	
		High to very high	None	High	CH	Inorganic clays of high organic plasticity	EXAMPLE:
		Medium to high	None to very slow	Slight to medium	OH	Organic clays of medium to high plasticity	Clayey silt, brown, slightly plastic; small percentage of fine sand; numerous vertical root holes; firm and dry in place; loess, (ML)
HIGHLY ORGANIC SOILS		Readily identified by color, odor, spongy feel and frequently by fibrous texture			Pt	Peat and other organic soils	

PLASTICITY CHART

FOR LABORATORY CLASSIFICATION OF FINE GRAINED SOILS

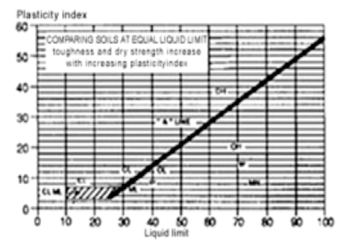

UNIFIED SOIL CLASSIFICATION INCLUDING IDENTIFICATION AND DESCRIPTION

Major division	Subdivision	FIELD IDENTIFICATION PROCEDURES (excluding particles larger than 3 inches and basing fractions on stimated weights)	GROUP SYMBOLS	TYPICAL NAMES	INFORMATION REQUIRED FOR DESCRIBING SOILS
COARSE GRAINED SOILS More than half of materials is <u>larger</u> than No. 200 sieve size	GRAVELS More than half of coarse fraction is larger than No. 4 sieve size (For visual classification, the 1/4" size may be used as equivalent for the No. 4 sieve size) — CLEAN GRAVELS (Little or no fines)	Wide range in grain size and substantial amounts of all intermediate particle sizes	GW	Well graded gravels, gravel-sand mixtures, little or no fines	Give typical name; indicate approximate percentage of sand and gravel, max. size; angularity, surface condition, and hardness of the coarse grains; local or geological name and other pertinent descriptive information, and symbol in parentheses
		Predominantly one size or a range of sizes with same intermediate sizes missing	GP	Poorly graded gravels, gravel-sand mixtures, little or no fines	
	GRAVELS WITH FINES (Appreciable amount of fines)	Non-plastic fines (for identification procedures see ML below)	GM	Silty gravel, poorly graded gravel-sand silt mixtures	For undisturbed soils add information on stratification, degree of compactness, cementation, moisture conditions and drainage characteristics
		Plastic fines (for identification procedures see CL below)	GC	Clayey gravels, poorly graded gravel-sand clay mixtures	
	SANDS More than half of coarse fraction is smaller than No. 4 sieve size — CLEAN SANDS (Little or no fines)	Wide range in grain sizes and substantial amount of all intermediate particle sizes	SW	Well graded sands, gravelly sands, little or no fines	
		Predominantly one size or a range of sizes with some intermediate sizes missing	SP	Poorly graded sand, gravelly sands, little or no fines	EXAMPLE: <u>Silty sand</u> gravelly; about 20% hard, angular gravel particle $\frac{1}{2}$ - in maximum size; rounded and subangular sand grains coarse to fine; about 15% non-plastic fines with low dry strength; well compacted and moist in place; alluvial sand; (SM)
	SANDS WITH FINES (Appreciable amount of fines)	Non-plastic fines (for identification procedures see CL below)	SM	Silty sand, poorly graded sand-silt mixtures	
		Plastic fines (for identification procedures see CL below)	SC	Clayey sand, poorly graded sand-clay mixtures	

(The No. 200 sieve size is about the smallest particle visible to the naked eye)

Major division	Subdivision	DRY STRENGTH (CRUSHING CHARACTERISTICS)	DILATANCY (REACTION TO SHAKING)	TOUGHNESS (CONSISTENCY NEAR PLASTIC LIMIT)	GROUP SYMBOLS	TYPICAL NAMES	INFORMATION REQUIRED FOR DESCRIBING SOILS
FINE GRAINED SOILS More than half of materials is <u>smaller</u> than No. 200 sieve size	IDENTIFICATION PROCEDURES ON FRACTION SMALLER THAN No 40 SIEVE SIZE						
	SILTS AND CLAYS Liquid limit less than 50	None to slight	Quick to slow	None	ML	Inorganic silts and very fine sands, rock flour, silty or clayey fine sand with slight plasticity	Give typical name; indicate degree and character of plasticity, amount and maximum size of coarse grains; color in wet condition, odor, if any, local or geologic name, and other pertinent descriptive information, and symbol in parentheses
		Medium to high	None to very slow	Medium	OL	Inorganic clays of low to medium plasticity, gravelly clays, sandy clays, silty clays, lean clays	
		Slight to medium	Slow	Slight	MN	Organic silts and organic silt-clays of low plasticity	For undisturbed soils add information on structure, stratification, consistency in undisturbed and remolded strates, moisture and drainage conditions
	SILTS AND CLAYS Liquid limit greater than 50	Slight to medium	Slow to none	Slight to medium	OL	Inorganic silt, micaceous or diatomaceus fine sandy or silty soils, elastic silts	
		High to very high	None	High	CH	Inorganic clays of high organic plasticity	EXAMPLE:
		Medium to high	None to very slow	Slight to medium	OH	Organic clays of medium to high plasticity	Clayey silt, brown, slightly plastic; small percentage of fine sand; numerous vertical root holes; firm and dry in place; loess, (ML)
HIGHLY ORGANIC SOILS		Readily identified by color, odor, spongy feel and frequently by fibrous texture			Pt	Peat and other organic soils	

	LABORATORY CLASSIFICATION CRITERIA	
Determine percentages of gravel and sand from grain size curve. Depending on percentage of fines (fraction smaller than No. 200 sieve size) coarse grained soils are classified as follow: Less than 5% GW, GP, SW, SP. More than 12% GM, GC, SM, SC. 5% to 12% Borderline cases requiring use of dual symbols	$C_u = \frac{D_{60}}{D_{10}}$ Greater than 4 $C_c = \frac{(D_{30})^2}{D_{10} \times D_{60}}$ between one and 3	
	Not meeting all gradation requirements for GW	
	Atterberg limits above "A" line with PI greater than 7	Above "A" line with PI between 4 and 7 are borderline cases requiring use of dual symbols
	Atterberg limits below "A" line or PI greater than 7	
	$C_u = \frac{D_{60}}{D_{10}}$ Greater than 6 $C_c = \frac{(D_{30})^2}{D_{10} \times D_{60}}$ between one and 3	
	Not meeting all gradation requirements for SW	
	Atterberg limits below "A" line or PI less than 4	Above "A" line with PI between 4 and 7 are borderline cases requiring use of dual symbols
	Atterberg limits above "A" line with PI greater than 7	

Use grain size curve in indentifying the fractions as given under field identification

PLASTICITY CHART

FOR LABORATORY CLASSIFICATION OF FINE GRAINED SOILS

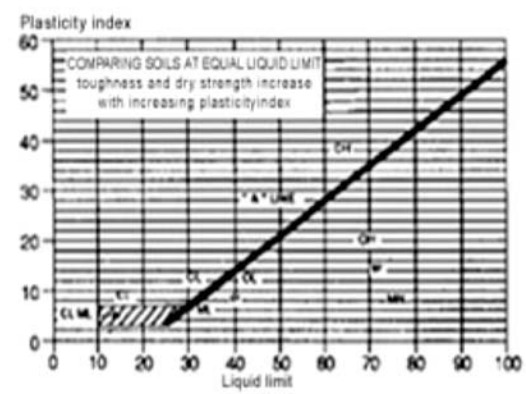

UNIFIED SOIL CLASSIFICATION SYSTEM

Soils are visually classified for engineering purposes by the Unified Soil Classification System. Grain-size analyses and Atterberg Limits tests often are performed on selected samples to aid in classification. The classification system is briefly outlined on this chart. Graphic symbols are used on boring logs presented in this report. For a more detailed description of the system, see "Standard Practice for Description and Identification of Soils (Visual-Manual Procedure)" ASTM Designation: 2488-84 and "Standard Test Method for Classification of Soils for Engineering Purposes" ASTM Designation: 2487-85.

MAJOR DIVISIONS				GRAPHIC SYMBOL	GROUP SYMBOL	TYPICAL NAMES
COARSE-GRAINED SOILS (Less than 50% passes No. 200 sieve)	GRAVELS (50% or less of coarse fraction passes No. 4 sieve)	CLEAN GRAVELS (Less than 5% passes No. 200 sieve)			GW	Well graded gravels, gravel-sand mixtures, or sand-gravel-cobble mixtures
					GP	Poorly graded gravels, gravel-sand mixtures, or sand-gravel-cobble mixtures
		GRAVELS WITH FINES (More than 12% passes No. 200 sieve)	Limits plot below "A" line & hatched zone on plasticity chart		GM	Silty gravels, gravel-sand-silt mixtures
			Limits plot above "A" line & hatched zone on plasticity chart		GC	Clayey gravels, gravel-sand-clay mixtures
	SANDS (50% or more of coarse fraction passes No. 4 sieve)	CLEAN SANDS (Less than 5% passes No. 200 sieve)			SW	Well graded sands, gravelly sands
					SP	Poorly graded sands, gravelly sands
		SANDS WITH FINES (More than 12% passes No. 200 sieve)	Limits plot below "A" line & hatched zone on plasticity chart		SM	Silty sands, sand-silt mixtures
			Limits plot above "A" line & hatched zone on plasticity chart		SC	Clayey sands, sand-clay mixtures
FINE-GRAINED SOILS (50% or more passes No. 200 sieve)	SILTS (Limits plot below "A" line & hatched zone on plasticity chart)	SILTS OF LOW PLASTICITY (Liquid Limit less than 50)			ML	Inorganic silts, clayey silts of low to medium plasticity
		SILTS OF HIGH PLASTICITY (Liquid Limit 50 or more)			MH	Inorganic silts, micaceous or diatomaceous silty soils, elastic silts
	CLAYS (Limits plot above "A" line & hatched zone on plasticity chart)	CLAYS OF LOW PLASTICITY (Liquid Limit less than 50)			CL	Inorganic clays of low to medium plasticity, gravelly, sandy, and silty clays
		CLAYS OF HIGH PLASTICITY (Liquid Limit 50 or more)			CH	Inorganic clays of high plasticity, fat clays, sandy clays of high plasticity
	ORGANIC SILTS AND CLAYS	ORGANIC SILTS AND CLAYS OF LOW PLASTICITY (Liquid Limit less than 50)			OL	Organic silts and clays of low to medium plasticity, sandy organic silts and clays
		ORGANIC SILTS AND CLAYS OF HIGH PLASTICITY (Liquid Limit 50 or more)			OH	Organic silts and clays of high plasticity, sandy organic silts and clays
ORGANIC SOILS		PRIMARILY ORGANIC MATTER (dark in color and organic odor)			PT	Peat

NOTE: Coarse-grained soils with between 5% and 12% passing the No. 200 sieve and fine-grained soils with limits plotting in the hatched zone on the plasticity chart have dual classifications.

PLASTICITY CHART

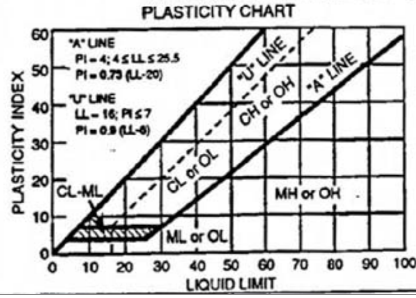

DEFINITION OF SOIL FRACTIONS

SOIL COMPONENT	PARTICLE SIZE RANGE
Boulders	Above 12 in.
Cobbles	12 in. to 3 in.
Gravel	3 in. to No. 4 sieve
Coarse gravel	3 in. to 3/4 in.
Fine gravel	3/4 in. to No. 4 sieve
Sand	No. 4 to No. 200 sieve
Coarse sand	No. 4 to No. 10 sieve
Medium sand	No. 10 to No. 40 sieve
Fine sand	No. 40 to No. 200 sieve
Fines (silt and clay)	Less than No. 200 sieve

Additional Related References (Fine Grained Soils)

Bray, J. D., Sancio, R. B., Riemer, M. F., and Durgunoglu, T. (2004). "Liquefaction susceptibility of fine-grained soils." Proc., 11th Int. Conf. On Soil Dynamics and Earthquake Engineering and 3rd Int. Conf. On Earthquake Geotechnical Engineering, Stallion Press, Berkeley, Calif., Vol. 1, 655–662.

Guo, T., and Prakash, S. (2000). "Liquefaction of silt-clay mixtures." Proc., 12th World Conf. on Earthquake Engineering, Upper Hutt, New Zealand, NZ Soc. for EQ Engrg., Paper No. 0561.

Perlea, V. G. (2000). "Liquefaction of cohesive soils." Soil dynamics and liquefaction 2000, The 2000 Specialty Conf., Denver, ASCE geotechnical special publication No. 107, 58–75.

Polito, C. (2001). "Plasticity based liquefaction criteria." Proc., 4th Int. Conf. On Recent Advances In Geotechnical Earthquake Engineering and Soil Dynamics, Univ. of Missouri-Rolla, Rolla, Mo., Paper No. 1.33.

Polito, C. P., and Martin, J. R., II. (2001). "Effects of nonplastic fines on the liquefaction resistance of sands." J. Geotech. Geoenviron. Eng., 127, 5, 408–415.

Sancio, R. B. (2003). "Ground failure and building performance in Adapazari, Turkey." Ph.D. thesis, Univ. of California at Berkeley, Berkeley, Calif.

Seed, H. B., and Idriss, I. M. (1982). "Ground motions and soil liquefaction during earthquakes." EERI Monograph, Berkeley, Calif. (where Chinese Criteria are proposed)

Thevanayagam, S., and Martin, G. R. (2002). "Liquefaction in silty soils: screening and remediation issues." Soil Dyn. Earthquake Eng., 229–12, 1035–1042.

Wang, W. (1979). Some findings in soil liquefaction, Water Conservancy and Hydroelectric Power Scientific Research Institute, Beijing, China. (Chinese Criteria was derived based on the data in this ref.)

Wijewickreme, D., and Sanin, M. (2004). "Cyclic shear loading response of Fraser River Delta Silt." Proc., 13th World Conf. on EQ Engineering, Mira Digital Publishing, Vancouver, Canada, Paper No. 499.

Wijewickreme, D., Sanin, M.V., and Greenaway, G. R. (2005). "Cyclic shear response of fine-grained mine tailings." Can. Geotech. J., 42, 1408–1421.

Yamamuro, J. A., and Lade, P.V. (1998). "Steady-state concepts and static liquefaction of silty sands," J. Geotech. Geoenviron. Eng., 124, 9, 868–877.

Yamamuro, J. A., and Covert, K. M. (2001). "Monotonic and cyclic liquefaction of very loose sands with high silt content." J. Geotech. Geoenviron. Eng., 127, 4 314–324.

Lateral Spreading: Empirical Approach

Primary References

T. L. Youd, C. M. Hansen, and S. F. Bartlett, Revised MLR Equations for Predicting Lateral Spread Displacement, Proc. 7th U.S.-Japan Workshop on Earthquake Resistant Design of Lifeline Facilities and Countermeasures Against Soil Liquefaction, T. D. O'Rourke, J.-P. Bardet, and M. Hamada, Eds., Technical MCEER Report 99-6002, Buffalo, NY, 1999, pp. 100-114.

S. F. Bartlett and T. L. Youd, Empirical Analysis of Horizontal Ground Displacement Generated by Liquefaction-Induced Lateral-Spread, Technical Report NCEER 92-0021, 114p.

S. F. Bartlett, and T. L. Youd, Empirical Prediction of Liquefaction-Induced Lateral-Spread, Journal of Geotechnical Engineering, ASCE, Vol. 121, No. 4, pp. 316-329.

Additional Reference

J.-P. Bardet, N. Mace, T. Tobita, and J. Hu, Large-Scale Modeling of Liquefaction-Induced Ground Deformation Part I: A Four Parameter MLR Model, Proc. 7th U.S.-Japan Workshop on Earthquake Resistant Design of Lifeline Facilities and Countermeasures Against Soil Liquefaction, T. D. O'Rourke, J.-P. Bardet, and M. Hamada, Eds., Technical MCEER Report 99-6002, Buffalo, NY, pp. 155-173.

Empirical MLR Procedure

1) Large Case History Data Set

2) Multi-Linear Regression Analysis (MLR)

Presented in 1992, 1995, with latest modification 1999

New predictive equation is based on additional new data sets from US and Japan, and some corrections and modifications

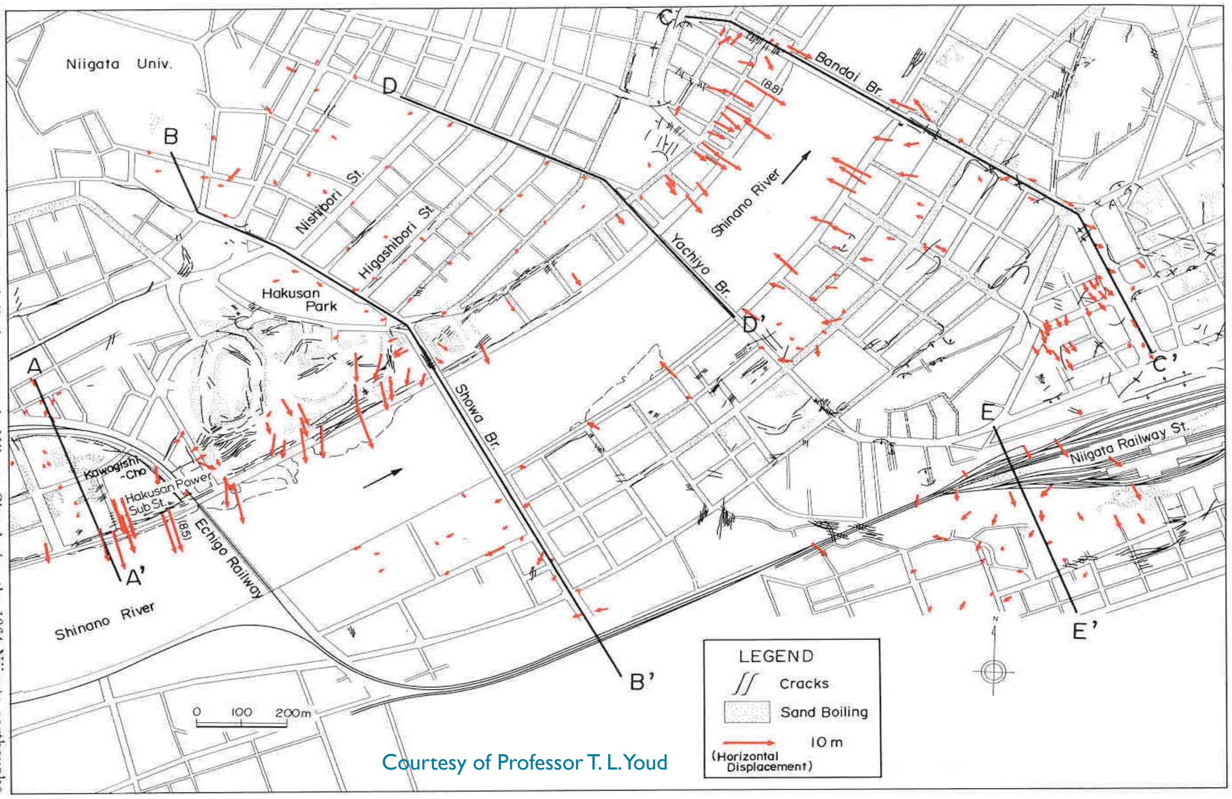

Fig. 3-2 Permanent horizontal ground displacements in Niigata City during the 1964 Niigata earthquake

Courtesy of Professor T. L. Youd

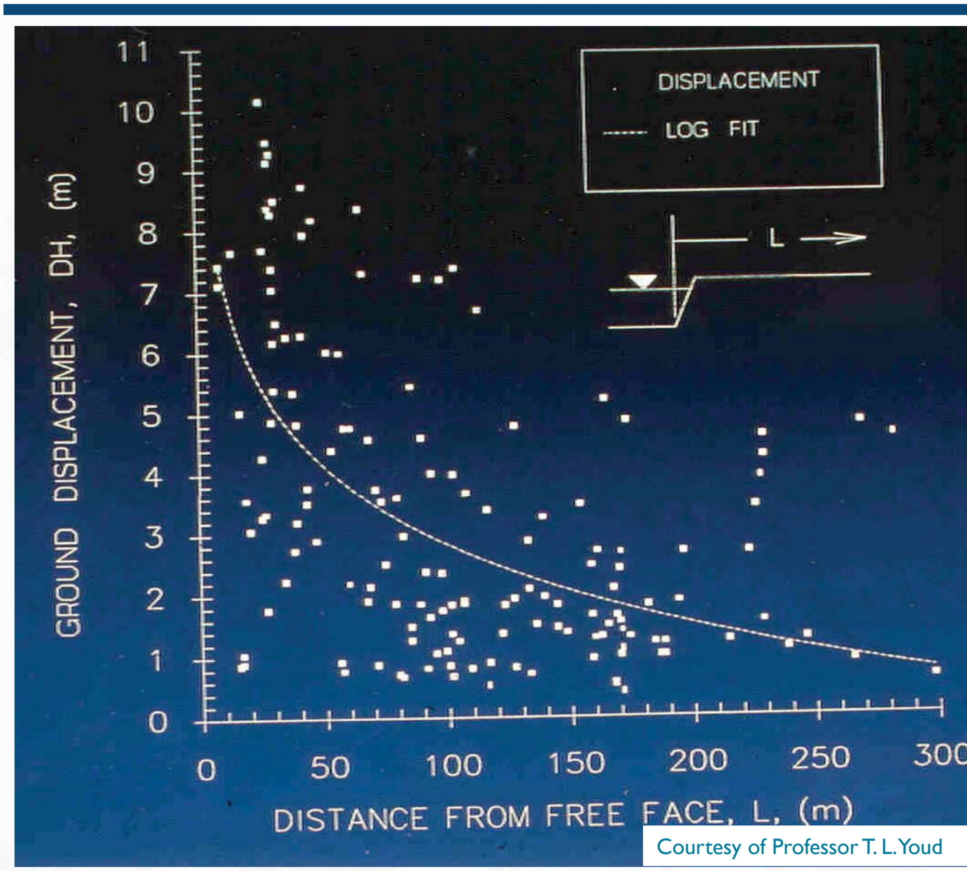

Courtesy of Professor T. L. Youd

Displacement Versus Distance From Free Face for Lateral Spread Displacements Generated in Niigata, Japan During 1994 Earthquake

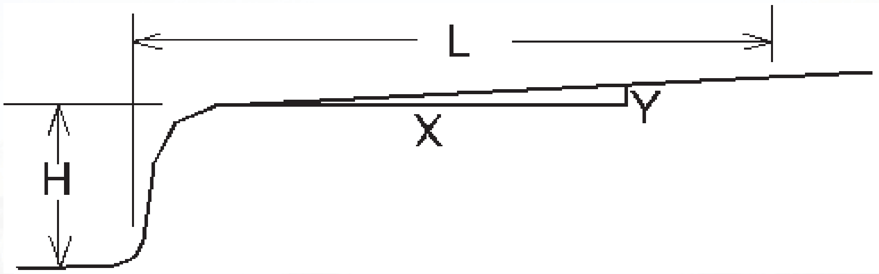

D_H = horizontal displacement (m),

M = moment magnitude,

R = distance from seismic energy source (km),

W = free face ratio = (H/L)(100) in percent (see figure above),

S = ground slope = (Y/X)(100) in percent (see figure above),

T_{15} = thickness of layer with $(N_1)_{60} < 15$ (m),

F_{15} = fines content in T_{15} layer (%),

$D50_{15}$ = average mean grain size in T_{15} layer (mm).

Recommended MLR Equations

Youd, T.L., Hansen, C.M., and Bartlett, S.F. (1999)

Free face conditions:

$$\text{Log } D_H = -18.084 + 1.581 M - 1.518 \text{ Log } R^* - 0.011 R + 0.551 \text{ Log } W + 0.547 \text{ Log } T_{15} + 3.976 \text{ Log } (100-F_{15}) - 0.923 \text{ Log } (D50_{15}+0.1)$$

Ground slope conditions:

$$\text{Log } D_H = -17.614 + 1.581 M - 1.518 \text{ Log } R^* - 0.011 R + 0.343 \text{ Log } S + 0.547 \text{ Log } T_{15} + 3.976 \text{ Log } (100-F_{15}) - 0.923 \text{ Log } (D50_{15}+0.1)$$

where $R^* = R+R_0$ and $R_0 = 10^{(0.89M-5.64)}$

Note:

- This model is valid for coarse-grained sites ($D50_{15}$ up to 10mm for silty sediments)
- Predicted displacements greater than 6 m are poorly constrained by observational data and are highly uncertain

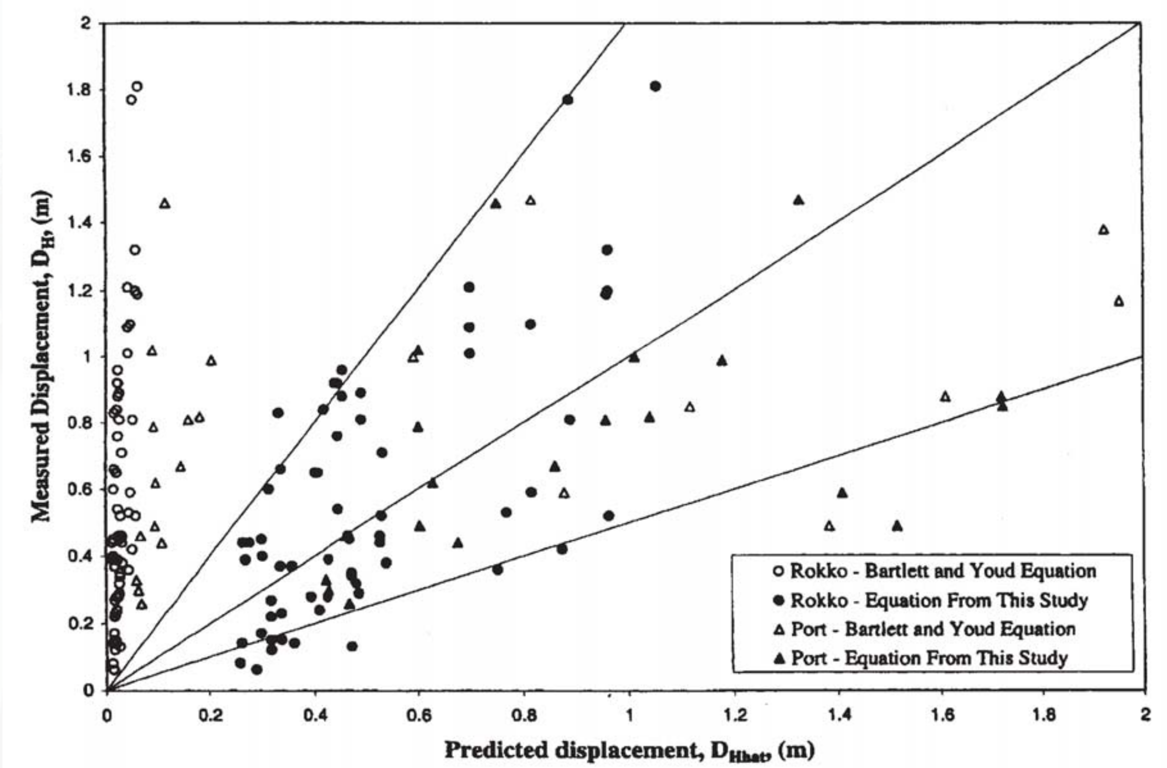

Measured versus predicted displacements for Port and Rokko Islands, Japan showing that Bartlett and Youd Equations greatly under-predict displacements at coarse-grained sites (Youd et al. 1999).

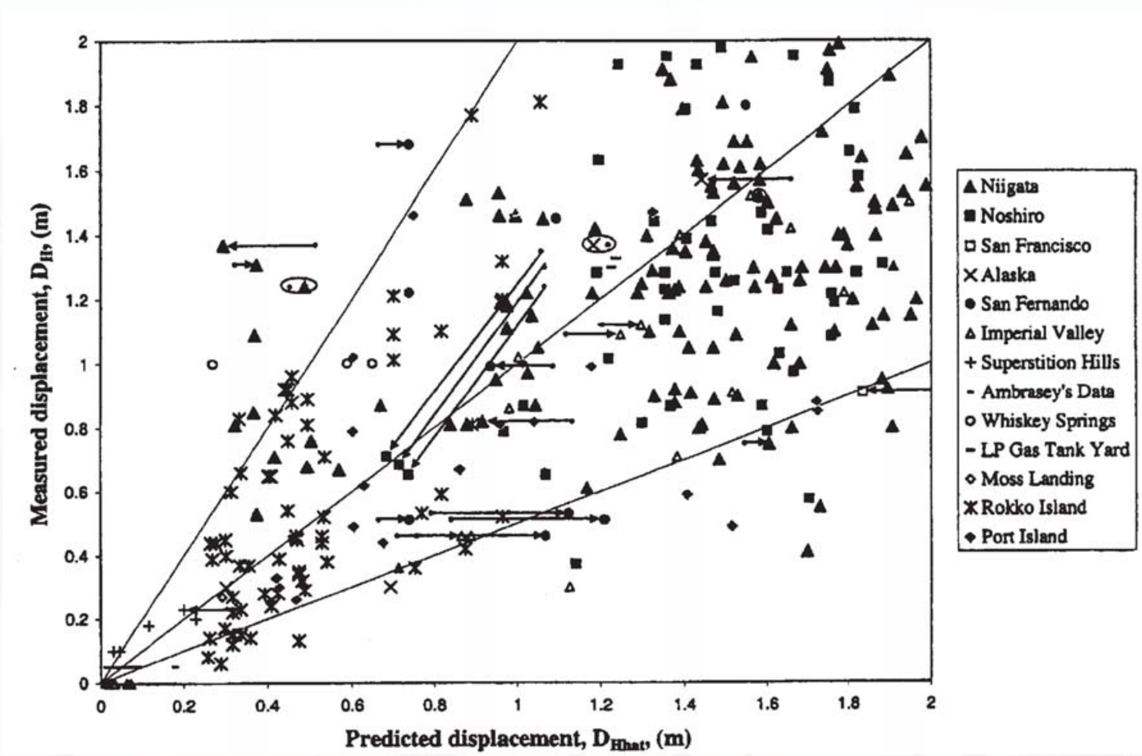

Measured versus predicted displacements using Youd et al. Equation (1999) with comparisons of values predicted using the Bartlett and Youd (1992) model for 22 tracked points.

Liquefaction Countermeasures

Ahmed Elgamal

Liquefaction Countermeasures

Source: Hayward Baker
http://www.haywardbaker.com/

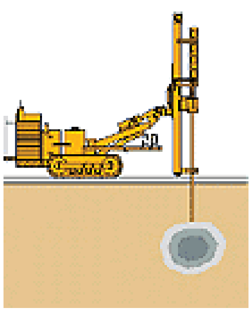

Compaction Grouting

When low-slump compaction grout is injected into granular soils, grout bulbs are formed that displace and densify the Surrounding loose soils. The technique is ideal for remediating or preventing structural settlements, and for site improvement of loose soil strata.

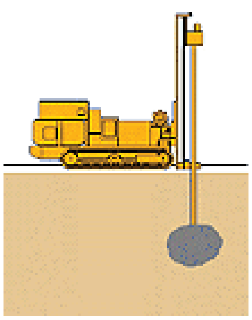

Chemical Grouting

The permeation of very low-viscosity chemical grout into granular soil improves the strength and rigidity of the soil to limit ground movement during construction. Chemical grouting is used extensively to aid soft ground tunneling and to control groundwater intrusion. As a remedial tool, chemical grouting is effective in waterproofing leaking subterranean structures.

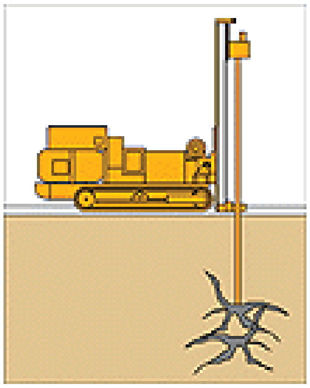

Cement Grouting Primarily used for water control in fissured rock, Portland and microfine cement grouts play an important role in dam rehabilitation, not only sealing water passages but also strengthening the rock mass. Fast-set additives allow cement grouting in moving water and other hard-to-control conditions.

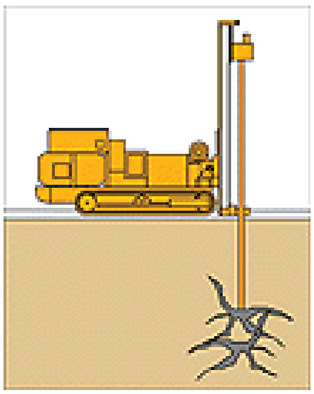

Soilfrac Grouting Soilfrac^{sm} grouting is used where a precise degree of settlement control is required in conjunction with soft soil stabilization. Cementitious or chemical grouts are injected in a strictly controlled and monitored sequence to fracture the soil matrix and form a supporting web beneath at-risk structures.

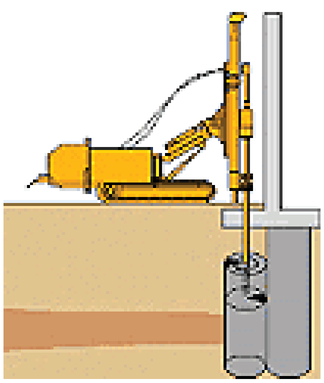

Jet Grouting Jet grouting is an erosion/replacement system that creates an engineered, in situ soil/cement product known as Soilcrete^{sm}. Effective across the widest range of soil types, and capable of being performed around subsurface obstructions and in confined spaces, jet grouting is a versatile and valuable tool for soft soil stabilization, underpinning, excavation support and groundwater control.

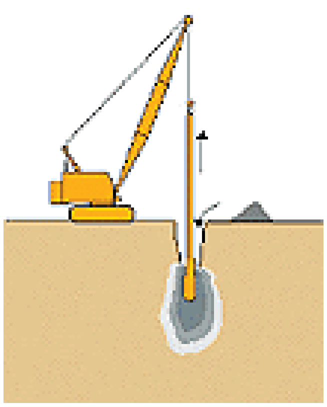

Vibro-Compaction A site improvement technique for granular material, Vibro-Compaction uses company-designed probe-type vibrators to densify soils to depths of up to 120 feet. Vibro-Compaction increases bearing capacity for shallow-footing construction, reduces settlements and also mitigates liquefaction potential in seismic areas.

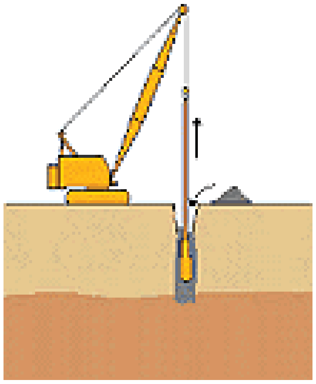

Vibro-Replacement Related to Vibro-Compaction, Vibro-Replacement is used in clays, silts, and mixed or stratified soils. Stone backfill is compacted in lifts to construct columns that improve and reinforce the soil strata and aid in the dissipation of excess pore water pressures. Vibro-Replacement is well suited for stabilization of bridge approach soils, for shallow footing construction, and for liquefaction mitigation.

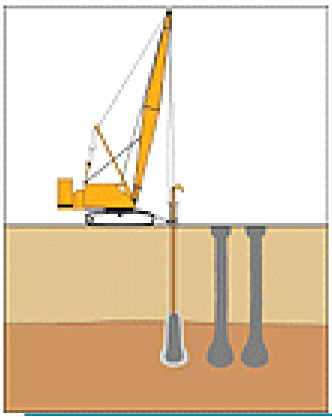

Vibro Concrete Columns Very weak, cohesive and organic soils that are not suitable for standard Vibro techniques can be improved by the installation of Vibro Concrete Columns. Beneath large area loads, Vibro Concrete Columns reduce settlement, increase bearing capacity, and increase slope stability.

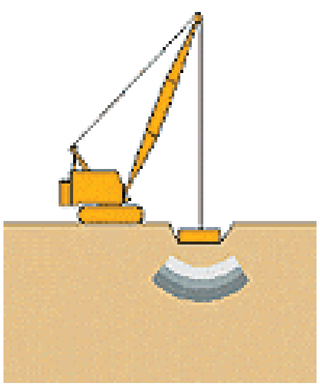

Dynamic Deep Compaction Dynamic Deep Compaction™ is an economic site improvement technique used to treat a range of porous soil types and permit shallow, spread footing construction. Soils are densified at depth by the controlled impact of a crane-hoisted, heavy weight (15-35 tons) on the ground surface in a pre-determined grid pattern. Dynamic Deep Compaction is also successful in densifying landfill material for highway construction or recreational landscaping.

Soil Mixing Typically used in soft soils, the soil mixing technique relies on the introduction of an engineered grout material to either create a soil-cement matrix for soil stabilization, or to form subsurface structural elements to support earth or building loads. Soil mixing can be accomplished by many methods, with a wide range of mixing tools and tool configurations available.

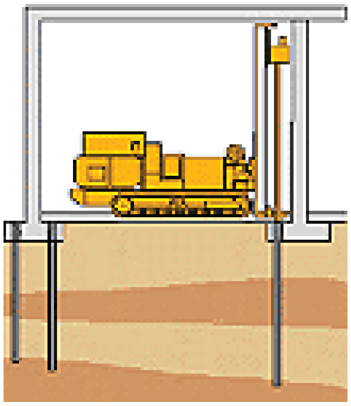

Minipiles Underpinning of settling or deteriorating foundations, and support of footings for increased capacity are prime candidates for minipile installation, particularly where headroom is limited or access restricted. These small diameter, friction and/or end bearing elements can transfer ultimate loads of up to 350 tons to a competent stratum.

Extensive Literature is available at the Hayward Baker Web-site:
http://www.haywardbaker.com/

NICHOLSON
A Rodio Group Company

Nicholson Construction Company

http://www.nicholsonconstruction.com/

Grouting Applications

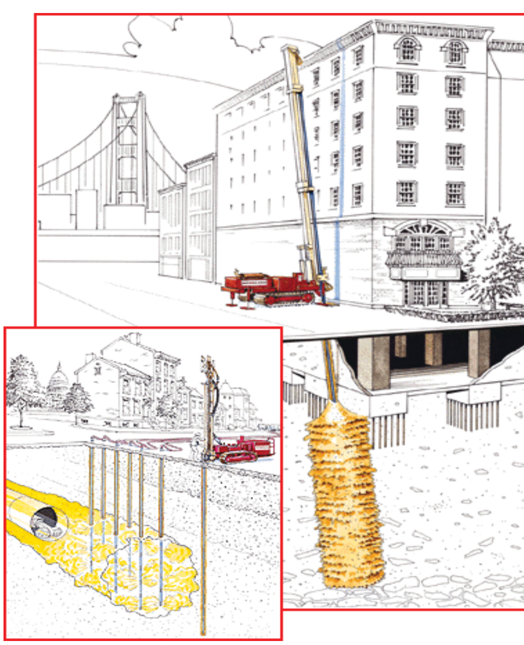

Pin Piles

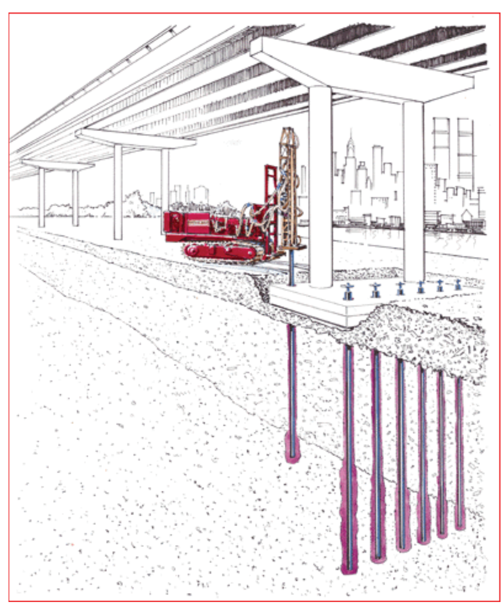

Vibro Technologies

http://www.nicholsonconstruction.com/

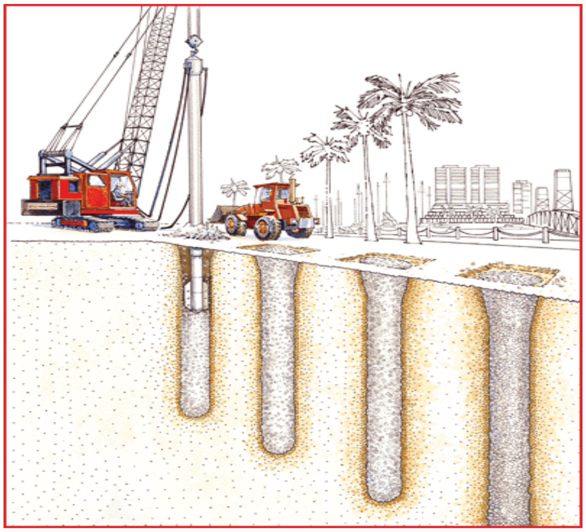

For Publications
http://www.nicholsonconstruction.com/techResources/technicalPapers.aspx